Macroscopic stochastic thermodynamics

Gianmaria Falasco*

Department of Physics and Astronomy, University of Padova, Via Marzolo 8, I-35131 Padova, Italy

Massimiliano Esposito†

Department of Physics and Materials Science, University of Luxembourg, 30 Avenue des Hauts-Fourneaux, L-4362 Esch-sur-Alzette, Luxembourg

(published 22 January 2025)

Starting at the mesoscopic level with a general formulation of stochastic thermodynamics in terms of Markov jump processes, the scaling conditions that ensure the emergence of a (typically nonlinear) deterministic dynamics and an extensive thermodynamics at the macroscopic level are identified. Large deviations theory is then used to build a macroscopic fluctuation theory around this deterministic behavior, which are shown to preserve the fluctuation theorem. For many systems (such as chemical reaction networks, electronic circuits, and Potts models), this theory does not coincide with Langevin-equation approaches (obtained by adding Gaussian white noise to the deterministic dynamics), which if used are thermodynamically inconsistent. Einstein-Onsager theory of Gaussian fluctuations and irreversible thermodynamics are recovered at equilibrium and close to it, respectively. Far from equilibirum the free energy is replaced by the dynamically generated quasipotential (or self-information), which is a Lyapunov function for the macroscopic dynamics. Thermodynamics connects the dissipation along deterministic and escape trajectories to the Freidlin-Wentzell quasipotential, thus constraining the transition rates between attractors induced by rare fluctuations. A coherent perspective on minimum and maximum entropy production principles is also provided. For systems that admit a continuous-space limit, a nonequilibrium fluctuating field theory with its associated thermodynamics is derived. Finally, the macroscopic stochastic dynamics is coarse grained into a Markov jump process describing transitions among deterministic attractors, and the stochastic thermodynamics emerging from it is formulated.

DOI: 10.1103/RevModPhys.97.015002

CONTENTS

*Contact author: gianmaria.falasco@unipd.it
†Contact author: massimiliano.esposito@uni.lu

I. INTRODUCTION

A. The challenge

Thermodynamics is a theory describing energy transfers among systems and energy transformations from one form into another. It constitutes a significant scientific achievement that started more than three centuries ago with the study of vacuum pumps. During the 19th century its developments were noteworthy and instrumental in mastering the technology of steam engines that powered the industrial revolution. In its traditional formulation thermodynamics applies to macroscopic systems at thermodynamic equilibrium. The microscopic foundation of the theory, *statistical mechanics*, was established during the late 19th and early 20th centuries. It explains how the observed macroscopic behavior results from large numbers of microscopic degrees of freedom giving rise to sharply peaked probability distributions. The 20th century witnessed the first development of *irreversible thermodynamics* to explain transport phenomena, which is based on the assumption that the bulk properties of macroscopic systems remain close to thermodynamic equilibrium (Prigogine, 1961; de Groot and Mazur, 1984).

Since the end of the 20th century, a statistical formulation of nonequilibrium thermodynamics, called stochastic thermodynamics (ST), was established to describe small fluctuating systems (Seifert, 2012; Van den Broeck and Esposito, 2015; Peliti and Pigolotti, 2021; Gaspard, 2022; Shiraishi, 2023). In its general formulation (Rao and Esposito, 2018b), ST constructs thermodynamic observables (for example, heat, work, and dissipation) on top of the stochastic dynamics of open systems. The key assumption is that all the degrees of freedom that are not explicitly described by the dynamics—i.e., the internal structure of the system states and the reservoirs—must be at equilibrium. The link between observables and dynamics is then provided by the *local detailed balance* property (Bergmann and Lebowitz, 1955; Esposito, 2012; Bauer and Cornu, 2015; Falasco and Esposito, 2021; Maes, 2021): when an elementary process (such as an elementary chemical reaction) induces a transition between two states (such as the number of molecules before and after the reaction), the Boltzmann constant k_B times the log ratio of the forward and backward currents of that process between the two states is the entropy production (or dissipation) of the process; i.e., the sum of the entropy changes in the environment and in the system. The successes of ST over recent years have been impressive both theoretically and experimentally. Since the theory predicts the temporal changes of thermodynamic quantities, it can be used to address typical *finite-time thermodynamics* questions such as identifying optimal driving protocols leading to maximum power extraction (Seifert, 2012; Benenti *et al.*, 2017). For instance, driven colloidal particles, molecular motors, Brownian ratchets, and electrical circuits have been considered (Blickle *et al.*, 2006; Mehl *et al.*, 2012; Pekola, 2015; Ciliberto, 2017; Brown and Sivak, 2020). ST also predicts the nonequilibrium fluctuations of thermodynamic observables. The central discovery of the field is the *fluctuation theorem* asserting that the probability to observe a given positive dissipation is exponentially larger than the probability of its negative counterpart (Jarzynski, 2011; Seifert, 2012; Rao and Esposito, 2018c; Gaspard, 2022). This relation generalizes the second law, which states only that on average the dissipation cannot decrease. Previous results such as Onsager reciprocity relations or fluctuation-dissipation relations can be recovered from it. ST also provides natural connections with information theory (Wolpert, 2019): the system entropy contains a Shannon entropy contribution, dissipation can be expressed as a Kullback-Leibler entropy quantifying how different probabilities of forward trajectories are from their time-reversed counterpart, and the difference between the nonequilibrium and equilibrium thermodynamic potential takes the form of a Kullback-Leibler entropy between the system nonequilibrium and equilibrium probability distributions. These results provide a rigorous ground to assess, both theoretically (Horowitz and Esposito, 2014; Parrondo, Horowitz, and Sagawa, 2015) and experimentally (Toyabe *et al.*, 2010; Bérut *et al.*, 2012; Jun, Gavrilov, and Bechhoefer, 2014; Koski *et al.*, 2015), the cost of various information processing operations such as Landauer erasure or Maxwell's demons. More recently, ST was also used to show that dissipation sets universal bounds—called thermodynamic uncertainty relations and speed limits—on the precision (Barato and Seifert, 2015; Falasco, Esposito, and Delvenne, 2020; Horowitz and Gingrich, 2020) as well as the duration (Shiraishi, Funo, and Saito, 2018; Falasco and Esposito, 2020; Vo, Van Vu, and Hasegawa, 2020; Van Vu and Saito, 2023) of nonequilibrium processes.

Despite these significant achievements, the focus of ST has been the study of small and simple systems far from equilibrium, and important questions remain open when considering larger and more complex systems. In particular: (i) What happens in the thermodynamic limit of ST? and (ii) How should ST be modified when detailed balance is broken? These questions remain poorly explored except for specific model-system studies.

(i) More specifically, what happens when one considers systems whose number of degrees of freedom becomes large? Can one derive from ST a macroscopic thermodynamics valid far from equilibrium and connect it close to equilibrium to irreversible thermodynamics? These general questions largely remain unanswered. This is surprising given that a motivation for the early developments (Hatano and Sasa, 2001, 2005; Sekimoto, 2010) that led to the present form of ST was the derivation of a nonequilibrium version of traditional thermodynamics (Keizer, 1978; Oono and Paniconi, 1998). In recent years only specific classes of systems that exhibit a macroscopic limit have been considered, such as chemical reaction networks (Rao and Esposito, 2016; Falasco, Rao, and Esposito, 2018; Falasco *et al.*, 2019; Avanzini *et al.*, 2021), electronic circuits (Freitas, Delvenne, and Esposito, 2020, 2021), and mean-field Ising and Potts models (Herpich, Thingna, and Esposito, 2018; Herpich and Esposito, 2019; Herpich *et al.*, 2020). These results suggest that, for these macroscopic systems, one can derive not only a deterministic

formulation of nonequilibrium thermodynamics but also, with the help of large deviations theory (Touchette, 2009), a theory of macroscopic fluctuations around the deterministic behavior that is similar in spirit to the one valid for diffusive systems (Bertini *et al.*, 2015). The macroscopic fluctuation theories derived for most of the model systems studied are incompatible with a naive approach consisting of adding Gaussian white noise to the deterministic dynamics. A general theory is needed to clarify these crucial questions.

(ii) Most dynamics used to describe complex phenomena are highly coarse grained and do not resolve all the out-of-equilibrium degrees of freedom, thus compromising the detailed balance assumption essential to build a consistent ST. This situation is ubiquitous in active and biological systems, for instance (Marchetti *et al.*, 2013; Bechinger *et al.*, 2016). While the dynamics of some motile cells can be modeled by active Brownian dynamics (Fodor *et al.*, 2016), their energetic cost cannot be deduced from the motion of the cells alone, as a large number of hidden subcellular processes are also dissipating energy. The practical relevance of a thermodynamics of complex systems is enormous. It is necessary to address questions such as the following: To what extent are biology and ecology shaped by the energy flows sustaining them (Garvey and Whiles, 2016; Yang *et al.*, 2021)? and What are energy efficient design principles for information, computation, and communication technologies (Wolpert, Kolchinsky, and Owen, 2019; Lange, Pohl, and Santarius, 2020; Auffèves, 2022)?

A crucial difference between these complex systems and those typically considered in irreversible thermodynamics is that the nonequilibrium constraints or thermodynamic driving forces are imposed not only at the boundaries of the system but also throughout the system itself. In biology, for instance, the energy input is chemical (for example, from adenosine triphosphate hydrolysis) and arises at the molecular scale. This fact *a priori* jeopardizes notions of equilibrium used to build traditional macroscopic fluctuation theories (de Zárate and Sengers, 2006; Bertini *et al.*, 2015). Despite much ongoing work on coarse-graining stochastic dynamics (Rahav and Jarzynski, 2007; Puglisi *et al.*, 2010; Toyabe *et al.*, 2010; Esposito, 2012; Bo and Celani, 2014, 2017; Esposito and Parrondo, 2015; Polettini and Esposito, 2017; Strasberg and Esposito, 2019; Herpich, Shayanfard, and Esposito, 2020; Maes, 2020), aside from a few exceptions in simple models (Pietzonka and Seifert, 2018; Speck, 2022; Bebon, Robinson, and Speck, 2024) and in the linear regime (Gaspard and Kapral, 2020), little is known about how to establish a thermodynamically consistent theory of active systems, particularly at a macroscopic level, where nonequilibrium field theoretical descriptions (formulated in physical space) would be useful.

B. What we achieve

Starting with a general formulation of ST, we identify the scaling conditions ensuring that a *deterministic* (typically nonlinear) dynamics and a corresponding *extensive* thermodynamics emerge in the macroscopic limit. We find that the same conditions ensure the validity of a thermodynamically consistent macroscopic fluctuation theory (based on large deviations theory) describing fluctuations around the deterministic behavior. The importance of these results is manifold. First, ST is proved to be compatible with macroscopic thermodynamics and equilibrium statistical mechanics, thus resolving some controversy concerning the definition of entropy on the basis of information theory (Goldstein *et al.*, 2019). Second, irreversible thermodynamics and the Einstein-Onsager theory of small fluctuations (Rytov, 1958; Landau and Lifshitz, 1959; Rytov, Kravtsov, and Tatarskii, 1989; de Zárate and Sengers, 2006; Henkel, 2017) are derived from our unified framework for close-to-equilibrium conditions, thus providing a more microscopic foundation for these two originally phenomenological theories. Third, we explain how thermodynamic quantities shape the far-from-equilibrium behavior, both the deterministic relaxation and the exponentially rare fluctuations (in the system size). By doing so, we connect the Freidlin-Wentzell theory of large deviations (Graham, 1987; Freidlin and Wentzell, 1998) to thermodynamics. This allows us to retrieve the minimum entropy production principle close to equilibrium, relate the lifetime of nonequilibrium metastable states to dissipation, and rigorously discuss a maximum entropy production principle. Fourth, we identify the pitfalls of commonly used approximations [such as nonlinear Langevin equations with multiplicative noise (Gillespie, 2000)] and offer as a result a systematic framework to derive thermodynamically consistent fluctuating field theories, for example, for active matter. Finally, we show that ST allows one to perform a physically motivated coarse graining tailored to reveal emergent states and transitions between them in complex nonequilibrium systems.

C. Outline

In Sec. II we introduce a dynamical description of the systems based on the classical master equation for occupation-like variables, for example, the number of particles in the physical space, of electrons on a conductor, of spins with a certain orientation, and of excitations in some mode space. At this level of description, which we called mesoscopic, all unresolved degrees of freedom (internal and environmental) are assumed to be thermalized. Detailed balance thus ensues, allowing us to introduce a complete thermodynamic superstructure given by standard ST, which we recapitulate.

We then introduce the macroscopic limit in Sec. III.A, which is akin to a nonequilibrium thermodynamic limit. We derive the conditions on the transition rate and thermodynamic forces of the mesoscopic dynamics that asymptotically ensure a deterministic dynamics (Sec. III.B) and an extensive thermodynamics (Sec. III.D). Large deviations theory, the appropriate language to describe the concentration of probability in the macroscopic limit, is utilized. Thanks to this theory, we explain that the macroscopic entropy of a system is independent of the probability distribution at the mesoscopic level and made up only of the internal entropy of the mesoscopic states. We link the phenomenon of dissipative metastability in the stochastic dynamics with the ergodicity breaking and multistability of the macroscopic deterministic dynamics (Sec. III.C). In Sec. III.E we consider the macroscopic nonlinear dynamics, identifying the weak-noise

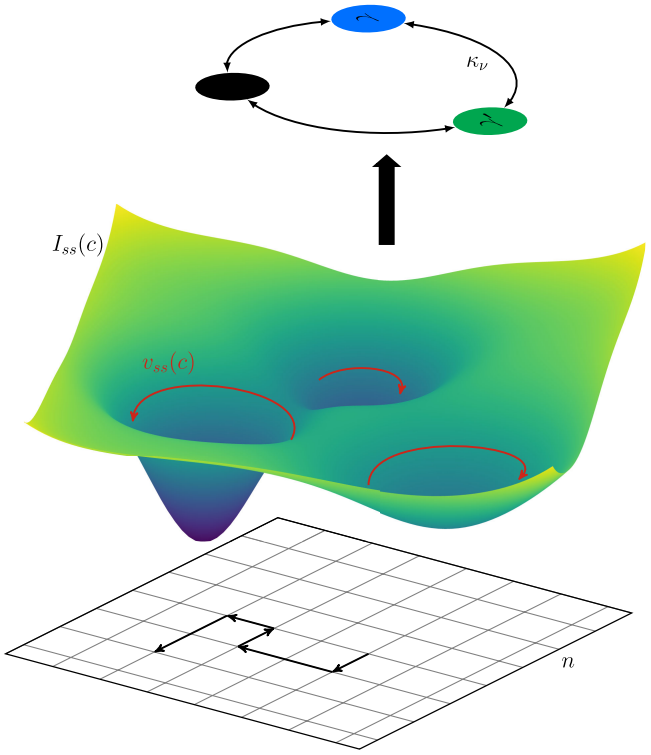

FIG. 1. Sketch of the different levels of the description emerging with a growing size V and timescale τ. Bottom sketch: the mesoscopic level consists of a Markov jump process in the discrete space n that enjoys local detailed balance. Middle sketch: for large V the dynamics of the intensive variable $c = n/V$ is dictated by the quasipotential $I_{\rm ss}$ and the nonconservative drift $v_{\rm ss}$. Top sketch: for large τ the dynamics again reduces to a Markov jump process on the space of the attractors, which are regarded as emergent states with internal dissipation.

quasipotential as the Lyapunov function and connecting it to thermodynamics. We split the deterministic relaxation in its gradient part and the nonequilibrium circulation due to state-space probability currents; see Fig. 1. In Sec. III.F we examine the linear deterministic relaxation close to nonequilibrium fixed points. Close to equilibrium we retrieve linear irreversible thermodynamics and the minimum entropy production principle.

Next we obtain in Sec. IV.A the macroscopic fluctuations from the extremum action principle. In Sec. IV.B we formulate the thermodynamics along macroscopic fluctuating trajectories by deriving an emergent second law and connecting the quasipotential to dissipation close to equilibrium. We focus on the asymptotic form of both small Gaussian fluctuations and rare large ones. The former are described by linear Langevin equations that reduce to the Onsager-Machlup theory at equilibrium (Sec. IV.C). We highlight the failure in capturing the rare events (Sec. IV.D) and the thermodynamics (Sec. IV.E) of the unsystematic truncation of the mesoscopic master equation that gives rise to a nonlinear Langevin equation with multiplicative noise. In Sec. IV.G we quantify the time-reversal asymmetry between the relaxation path within an attractor and the escape path out of it (called an instanton). In addition, the likelihood of rare large fluctuations, encoded into the quasipotential, allows us to quantify the transition rate out of a basin of attraction. For them we derive in Sec. IV.H upper and lower bounds in terms of the entropy produced in relaxation and escape trajectories, which constitute a novel maximum entropy production principle under certain conditions. In Sec. IV.I we discuss the asymptotic full counting statistics of thermodynamic currents and the fluctuation theorems showing how the multiplicative Gaussian noise approximations break them.

In Sec. V.A we consider a continuous-space limit, making contact with macroscopic fluctuation theory. We explain how fluxes become linear functions of the thermodynamic forces and the notion of local equilibrium appears. The associated thermodynamics is discussed in Sec. V.B, showing that the continuous-space limit of the mesoscopic entropy production differs from the apparent one defined in configuration space only unless all processes are diffusive.

In Sec. VI we formulate ST for the long-time jump dynamics between attractors. This provides a natural way to coarse grain the original system into emergent states sustained by an internal dissipation. We discuss the conditions of the underlying mesoscopic dynamics required to obtain the standard form of ST for this emergent jump process; see Fig. 1.

In Sec. VII we provide examples of the general theory, including chemical reaction networks, electronic circuits, and driven Potts models. In Sec. VIII we conclude by discussing the strength of our framework, its limitations, and open issues.

II. STOCHASTIC THERMODYNAMICS

We consider a small system in contact with several reservoirs, each characterized by prescribed intensive thermodynamic variables (temperature, chemical potential, electric voltage, etc.). We assume that the system's microscopic degrees of freedom are equilibrated and can be grouped into $i = \{1, \dots, N\}$ mesoscopic states, with occupation number n_i evolving under a stochastic dynamics; see Fig. 2. Namely, the occupation number vector $n = \{n_i\}_{i=1}^N$ changes at random times t_k by a finite vector $\Delta_\rho = \{\Delta_\rho^i\}_{i=1}^N$ due to transitions of type ρ induced by the coupling with the reservoirs,

$$d_t n(t) = \sum_\rho \Delta_\rho J_\rho(t) = \sum_{\rho>0} \Delta_\rho I_\rho(t). \tag{1}$$

In Eq. (1) $J_\rho(t) = \sum_k \delta_{\rho\rho(t)}\delta(t-t_k)$ is the rate of transitions ρ occurring at time t and $I_\rho(t) = J_\rho(t) - J_{-\rho}(t)$ is the net current (Rao and Esposito, 2018a). We have used microscopic reversibility, which imposes that for each transition $+\rho$ there exists an inverse transition denoted $-\rho$ and satisfying $\Delta_\rho = -\Delta_{-\rho}$. Equation (1) is taken to be Markovian when one chooses for $J_\rho(t)$ a Poissonian distribution[1] conditioned on the present state $n(t)$ with the average value $R_\rho(n(t))$.[2] We might also consider systems driven by reservoirs whose

[1]Or, equivalently, an exponential distribution for the waiting times $t_{k+1} - t_k$.

[2]We chose a compact notation such that the argument of $R_\rho(n)$ [$\Gamma_\rho(n)$, $\Sigma_\rho(n)$, etc.] denotes the starting state of the transition ρ, but the function can also depend on the final state $n + \Delta_\rho$.

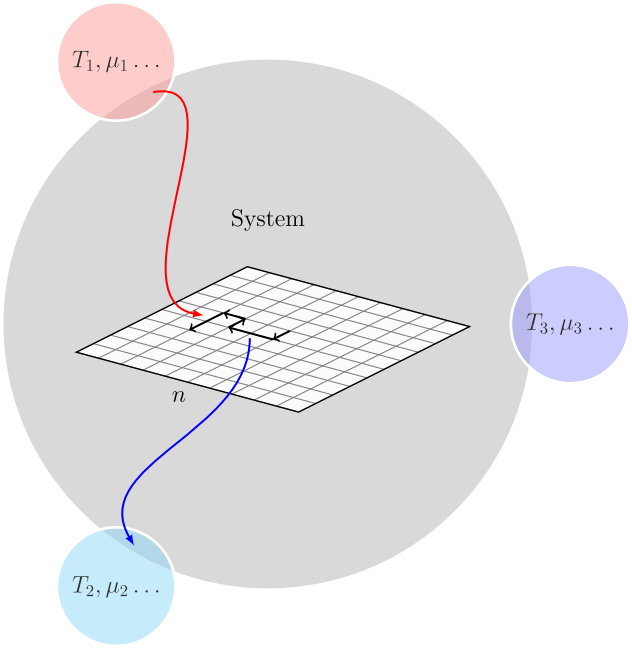

FIG. 2. Schematic representation of a system coupled to three reservoirs with fixed temperature T, (electro)chemical potential μ, etc. Each of them can exchange energy, (charged) particles, etc., through various transition mechanisms that result in jumps of the system state n.

intensive thermodynamic properties are externally changed in time. This corresponds to nonautonomous dynamics with rates $R_\rho(n(t), \vartheta(t))$ that carry an explicit dependence on time via a protocol $\vartheta(t)$ (although we do not write this dependence, to avoid clutter). For concreteness, we can think of n_i as the number of molecules of chemical species i, the number of charges of conductors i, or the number of excitations of modes i; see Sec. VII.

A trajectory $\mathcal{X}$ is the ordered set of states $n(t)$ and jumps $\rho(t_k)$ in the time span $t \in [0, \tau]$. The entire dynamical description of the system, equivalent to Eq. (1), is given by the probability density of a trajectory (Sun, 2006; Maes and Netočný, 2008)

$$P[\mathcal{X}] = P(n(0), 0) e^{-\sum_\rho \int_0^\tau dt R_\rho(n(t))} \prod_k R_{\rho(t_k)}(n(t_k^-)). \quad (2)$$

Shown in order in Eq. (2) are the probability density of the initial state $n(0)$, the product of probabilities for remaining in a certain state, and the product of probability densities for the changing state.

The dynamics in the configuration space corresponding to the mesoscopic description provided in Eq. (1) or (2) is given by the master equation for the probability density of occupation numbers,

$$\begin{aligned} \partial_t P(n,t) &= \sum_\rho [R_\rho(n-\Delta_\rho) P(n-\Delta_\rho, t) - R_\rho(n) P(n,t)] \\ &= \sum_{n'} \mathcal{R}_{nn'} P(n', t), \end{aligned} \quad (3)$$

with $\mathcal{R}_{nn'} = \sum_\rho R_\rho(n')(\delta_{n', n-\Delta_\rho} - \delta_{n',n})$ the transition rate matrix, i.e., the generator of the Markovian dynamics. We assume that the Markov jump process has a connected graph and thus is ergodic. For transition rates that carry an explicit time dependence, the instantaneous stationary probability density is defined by

$$\sum_{n'} \mathcal{R}_{nn'} P_t^{\mathrm{ss}}(n') = 0. \quad (4)$$

For transition rates that do not have any explicit time dependence, the solution of Eq. (4) is the unique stationary probability density function $P^{\mathrm{ss}}(n) = \lim_{t\to\infty} P(n,t)$ reached by the system at long times.

The transition rates satisfy the condition of local detailed balance (Bergmann and Lebowitz, 1955; Esposito, 2012; Bauer and Cornu, 2015; Falasco and Esposito, 2021; Maes, 2021),

$$\Sigma_\rho(n) \coloneqq \ln \frac{R_\rho(n)}{R_{-\rho}(n+\Delta_\rho)} = -\Phi(n+\Delta_\rho) + \Phi(n) + a_\rho, \quad (5)$$

which states that the logarithm of the ratio between forward and backward rates of a given transition ρ is the entropy production Σ_ρ of such a process; the Boltzmann constant k_B is set to 1 hereafter. Physically, Eq. (5) holds when the transitions $\pm\rho$ are caused by reservoirs in thermodynamic equilibrium, and all microscopic (internal) degrees of freedom of a mesostate n are equilibrated as well. In Eq. (5) $\Phi(n)$ is the negative of the Massieu potential, also called the free entropy (Callen, 1991), defined by subtracting the internal entropy $S_{\mathrm{int}}(n)$ of the mesostate n from the energetic contribution of conserved quantities exchanged with the baths.[3] For example, in the particular case of a system exchanging only energy with a single thermal bath at a temperature T,

$$T\Phi(n) = U(n) - TS_{\mathrm{int}}(n) \quad (6)$$

corresponds to the Helmholtz free energy, with $U(n)$ the internal energy of state n. The quantity

$$a_\rho = \mathbb{X}_\rho \cdot \mathscr{F}_{\mathrm{nc}} = -a_{-\rho} \quad (7)$$

in Eq. (5) denotes the nonconservative entropy flow in the transition ρ. It is the projection on ρ of the fundamental nonconservative forces $\mathscr{F}_{\mathrm{nc}}$, i.e., the minimal set of independent forces generated by the reservoirs, with $\mathbb{X}_\rho$ the variation in the reservoirs of the associated physical quantity due to the transition ρ. For these reasons a_ρ is expressed solely in terms of differences of intensive quantities of the reservoirs (inverse temperatures, chemical and electrical potentials, etc.); i.e., it is independent of the state of the system n. This decomposition into Massieu potential and nonconservative forces can always be performed, as outlined by Rao and Esposito (2018b). We note that $\Sigma_\rho(n) = -\Sigma_{-\rho}(n+\Delta_\rho)$.

[3] In the case of nonautonomous dynamics, $\Phi(n,t)$ carries an explicit time dependence due to $\vartheta(t)$ that we avoid writing, though.

The total entropy production rate (Seifert, 2005) along a fluctuating trajectory solution of Eq. (1),

$$\dot{\Sigma}(t) = \dot{\Sigma}_e(t) + d_t S_{\rm syst}(n(t), t), \tag{8}$$

is the sum of the entropy flow in the environment,

$$\dot{\Sigma}_e(t) \coloneqq \sum_\rho J_\rho(t)\Sigma_\rho(n(t)) - d_t S_{\rm int}(n(t)), \tag{9}$$

plus the time derivative of the system entropy,

$$S_{\rm syst}(n,t) \coloneqq -\ln P(n,t) + S_{\rm int}(n). \tag{10}$$

The first term on the right-hand side of Eq. (10) is the system's self-information or surprisal, whose mean value is the Shannon entropy

$$S_{\rm Sh}(t) \coloneqq -\sum_n P(n,t)\ln P(n,t). \tag{11}$$

The stochastic entropy production, i.e., the time integral of Eq. (8), can be obtained by comparing the forward and backward trajectory probabilities

$$\Sigma[\mathcal{X}] = \int_0^\tau dt\, \dot{\Sigma}(t) = \ln\frac{P[\mathcal{X}]}{\bar{P}[\mathcal{X}]}, \tag{12}$$

where $\bar{P}[\mathcal{X}]$ is the probability of the time-reversed trajectory obtained from Eq. (2) via the change of variable $t_k \mapsto \tau - t_k$ and reversing the protocol $\vartheta(t) \mapsto \vartheta(\tau - t)$. Therefore, the mean entropy production is the Kullback-Leibler divergence

$$\langle \Sigma[\mathcal{X}]\rangle = \int \mathcal{D}\mathcal{X} P[\mathcal{X}] \ln\frac{P[\mathcal{X}]}{\bar{P}[\mathcal{X}]} \geq 0. \tag{13}$$

Hereafter, the symbol $\langle\cdots\rangle$ denotes the expectation value of an observable computed with the appropriate probability, namely, $P[\mathcal{X}]$ for trajectory functionals or $P(n,t)$ for functions of the state at a single time t.

The mean entropy production rate (Schnakenberg, 1976) follows from averaging Eqs. (8)–(10),

$$\begin{aligned}\langle\dot{\Sigma}\rangle &= \sum_{n,\rho} R_\rho(n)P(n,t)\Sigma_\rho(n) + d_t S_{\rm Sh}(t)\\ &= \sum_{n,\rho>0}\left[R_\rho(n)P(n,t) - R_{-\rho}(n+\Delta_\rho)P(n+\Delta_\rho,t)\right]\\ &\quad\times \ln\frac{R_\rho(n)P(n,t)}{R_{-\rho}(n+\Delta_\rho)P(n+\Delta_\rho,t)} \geq 0.\end{aligned} \tag{14}$$

The non-negativity follows from $(x-y)\ln(x/y) \geq 0$, which is valid for all positive x and y.

The dynamics is said to be detailed balanced when $a_\rho = 0$ for all ρ. Thus, in the absence of parametric time dependence of the rates in the long-time limit, when the initial condition $P(n,0)$ is relaxed, $\Sigma(t)$ is identically zero, and the stationary solution of Eq. (3) is the equilibrium Gibbs distribution $P^{\rm eq}(n)$,

$$P^{\rm ss}(n) \underset{a_\rho=0}{=} \frac{e^{-\Phi(n)}}{\sum_n e^{-\Phi(n)}} =: P^{\rm eq}(n). \tag{15}$$

In view of Eqs. (5) and (15), when $a_\rho = 0$, the local detailed balance condition on the transition rates can also be written as the equality of forward and backward fluxes at equilibrium,

$$P^{\rm eq}(n)R_\rho(n) = P^{\rm eq}(n+\Delta_\rho)R_{-\rho}(n+\Delta_\rho). \tag{16}$$

Two other useful decompositions of the entropy production rate [Eq. (8)] can be introduced. First, rearranging Eq. (8), we get

$$\dot{\Sigma}(t) = \dot{\Sigma}_{\rm nc}(t) + \dot{\Sigma}_{\rm d}(t) - d_t[\Phi(n(t),t) + \ln P(n(t),t)], \tag{17}$$

where $\dot{\Sigma}_{\rm nc}(t) \coloneqq \sum_\rho J_\rho(t)a_\rho$ is the dissipation rate due to nonconservative forces, $\dot{\Sigma}_{\rm d}(t) \coloneqq \partial_t\Phi(n,t)|_{n=n(t)}$ is the dissipation rate caused by parametrically driving the reference equilibrium, and $-[\Phi(n,t) + \ln P(n,t)]$ is the stochastic Massieu potential (Rao and Esposito, 2018b). The decomposition [Eq. (17)] is useful to rationalize which mechanism keeps the system out of equilibrium. In particular, we can name three limiting scenarios: in nonequilibrium stationary states only $\dot{\Sigma}_{\rm nc}$ is on average nonzero, in periodic detailed balance dynamics only $\dot{\Sigma}_{\rm d}$ is on average nonzero, and in detailed balance dynamics relaxing from an initial nonequilibrium probability distribution only $d_t(\Phi + \ln P)$ is nonzero. The nonconservative dissipation rate $\dot{\Sigma}_{\rm nc}(t)$ can be cast in terms of the physical currents $\sum_{\rho>0}\mathbb{X}_\rho I_\rho$ between the reservoirs that generate the fundamental forces $\not{f}_{\rm nc}$. Note that, for systems in contact with reservoirs at the same temperature T, the nonconservative and driving contributions to the entropy production correspond to work contributions divided by the temperature T.

Second, for systems with nonautonomous dynamics, or with relaxation from a nonstationary initial condition, it is worth recasting the entropy production rates into the adiabatic and nonadiabatic components (Hatano and Sasa, 2001; Speck and Seifert, 2005; Esposito, Harbola, and Mukamel, 2007; Esposito and Van den Broeck, 2010),

$$\dot{\Sigma}(t) = \dot{\Sigma}_{\rm ad}(t) + \dot{\Sigma}_{\rm na}(t), \tag{18}$$

with the adiabatic entropy production rate

$$\dot{\Sigma}_{\rm ad}(t) \coloneqq \sum_\rho J_\rho(t)\left(\Sigma_\rho(t) + \ln\frac{P_t^{\rm ss}(n(t))}{P_t^{\rm ss}(n(t)+\Delta_\rho)}\right) \tag{19}$$

and the nonadiabatic entropy production rate

$$\dot{\Sigma}_{\rm na}(t) \coloneqq -d_t\ln P(n(t),t) + \sum_\rho J_\rho(t)\ln\frac{P_t^{\rm ss}(n(t)+\Delta_\rho)}{P_t^{\rm ss}(n(t))}. \tag{20}$$

We recall that $P_t^{\rm ss}(n)$ denotes the stationary solution of the master equation (3) with transition rates held fixed at their

instantaneous values $R_\rho(n,\vartheta(t))$. Loosely speaking, the splitting in Eq. (18) is in terms of the dissipation to maintain a stationary state and to drive it. This consideration becomes exact in two limiting cases: for autonomous systems at stationarity in which $P(n,t)=P_t^{\rm ss}(n)$, such that Eq. (20) is identically zero and the adiabatic entropy production rate [Eq. (19)] equals $\dot\Sigma(t)$, and for nonautonomous detailed balance dynamics for which $P_t^{\rm ss}(n)=P_t^{\rm eq}(n)$, such that Eq. (19) is identically zero and the nonadiabatic entropy production rate [Eq. (20)] is equal to $\dot\Sigma(t)$. It can be shown that both $\dot\Sigma_{\rm ad}(t)$ and $\dot\Sigma_{\rm na}(t)$ are on average positive (Esposito, Harbola, and Mukamel, 2007; Esposito and Van den Broeck, 2010; Ge and Qian, 2010; Rao and Esposito, 2018c). Adiabatic and nonadiabatic components are also called housekeeping and excess ones, respectively, even though such names were originally assigned to the decomposition of entropy production of systems in contact with isothermal baths.

There is another measure of the time irreversibility of the dynamics obtained by lumping together in the master equation (3) all the transition rates $R_\rho(n)$ associated with jumps with the same size $\tilde\Delta_\rho$ as $\tilde R_\rho(n):=\sum_{\rho:\Delta_\rho=\tilde\Delta_\rho}R_\rho(n)$.[4] On the resulting trajectories $\mathcal{X}'$ (which are identical to $\mathcal{X}$ when restricted to the state space) one can define the Kullback-Leibler divergence as

$$\langle\tilde\Sigma[\mathcal{X}']\rangle:=\int\mathcal{D}\mathcal{X}'P[\mathcal{X}']\ln\frac{P[\mathcal{X}']}{\tilde P[\mathcal{X}']}\geq 0. \tag{21}$$

Such trajectories carry no detailed information about the elementary transitions; therefore, Eq. (21) is a mere information-theoretic quantity with no general connection to thermodynamics. The rate of Eq. (21) is obtained like Eq. (14),

$$\langle\dot{\tilde\Sigma}(t)\rangle=\sum_{\substack{n,\rho>0\\ \rho:\Delta_\rho=\tilde\Delta_\rho}}[\tilde R_\rho(n)P(n,t)-\tilde R_{-\rho}(n+\Delta_\rho,t)P(n+\Delta_\rho)]\times\ln\frac{\tilde R_\rho(n)P(n,t)}{\tilde R_{-\rho}(n+\Delta_\rho)P(n+\Delta_\rho,t)}\geq 0. \tag{22}$$

When the log sum inequality is applied to Eq. (14), it follows that $\langle\dot{\tilde\Sigma}\rangle\leq\langle\dot\Sigma\rangle$.

We conclude this summary of the core structure of stochastic thermodynamics with three comments on the transition rates. First, they can be rewritten as

$$R_\rho(n)=\Gamma_\rho(n)e^{[-\Phi(n+\Delta_\rho)+\Phi(n)+a_\rho]/2} \tag{23}$$

by identifying a symmetric kinetic factor $\Gamma_\rho(n)=\sqrt{R_\rho(n)R_{-\rho}(n+\Delta_\rho)}=\Gamma_{-\rho}(n+\Delta_\rho)$ not constrained by thermodynamics (Maes, 2018). Second, on can introduce dual (also called adjoint, or reversed) rates,

$$R_\rho^\dagger(n):=\frac{R_{-\rho}(n+\Delta_\rho)P_t^{\rm ss}(n+\Delta_\rho)}{P_t^{\rm ss}(n)}, \tag{24}$$

which generate a stochastic process with the same stationary distribution as the original one, namely, $P_t^{\rm ss}=P_t^{\rm ss\dagger}$, and change the sign of the average stationary currents, $\langle I_\rho^\dagger\rangle=-\langle I_\rho\rangle$ (Norris, 1997). Third, by combining the escape rate $\sum_\rho R_\rho(n)$, which gives the mean time to leave the state n, with the entrance rate $\sum_\rho R_\rho(n-\Delta_\rho)$ in the same state, we introduce the inflow rate

$$\Lambda(n):=\sum_\rho[R_\rho(n-\Delta_\rho)-R_\rho(n)], \tag{25}$$

which measures the rate of contraction of a discrete volume centered on the state n (Baiesi and Falasco, 2015).

III. MACROSCOPIC LIMIT

A. Thermodynamic and kinetic conditions

We identify a large parameter V on which the rates R_ρ depend. This can be a mesoscopic volume, which is large when measured in units of molecular volumes, or a typical particle number per state, which is much larger than unity. We focus on systems such that $n\to\infty$ as $V\to\infty$ and thus define an intensive state variable $c:=n/V$. We fix the asymptotic behavior of the thermodynamic variables to match the extensivity prescribed by standard (macroscopic) thermodynamics,

$$\phi(c):=\lim_{V\to\infty}\frac{\Phi(n)}{V}. \tag{26}$$

Note that a_ρ is already a quantity of the order of $O(V^0)$ because the fundamental nonconservative forces are expressed in terms of intensive thermodynamic variables of the reservoirs that are macroscopic. We also assume that a deterministic macroscopic limit of the dynamics [Eq. (3)] exists, which requires that the transition rates scale asymptotically with V,

$$r_\rho(c):=\lim_{V\to\infty}\frac{R_\rho(n)}{V}=\gamma_\rho(c)e^{[-\Delta_\rho\cdot\partial_c\phi(c)+a_\rho]/2}, \tag{27}$$

which entails for the macroscopic kinetic coefficients

$$\gamma_\rho(c):=\lim_{V\to\infty}\frac{\Gamma_\rho(n)}{V}=\gamma_{-\rho}(c). \tag{28}$$

Thus, the macroscopic expression of the local detailed balance [Eq. (5)] reads

$$\sigma_\rho(c):=\lim_{V\to\infty}\Sigma_\rho(n)=\ln\frac{r_\rho(c)}{r_{-\rho}(c)}=-\Delta_\rho\cdot\partial_c\phi(c)+a_\rho. \tag{29}$$

Note that $\gamma_\rho(c)$ may depend in a symmetric fashion on the forces $-\Delta_\rho\cdot\partial_c\phi(c)$ and a_ρ.

Under these assumptions the master equation for the probability density of the intensive state variable, $p(c,t)=V^N P(n,t)$, reads

$$\partial_t p(c,t)=V\sum_\rho\left[r_\rho\left(c-\frac{\Delta_\rho}{V}\right)p\left(c-\frac{\Delta_\rho}{V},t\right)-r_\rho(c)p(c,t)\right]. \tag{30}$$

[4]This happens when a change in the state space can be realized via multiple pathways. See Sec. VII.A.1 for an example.

The scaling imposed in Eq. (27) leads to a concentration of probability in the macroscopic limit (Gardiner, 2004; van Kampen, 2007). Namely, the probability density $p(c,t)$ acquires the large-deviation form

$$p(c,t) \asymp e^{-VI(c,t)}, \tag{31}$$

where $I \geq 0$, called the rate function, is V-independent. The symbol $\asymp$ stands for the logarithm equality of the two sides of Eq. (31), that is, $-\lim_{V\to\infty}(1/V)\ln p(c,t) = I(c,t)$. The scaling captures the fact that p is singular in the limit $V \to \infty$, wherein the system is described by the deterministic dynamics of the minima of $I(c,t)$, as we show in Sec. III.B.

Plugging Eq. (31) into Eq. (30) and expanding to leading order in V yields the evolution equation for the rate function,

$$-\partial_t I(c,t) = \sum_\rho (e^{\Delta_\rho\cdot\partial_c I(c,t)} - 1) r_\rho(c), \tag{32}$$

which is a Hamilton-Jacobi equation with momenta $\pi = \partial_c I$ and Hamiltonian function (Kubo, Matsuo, and Kitahara, 1973; Gang, 1987)

$$\mathcal{H}(c,\pi) := \sum_\rho (e^{\Delta_\rho\cdot\pi} - 1) r_\rho(c). \tag{33}$$

The stationary rate function $I_{\rm ss}(c)$, also called the quasipotential—where it exists and is differentiable—satisfies the time-independent version of Eq. (32) (Maes and Netočný, 2007),

$$\mathcal{H}(c, \partial_c I_{\rm ss}) = 0, \tag{34}$$

and gives the stationary probability density function

$$p_{\rm ss}(c) \asymp e^{-VI_{\rm ss}(c)}. \tag{35}$$

For detailed balance dynamics, the quasipotential coincides (up to a constant) with the negative Massieu potential ϕ, whose minima is denoted in this review by $x^{\rm eq}$. This can be seen by rewriting Eq. (34) as

$$\sum_\rho (r^{(0)}_{-\rho} - r^{(0)}_\rho e^{\Delta_\rho\cdot\partial_c I_{\rm ss}}) = 0, \tag{36}$$

with detailed balance rates

$$r^{(0)}_\rho := \lim_{a_\rho\to 0} r_\rho = \gamma^{(0)}_\rho e^{-(1/2)\Delta_\rho\cdot\partial_c\phi}, \tag{37}$$

and noting that $I_{\rm ss} = \phi + \text{const}$ nullifies each summand in Eq. (36) by virtue of Eq. (29). Hence, the large-scale stochastic dynamics preserves the equilibrium Gibbs distribution [Eq. (15)] and yields Einstein's fluctuation formula (Einstein, 1910),

$$p_{\rm eq}(c) \asymp e^{-V[\phi(c)-\phi(x^{\rm eq})]}, \tag{38}$$

with the partition function $\sum_n e^{-\Phi(n)} \asymp e^{-V\phi(x^{\rm eq})}$ obtained by the Laplace approximation. Note that the equilibrium state $x^{\rm eq}$ is the one that minimizes the thermodynamic potential ϕ.

For transition rates that carry an explicit time dependence, we introduce the instantaneous stationary rate function $I^t_{\rm ss}(c)$, which satisfies

$$\mathcal{H}_t(c, \partial_c I^t_{\rm ss}) = 0, \tag{39}$$

where $\mathcal{H}_t$ is the Hamiltonian [Eq. (33)] with transition rates $r_\rho(c,\vartheta(t))$ held fixed at their instantaneous value at time t. We end by noting that, using Eq. (24), the scaled dual rate is given by

$$r^\dagger_\rho(c) := \lim_{V\to\infty} \frac{R^\dagger_\rho(n)}{V} = r_{-\rho}(c) e^{-\Delta_\rho\cdot\partial_c I_{\rm ss}(c)} \tag{40}$$

and is associated with the macroscopic log ratio

$$\begin{aligned}\sigma^{\rm ad}_\rho(c) &:= \lim_{V\to\infty} \ln\frac{R_\rho(n)}{R^\dagger_\rho(n)} = \ln\frac{r_\rho(c)}{r^\dagger_\rho(c)} \\ &= \Delta_\rho\cdot\partial_c[I_{\rm ss}(c) - \phi(c)] + a_\rho.\end{aligned} \tag{41}$$

Equation (41) corresponds to the macroscopic limit of the adiabatic entropy production of transition ρ, as can be directly seen from Eq. (19). The importance of these quantities for the macroscopic dynamics and thermodynamics is elucidated in Sec. IV.

B. Deterministic dynamics

The macroscopic dynamical equation for the intensive state variable can be obtained multiplying both sides of Eq. (30) by c and integrating over c with the change of variable $c \mapsto c + \Delta_\rho/V$ on the right-hand side,

$$d_t\langle c\rangle = \sum_\rho \Delta_\rho \langle r_\rho(c)\rangle = \sum_{\rho>0} \Delta_\rho[\langle r_\rho(c)\rangle - \langle r_{-\rho}(c)\rangle]. \tag{42}$$

The mean value of a generic state observable $\mathcal{O}$ at time t is calculated as $\langle \mathcal{O}(c(t))\rangle = \int dc \mathcal{O}(c) p(c,t)$. In view of the large-deviation scaling of the probability [Eq. (31)], the probability density concentrates around its most likely state $x(t)$, which corresponds to the global minimum of $I(c,t)$ (Hao and Hong, 2011; Qian *et al.*, 2016; Huang *et al.*, 2017), namely,

$$x(t) := \operatorname{argmin}_c I(c,t), \tag{43}$$

and therefore

$$I(x(t),t) = \partial_c I(x(t),t) = 0, \qquad \partial_c^2 I(x(t),t) > 0. \tag{44}$$

This implies that, using the Laplace method, $\lim_{V\to\infty}\langle \mathcal{O}(c(t))\rangle = \mathcal{O}(x(t))$ and Eq. (42) approaches the dynamics

$$d_t x(t) = F(x(t)), \tag{45}$$

with the deterministic drift field

$$F(c) \coloneqq \sum_{\rho} \Delta_\rho r_\rho(c) = \partial_\pi \mathcal{H}(c,\pi)|_{\pi=0}, \tag{46}$$

which we recognize as the derivative of the Hamiltonian [Eq. (33)] with respect to the momenta π. We explore the connection with the Hamiltonian dynamics in Sec. IV.A. Notably, the macroscopic limit of the inflow rate [Eq. (25)] is the negative divergence of the drift field [Eq. (46)],

$$\lambda(c) \coloneqq \lim_{V\to\infty} \Lambda(n) = -\partial_c \cdot F(c). \tag{47}$$

The latter is a key quantity in the dynamical systems theory as it represents the phase-space volume contraction rate (Dorfman, 1999; Gaspard, 2005), that is, the negative sum of the Lyapunov exponents (Benettin *et al.*, 1980) of the deterministic dynamics [Eq. (45)]. The phase-space contraction rate plays a key role in the statistical mechanics of deterministic thermostatted systems (Evans and Morriss, 1990) as it enters the steady state [Gallavotti-Cohen (Evans, Cohen, and Morriss, 1993; Gallavotti and Cohen, 1995a, 1995b)] and the transient [Evans-Searles (Evans and Searles, 1994, 2002)] fluctuation theorems and can sometimes be identified with the entropy production rate (Cohen and Rondoni, 1998).

For any autonomous dynamics [Eq. (45)], the quasipotential $I_{\rm ss}$ always decreases along the solution, i.e.,

$$d_t I_{\rm ss}(x(t)) = F(x(t)) \cdot \partial_c I_{\rm ss}(x(t)) \le 0, \tag{48}$$

where the inequality is proved using the explicit form of Eq. (34) along with the fact that $e^x - 1 \ge x$. Since Eq. (43) implies that $I_{\rm ss}$ always reaches a minimum on the long-time solutions of Eq. (45), be they stable fixed points x^* [defined by $F(x^*) = 0$; see Sec. III.C] or time-dependent attractors $x^*(t)$, the quasipotential is a Lyapunov function of the deterministic dynamics [Eq. (45)]. When the dynamics is detailed balanced ($a_\rho = 0$), Eq. (48) reduces to

$$d_t \phi(x(t)) \le 0, \tag{49}$$

and we recover a central tenet of macroscopic thermodynamics, namely, that the thermodynamic potential ϕ is minimized by the dynamics.

We end by introducing the Hamiltonian of the dual process

$$\mathcal{H}^\dagger(c,\pi) \coloneqq \sum_{\rho} (e^{\Delta_\rho \cdot \pi} - 1) r_\rho^\dagger(c) \tag{50}$$

and its deterministic drift field

$$F^\dagger(c) \coloneqq \sum_{\rho} \Delta_\rho r_\rho^\dagger(c) = \partial_\pi \mathcal{H}^\dagger(c,\pi)|_{\pi=0}. \tag{51}$$

The dual dynamics shares not only the same fixed point as the original one, $F^\dagger(x^*) = F(x^*) = 0$, but also the same steady state rate function,

$$\mathcal{H}^\dagger(c, \partial_c I_{\rm ss}) = -\mathcal{H}(c, \partial_c I_{\rm ss}) = 0. \tag{52}$$

The dual macroscopic trajectory $x^\dagger(t)$ solution of

$$d_t x^\dagger(t) = F^\dagger(x^\dagger(t)) \tag{53}$$

with the initial condition $x^\dagger(0) = x^*$ plays a central role in the description of macroscopic fluctuations; see Sec. IV.

C. Multistability vs metastability

A fixed point is stable and is denoted as x^* if all eigenvalues of the Jacobian matrix $\partial_c F(c)$ evaluated in $c = x^*$ have negative real parts. It is unstable when at least one eigenvalue has a positive real part. When F is nonlinear, multiple stable fixed points x_γ^* can be present; they are indicated with the label $\gamma \in \mathbb{N}$. More complex, time-dependent attractors such as limit cycles are merely mentioned later. We assume that the stable fixed points x_γ^* are separated by nondegenerate saddle points, denoted as x_ν, i.e., fixed points with real, nonzero eigenvalues, at least one of which is positive. They define the boundaries between the different basins of attraction of F. In this case the dynamics [Eq. (45)] is nonergodic and multistable since $x(t)$, due to Eq. (48), will relax within the basin of attraction selected by the initial condition $x(0)$ to its fixed point. This has to be contrasted with the uniqueness of the stationary solution of the underlying mesoscopic master equation (3). The discrepancy, known as Keizer's paradox (Keizer, 1978), stems from the fact that the long-time limit and the macroscopic limit do not commute in general. This phenomenon is understood within the spectral theory of the Markovian generator, which is summarized as follows (Gaveau and Schulman, 1998; Kurchan, 2009). The time evolution of the probability distribution can be expanded in the right eigenfunctions $\psi_\xi^{(R)}(n)$ of the matrix $\mathcal{R}$ in Eq. (3),

$$P(n,t) = \sum_{\xi} b_\xi \psi_\xi^{(R)}(n) e^{\omega_\xi t}, \tag{54}$$

where $b_\xi = \sum_n \psi_\xi^{(L)}(n) P(n,0)$ are the overlap of the initial condition with the left eigenfunctions $\psi_\xi^{(L)}(n)$. Since $\mathcal{R}$ is a stochastic generator on a finite state space, by the Perron-Frobenius theorem it has nonpositive eigenvalues [which can be ordered by their real part $\mathrm{Re}(\omega_\xi) \ge \mathrm{Re}(\omega_{\xi+1})$], of which $\omega_0 = 0$ is nondegenerate and associated with a constant left eigenfunction. Metastability appears when there exist eigenvalues $\omega_1, \ldots, \omega_{\tilde\xi}$ whose real part goes to $0 = \omega_0$ as $V \to \infty$, while all other ω_ξ with $\xi > \tilde\xi$ stay finite. The inverse of this spectral gap corresponds to a diverging timescale separating the fast dynamics within basins of attractions from the slow dynamics between them. Ultimately, if $V \to \infty$ at finite t, the system probability can converge only to linear combinations of those $\psi_\xi^{(R)}(n)$ with $\xi \le \tilde\xi$ that are selected by the initial conditions, i.e., those with a finite overlap $b_\xi \neq 0$.

In general, $\mathcal{R}$ is not similar to a symmetric matrix unless detailed balance holds; hence, the eigenvalue ω_ξ can have a nonzero imaginary part. In this case metastable states can be time dependent, as with stable limit cycles at $V \to \infty$

(Herpich, Thingna, and Esposito, 2018). A limit cycle is a closed trajectory in state space not surrounded by other closed trajectories. It is called stable or attracting if all neighboring trajectories approach it for large times. It appears as a periodic solution of Eq. (45), $x^*(t) = x^*(t + t_p)$, with a period $t_p = 2\pi/\mathrm{Im}(\omega_\xi)$, where $\xi \leq \tilde{\xi}$. Hereafter, we merely mention such periodic attractors and do not explicitly consider more general quasiperiodic and chaotic attractors; see the application in Sec. VII.C and the discussion in Sec. VIII, though.

For multistable systems a further comment is in order. For general nondetailed balance dynamics, the rate function I_{ss} is locally nondifferentiable and Eq. (34) can be solved only piecewise in each basin of attraction (Graham and Tél, 1986; Baek and Kafri, 2015) while obtaining the local quasipotential $I_{ss}^{(\gamma)}$. This stems from the fact that only the local stochastic dynamics can be directly determined when the macroscopic limit is taken before the long-time limit (Ge and Qian, 2012; Zhou and Li, 2016). The global quasipotential defined by first taking the long-time limit before the large V limit is obtained *a posteriori* by fixing the normalization constants, i.e., the relative weights α_γ of the attractors, and choosing at each c the minimum among the local quasipotentials (Bouchet, Gawredzki, and Nardini, 2016),

$$I_{ss}(c) = \min_\gamma [I_{ss}^{(\gamma)}(c) + \alpha_\gamma] - \min_\gamma \alpha_\gamma. \tag{55}$$

The last term in Eq. (55) ensures that I_{ss} is zero on the most likely attractor. The Markov jump process on attractors that is used to fix the normalization constants (Graham, 1987; Freidlin and Wentzell, 1998) is discussed in Sec. VI as a coarse-grained description for the long-time macroscopic fluctuating thermodynamics of the systems. If the limit $V \to \infty$ is taken before the limit $t \to \infty$, the relative weights are fixed by the initial condition (the relative probability to be on an attractor).

D. Deterministic thermodynamics

The first crucial observation regards the macroscopic Shannon entropy

$$S_{Sh}(t) = -\int dc\, p(c,t) \ln p(c,t), \tag{56}$$

where an irrelevant additive constant has been discarded. Its scaled macroscopic limit is identically null since the randomness associated with the distribution over states c has vanished [see Eq. (44)],

$$-\lim_{V\to\infty} \frac{1}{V} S_{Sh}(t) = I(x(t), t) = 0. \tag{57}$$

However, the mean of the scaled system entropy [Eq. (10)] is generally finite and entirely given by the internal entropy evaluated for the most likely state,

$$\lim_{V\to\infty} \frac{1}{V} \langle S_{syst}(n,t)\rangle = s_{int}(x(t)). \tag{58}$$

In Eq. (58) we have required the internal entropy s_{int} to be an extensive function of V.

The mean variation rate of thermodynamic observables depends on the average flux of transitions, which at leading order in V reads

$$\langle J_\rho(t)\rangle = V \int dc\, r_\rho(c) p(c,t). \tag{59}$$

The concentration of the probability [Eq. (31)] yields for the scaled macroscopic limit of the transition flux

$$\lim_{V\to\infty} \frac{1}{V} \langle J_\rho(t)\rangle = r_\rho(x(t)). \tag{60}$$

Hence, the function $[r_\rho(x(t)) - r_{-\rho}(x(t))]\mathscr{o}_\rho$ represents the mean rate of variation of an intensive quantity $\mathscr{o}_\rho = -\mathscr{o}_{-\rho}$ due to transition ρ. In particular, the mean of the scaled entropy production rate $\dot{\sigma} := \dot{\Sigma}/V$ reads in the macroscopic limit

$$\lim_{V\to\infty} \langle \dot{\sigma}\rangle = \sum_{\rho>0} [r_\rho(x(t)) - r_{-\rho}(x(t))]\sigma_\rho(x(t)) \geq 0, \tag{61}$$

where we have incorporated Eqs. (29) and (57) into Eq. (14); note the absence of the Shannon entropy with respect to Eq. (14). In the macroscopic limit all average quantities at time t are functions of $x(t)$. However, for brevity we avoid explicitly writing this dependence.

Taking the mean value of the decomposition [Eq. (17)] and using the concentration of the probability [Eqs. (31) and (60)], we obtain

$$\lim_{V\to\infty} \langle \dot{\sigma}\rangle = \lim_{V\to\infty} \langle \dot{\sigma}_{nc}\rangle + \lim_{V\to\infty} \langle \dot{\sigma}_d\rangle - d_t \phi(x(t), t), \tag{62}$$

which displays the scaled mean of the nonconservative dissipation rate

$$\lim_{V\to\infty} \langle \dot{\sigma}_{nc}\rangle = \sum_\rho r_\rho(x(t)) a_\rho, \tag{63}$$

the scaled mean of the driving dissipation rate

$$\lim_{V\to\infty} \langle \dot{\sigma}_d\rangle = \partial_t \phi(c,t)|_{c=x(t)}, \tag{64}$$

and the time derivative of the mean scaled thermodynamic potential. Proceeding in the same manner with Eq. (18), we can find the alternative decomposition

$$\lim_{V\to\infty} \langle \dot{\sigma}\rangle = \lim_{V\to\infty} \langle \dot{\sigma}_{ad}\rangle + \lim_{V\to\infty} \langle \dot{\sigma}_{na}\rangle \tag{65}$$

in terms of the mean scaled adiabatic entropy production rate

$$\lim_{V\to\infty} \langle \dot{\sigma}_{ad}\rangle = \sum_{\rho>0} [r_\rho(x(t)) - r_{-\rho}(x(t))]\sigma_\rho^{ad}(x(t)) \geq 0, \tag{66}$$

with Eq. (41), and the mean scaled nonadiabatic entropy production rate

$$\lim_{V\to\infty}\langle\dot\sigma_{\rm na}\rangle = -F(x(t))\cdot\partial_c I^t_{\rm ss}(x(t)) = \partial_t I^t_{\rm ss}(c)|_{c=x(t)} - d_t I^t_{\rm ss}(x(t)) \geq 0, \quad (67)$$

where we used Eqs. (29) and (46). We recall that the rate function $I^t_{\rm ss}(c)$ is the solution of Eq. (39) with the transition rates held fixed at their instantaneous value. Since Eqs. (19) and (20) are non-negative on average, $\langle\dot\sigma_{\rm ad}\rangle$ and $\langle\dot\sigma_{\rm na}\rangle$ are non-negative as well. As a consequence, for autonomous systems ($I^t_{\rm ss} = I_{\rm ss}$) the positivity of the nonadiabatic entropy production [Eq. (67)] provides an alternative proof that the quasipotential decreases along the solution of Eq. (45), as shown in Eq. (48).

Finally, thanks to Eqs. (27) and (31), the mean value of the scaled information-theoretic entropy production rate $\dot{\tilde\sigma} := \dot{\tilde\Sigma}/V$ [cf. Eq. (22)] reads

$$\lim_{V\to\infty}\langle\dot{\tilde\sigma}(t)\rangle = \sum_{\substack{\rho>0\\ \rho:\ \Delta_\rho=\tilde\Delta_\rho}} [\tilde r_\rho(x(t)) - \tilde r_{-\rho}(x(t))]\ln\frac{\tilde r_\rho(x(t))}{\tilde r_{-\rho}(x(t))} \geq 0, \quad (68)$$

with $\tilde r_\rho(c) := \lim_{V\to\infty}\tilde R_\rho(n)/V$. Again using the log sum inequality, we find that $\langle\dot{\tilde\sigma}\rangle \leq \langle\dot\sigma\rangle$.

E. Drift field decomposition

For simplicity, we focus on autonomous dynamics in this subsection. A useful decomposition of the macroscopic vector field $F(c)$ can be obtained by retaining the entire Kramers-Moyal expansion of the master equation (Gardiner, 2004). Namely, the Taylor expansion of the right-hand side of Eq. (30) yields a continuity equation with the probability current $\mathfrak{j}(c,t)$,

$$\partial_t p(c,t) = -\partial_c\cdot\mathfrak{j}(c,t),$$
$$\mathfrak{j}(c,t) := \sum_\rho\sum_{k=1}^\infty \frac{\Delta_\rho}{V^{k-1}k!}(-\Delta_\rho\cdot\partial_c)^{k-1}[r_\rho(c)p(c,t)]. \quad (69)$$

Plugging the large-deviation ansatz [Eq. (31)] into Eq. (69) and restricting to the stationary state, we identify the macroscopic limit of the probability velocity in configuration space (Wu and Wang, 2013),

$$v_{\rm ss}(c) := \lim_{V\to\infty}\lim_{t\to\infty}\frac{\mathfrak{j}(c,t)}{p(c,t)} = \sum_\rho \Delta_\rho r_\rho(c)\frac{e^{\Delta_\rho\cdot\partial_c I_{\rm ss}}-1}{\Delta_\rho\cdot\partial_c I_{\rm ss}}. \quad (70)$$

As a consequence, the deterministic drift vector field

$$F(c) = v_{\rm ss}(c) - \mathcal{F}(c) \quad (71)$$

splits into the asymptotic probability velocity [Eq. (70)] and a gradientlike vector field

$$\mathcal{F}(c) := \sum_\rho \Delta_\rho r_\rho(c)\frac{e^{\Delta_\rho\cdot\partial_c I_{\rm ss}} - \Delta_\rho\cdot\partial_c I_{\rm ss} - 1}{\Delta_\rho\cdot\partial_c I_{\rm ss}} = \mathcal{M}(c)\cdot\partial_c I_{\rm ss}, \quad (72)$$

with the symmetric positive semidefinite "mobility" matrix

$$\mathcal{M}(c) = \sum_\rho \Delta_\rho\Delta_\rho r_\rho(c)\frac{e^{\Delta_\rho\cdot\partial_c I_{\rm ss}} - \Delta_\rho\cdot\partial_c I_{\rm ss} - 1}{(\Delta_\rho\cdot\partial_c I_{\rm ss})^2}, \quad (73)$$

which itself depends on the rate function. Equations (70) and (73), respectively, can be rewritten in terms of the Hamiltonian [Eq. (33)] as

$$v_{\rm ss}(c) = \int_0^1 d\theta\,\partial_\pi\mathcal{H}(c,\pi)|_{\pi=\theta\partial_c I_{\rm ss}}, \quad (74)$$

$$\mathcal{M}(c) := \int_0^1 d\theta(1-\theta)\partial_\pi^2\mathcal{H}(c,\pi)|_{\pi=\theta\partial_c I_{\rm ss}}. \quad (75)$$

Equations (74) and (75) were given by Gao and Liu (2022) for polynomial transition rates but hold irrespective of the specific form of r_ρ.

Equation (71) is an extension of the well-known "orthogonal" decomposition valid for deterministic dynamical systems supplemented by weak Gaussian noise that lead to diffusion processes (Bertini *et al.*, 2015; Zhou and Li, 2016). This decomposition is generalized here to Markov jump processes, where the noise is Poissonian. It expresses the nonlinear downhill motion of $x(t)$ in the gradient of the Lyapunov function $I_{\rm ss}$ superimposed to the circulation on its level sets with the velocity $v_{\rm ss}(x(t))$. The major difference is that the mobility matrix $\mathcal{M}$ of the diffusive dynamics is independent of the gradient of the rate function.

To prove these properties, we first focus on the probability velocity $v_{\rm ss}(c)$. It is orthogonal to the gradient of the quasipotential $I_{\rm ss}$ since

$$v_{\rm ss}\cdot\partial_c I_{\rm ss} = \mathcal{H}(c,\partial_c I_{\rm ss}) = 0, \quad (76)$$

thanks to the definition [Eq. (70)] and the stationary state condition [Eq. (34)].[5] Additionally, the probability velocity is divergence-free on the fixed points

$$\partial_c\cdot v_{\rm ss}(x^*) = 0. \quad (77)$$

This follows from writing $v_{\rm ss} = \mathcal{N}(c)\cdot\partial_c I_{\rm ss}$, with $\mathcal{N}(c)$ an antisymmetric matrix that enforces Eq. (76), and using Eq. (44). Note that in general $\partial_c\cdot v_{\rm ss} \neq 0$ for $c \neq x^*$, as one can show by expanding the master equation (30) beyond the leading order approximation [Eq. (32)].

Now we turn to the gradient part of the dynamics. We showed in Eq. (48) that the quasipotential $I_{\rm ss}(c)$ is the Lyapunov function of Eq. (45); i.e., it decreases along solutions of Eq. (45) and reaches a local minimum at a stable

[5]Stationarity of the microscopic stochastic dynamics should not be taken for stationarity of the macroscopic rate equation (45). For example, a time-dependent attractor $x^*(t)$, such as a stable limit cycle, corresponds to a stationary probability density $p_{\rm ss}(c)$ with a rate function $I_{\rm ss}$ that is zero on the set $\{x^*(t)\}_{t=0}^{t_{\rm p}}$.

fixed point x^*_γ [or stable time-dependent attractor $x^*(t)$]. In fact, only the gradient part of the drift vector field $\mathcal{F}(c)$ contributes in Eq. (48) due to Eq. (76), i.e.,

$$d_t I_{\rm ss}(x(t)) = -\mathcal{F}(x(t)) \cdot \partial_c I_{\rm ss}|_{c=x(t)} \leq 0. \tag{78}$$

For detailed balance dynamics, the velocity $v_{\rm ss}$ is identically zero because $\lim_{t\to\infty} \mathrm{j} = 0$. This can also be proved starting from the explicit expression in Eq. (70). Using $I_{\rm ss} = \phi$, which is valid for $a_\rho = 0$, and Eq. (37) for detailed balance transition rates, we obtain

$$\begin{aligned} v_{\rm ss} &\underset{a_\rho=0}{=} \sum_\rho \Delta_\rho \gamma^{(0)}_\rho e^{-\Delta_\rho\cdot\partial_c\phi/2} \frac{e^{\Delta_\rho\cdot\partial_c\phi}-1}{\Delta_\rho\cdot\partial_c\phi} \\ &= 2\sum_\rho \Delta_\rho \gamma^{(0)}_\rho \frac{\sinh(\Delta_\rho\cdot\partial_c\phi/2)}{\Delta_\rho\cdot\partial_c\phi} = 0, \end{aligned}$$

where in the last passage we split the sum over forward and backward transitions $\pm\rho$ and use the antisymmetry of Δ_ρ and sinh. In this case the deterministic dynamics is a nonlinear gradient descent in the thermodynamic potential ϕ,

$$F(c) \underset{a_\rho=0}{=} -\mathcal{F}(c) \underset{a_\rho=0}{=} -D^{(0)}(c)\cdot\partial_c\phi(c) + O((\partial_c\phi)^2), \tag{79}$$

where we introduced

$$D^{(0)}(c) \coloneqq \lim_{a_\rho\to 0} D(c) = \tfrac{1}{2}\sum_\rho \Delta_\rho\Delta_\rho r^{(0)}_\rho(c), \tag{80}$$

the detailed balance limit of the positive-definite symmetric diffusion matrix, which generally reads

$$D(c) \coloneqq \tfrac{1}{2}\sum_\rho \Delta_\rho\Delta_\rho r_\rho(c) = \tfrac{1}{2}\partial^2_\pi \mathcal{H}(c,\pi)|_{\pi=0}. \tag{81}$$

Equation (79) indicates that detailed balance dynamics admit only time-independent attractors; i.e., limit cycles and chaos are ruled out in equilibrium. As indicated in the second equality of Eq. (79), neglecting higher order derivatives to get a linear gradient descent dynamics is possible only close to fixed points—or in a continuous limit where Δ_ρ becomes infinitesimal, as shown in Sec. V.A. We show in Sec. IV.B that, for small but not vanishing a_ρ, the quasipotential is still given by thermodynamic quantities.

The splitting [Eq. (71)] with the condition in Eq. (76) complies with the pre–general equation for the nonequilibrium reversible-irreversible coupling (pre-GENERIC) dynamics introduced by Kraaij *et al.* (2018), an extension of GENERIC (Öttinger, 2005). $\mathcal{F}$ entails a nonlinear gradient flow (Liero and Mielke, 2013; Mielke, Renger, and Peletier, 2016) since it can be recast as the product of the jump matrix with a gradient field in the space of transitions,

$$\mathcal{F}(c) = \sum_\rho \Delta_\rho \partial_{z_\rho}\psi(z)|_{z_\rho=\Delta_\rho\cdot\partial_c I_{\rm ss}}, \tag{82}$$

where the potential ψ is defined for all $z_\rho \neq 0$ as

$$\psi(z) \coloneqq \sum_\rho r_\rho[\mathrm{Ei}(z_\rho) - \ln(|z_\rho|) - z_\rho], \tag{83}$$

with Ei the exponential integral. One can verify that $\psi(z)$ is convex and non-negative with a minimum at $z \to 0$, but it is not symmetric in z_ρ. These properties imply that

$$\sum_\rho z_\rho \partial_{z_\rho}\psi \geq \psi(z) - \psi(0) \geq \min_z \psi(z) - \psi(0) = 0, \tag{84}$$

which corresponds to Eq. (78), with $z_\rho = \Delta_\rho\cdot\partial_c I_{\rm ss}$.

We note that the drift field on any attractor reduces to the probability velocity

$$F(x^*(t)) = v_{\rm ss}(x^*(t)), \qquad \mathcal{F}(x^*(t)) = 0, \tag{85}$$

since $\partial_c I_{\rm ss}(x^*(t)) = 0$ in Eq. (72). In the special case of time-independent attractors (i.e., fixed points), Eq. (85) becomes

$$F(x^*_\gamma) = v_{\rm ss}(x^*_\gamma) = \mathcal{F}(x^*_\gamma) = 0. \tag{86}$$

In other words, the probability velocity nullifies on the fixed points.

Finally, we consider the drift field decomposition of the dual process, $F^\dagger(c) = v^\dagger_{\rm ss}(c) - \mathcal{F}^\dagger(c)$. We find that the dual dynamics reverts the velocity $v^\dagger_{\rm ss}(c) = -v_{\rm ss}(c)$, the velocity remains orthogonal to the gradient of the quasipotential $v^\dagger_{\rm ss}\cdot\partial_c I_{\rm ss} = 0$, and the quasipotential remains a Lyapunov function of the dual dynamics $d_t I_{\rm ss}(x^\dagger(t)) = -\mathcal{F}^\dagger(x^\dagger(t))\cdot\partial_c I_{\rm ss}|_{c=x^\dagger(t)} \leq 0$.

F. Linearized dynamics and thermodynamics

The deterministic dynamics [Eq. (45)] linearized around a fixed point reads

$$d_t x(t) = (x(t) - x^*)\cdot\partial_c F(x^*), \tag{87}$$

where the matrix defining the relaxation coefficients is the Jacobian matrix of the dynamics. In turn, the nonadiabatic entropy production [Eq. (67)] around the fixed point reads

$$\lim_{V\to\infty}\langle\dot\sigma_{\rm na}\rangle = (x(t)-x^*)\cdot\mathcal{S}(x^*)\cdot(x(t)-x^*), \tag{88}$$

where we introduced the matrix

$$\mathcal{S}(c) \coloneqq -\partial_c F(c)\cdot\partial^2_c I_{\rm ss}, \tag{89}$$

which is symmetric and positive semidefinite when evaluated at a stable fixed point,

$$\mathcal{S}(x^*) = \partial^2_c I_{\rm ss}(x^*)\cdot D(x^*)\cdot\partial^2_c I_{\rm ss}(x^*). \tag{90}$$

We used Eqs. (71)–(73) with Eqs. (77) and (81).

We now turn to a thermodynamically motivated linearization. Using Eqs. (27) and (29), we can recast the drift field [Eq. (46)] as

$$F(c) = 2\sum_{\rho>0}\Delta_\rho\gamma_\rho(c)\sinh[\tfrac{1}{2}(-\Delta_\rho\cdot\partial_c\phi(c) + a_\rho)], \tag{91}$$

which shows that F is not a linear function of the thermodynamic forces unless some limiting cases are considered. First, F is a linear function when Δ_ρ and a_ρ become small in an appropriate sense, as in the continuous-space limit treated in Sec. V.A. Second, it is a linear function when the nonconservative force a_ρ is small and only small displacements $x(t) - x^{\mathrm{eq}}$ from the equilibrium state x^{eq} are considered.[6] In the latter case Eq. (91) can be linearized in $x - x^{\mathrm{eq}}$ and a_ρ to give

$$d_t x(t) = \big(x(t) - x^{\mathrm{eq}}\big) \cdot \partial_c F^{(0)}(x^{\mathrm{eq}}) + M^{(0)} \cdot \mathscr{f}_{\mathrm{nc}}, \tag{92}$$

where, as can be verified via Eqs. (46), (37), and (80),

$$\begin{aligned}\partial_c F^{(0)}(x^{\mathrm{eq}}) &\coloneqq \lim_{a_\rho \to 0} \partial_c F(x^{\mathrm{eq}}) \\ &= -D^{(0)}(x^{\mathrm{eq}}) \cdot \partial_c \partial_c \phi(x^{\mathrm{eq}}),\end{aligned} \tag{93}$$

and the matrix coupling the state dynamics to the fundamental nonconservative forces $\mathscr{f}_{\mathrm{nc}}$ reads

$$M^{(0)} \coloneqq \sum_{\rho>0} \gamma_\rho^{(0)}(x^{\mathrm{eq}}) \Delta_\rho \mathbb{X}_\rho. \tag{94}$$

The fact that the symmetric positive-definite matrix $D^{(0)}(x^{\mathrm{eq}})$ appears in Eq. (92) is a statement of the Onsager reciprocal relations (Onsager, 1931; Forastiere, Rao, and Esposito, 2022).

For $a_\rho \neq 0$ the fixed point x^* of the perturbed near-equilibrium dynamics differs from the equilibrium fixed point x^{eq} and is given by

$$-(x^* - x^{\mathrm{eq}}) \cdot \partial_c F^{(0)}(x^{\mathrm{eq}}) = M^{(0)} \cdot \mathscr{f}_{\mathrm{nc}}, \tag{95}$$

which we can use to write Eq. (92) as

$$d_t x(t) = \big(x(t) - x^*\big) \cdot \partial_c F^{(0)}(x^{\mathrm{eq}}). \tag{96}$$

Equation (96) shows that Eq. (93) is a fluctuation-dissipation relation since $\partial_c \partial_c \phi(x^{\mathrm{eq}})$ is related to the scaled correlations of the state variable (see Sec. IV) and $\partial_c F^{(0)}(x^{\mathrm{eq}})$ characterizes the rate of relaxation to equilibrium in an autonomous detailed balance system ($a_\rho = 0$), as one can see using Eq. (96) with $x^* = x^{\mathrm{eq}}$. For detailed balance systems we retrieve the setting of linear irreversible thermodynamics in which the only force is the linearized gradient of the Massieu potential (Prigogine, 1961; de Groot and Mazur, 1984).

Turning now to the dynamics of the scaled nonadiabatic entropy production using Eq. (88) to lowest order in a_ρ and Eq. (93), we find that

$$\lim_{V\to\infty} \langle \dot{\sigma}_{\mathrm{na}} \rangle = (x - x^*) \cdot \mathcal{S}^{(0)}(x^{\mathrm{eq}}) \cdot (x - x^*) \geq 0, \tag{97}$$

with the $a_\rho \to 0$ limit of the matrix [Eq. (89)]

$$\mathcal{S}^{(0)}(c) = \partial_c \partial_c \phi(c) \cdot D^{(0)}(c) \cdot \partial_c \partial_c \phi(c). \tag{98}$$

[6]We restrict to autonomous dynamics for simplicity.

The scaled entropy production rate corresponding to Eq. (92) follows by expanding Eq. (61) at second order in $x - x^{\mathrm{eq}}$ and a_ρ,

$$\lim_{V\to\infty} \langle \dot{\sigma} \rangle = \sum_{\rho>0} \gamma_\rho^{(0)}(x^{\mathrm{eq}}) y_\rho(x - x^{\mathrm{eq}}) y_\rho(x - x^{\mathrm{eq}}), \tag{99}$$

with the forces (nonconservative and conservative) acting along ρ,

$$y_\rho(c) \coloneqq a_\rho - \Delta_\rho \cdot \partial_c \partial_c \phi(x^{\mathrm{eq}}) \cdot c. \tag{100}$$

Rewriting $x - x^{\mathrm{eq}} = (x^* - x^{\mathrm{eq}}) + (x - x^*)$ and using the stationary condition [Eq. (95)] to eliminate the mixed terms, we simplify Eq. (99) to

$$\begin{aligned}\lim_{V\to\infty} \langle \dot{\sigma} \rangle &= (x - x^*) \cdot \mathcal{S}^{(0)}(x^{\mathrm{eq}}) \cdot (x - x^*) \\ &\quad + \sum_{\rho>0} \gamma^{(0)}(x^{\mathrm{eq}}) y_\rho(x^* - x^{\mathrm{eq}}) y_\rho(x^* - x^{\mathrm{eq}}).\end{aligned} \tag{101}$$

In view of Eq. (97), this is simply the nonadiabatic-adiabatic decomposition of the scaled entropy production [Eq. (18)] close to equilibrium. The first (nonadiabatic) contribution on the right-hand side of Eq. (101) describes the non-negative entropy produced as the system relaxes to the nonequilibrium steady state x^*. The second (adiabatic) one describes the non-negative entropy production to sustain that steady state. Hence, the structure of steady state thermodynamics proposed by Oono-Paniconi is recovered here (Oono and Paniconi, 1998). Furthermore, we retrieve the minimum entropy production principle since Eq. (101) states that the fixed point x^* minimizes the entropy production rate among all states solutions of Eq. (92) (Prigogine, 1961; Jiu-li, Van den Broeck, and Nicolis, 1984). In general, this result holds true only for states x^* close to detailed balance and linear dynamics. Nevertheless, we present in Sec. VII.C a class of model systems in which the minimum entropy production principle is valid far from equilibrium. Additionally, computing the time derivative of Eq. (101) with the aid of Eq. (96),

$$\begin{aligned}d_t \lim_{V\to\infty} \langle \dot{\sigma} \rangle &= 2 d_t x \cdot \mathcal{S}^{(0)}(x^{\mathrm{eq}}) \cdot (x - x^*) \\ &= -2 z \cdot \partial_c \partial_c \phi(x^{\mathrm{eq}}) \cdot z^T \leq 0,\end{aligned} \tag{102}$$

with $z = (x - x^*) \cdot \partial_c F^{(0)}(x^{\mathrm{eq}})$, we conclude that the entropy production rate monotonically decreases along solutions of Eq. (96) (Maes and Netočný, 2015).

IV. MACROSCOPIC FLUCTUATIONS

In this section we describe the asymptotic stochastic dynamics and the associated thermodynamics.

A. Dynamics of the state variable

The macroscopic master equation (30) can be recast as

$$\partial_t p(c,t) = V \mathcal{H}(c, -V^{-1}\partial_c) p(c,t) \tag{103}$$

by introducing the scaled generator of the stochastic dynamics

$$\mathcal{H}(c,-V^{-1}\partial_c)=\sum_\rho[e^{-V^{-1}\Delta_\rho\cdot\partial_c}-1]r_\rho(c), \tag{104}$$

which contains the operator $e^{-V^{-1}\Delta_\rho\cdot\partial_c}$ that shifts by $-V^{-1}\Delta_\rho$ the argument of the function that it is applied to. Its identification allows us to switch to an equivalent representation of the stochastic dynamics consisting of the probability density of stochastic trajectories conditioned on the initial value $c(0)$, namely, the ordered set of states $c(t)$ in some time interval $[0,\tau]\ni t$ (Doi, 1976; De Dominicis and Peliti, 1978; Grassberger and Manfred, 1980; Peliti, 1985; Weber and Frey, 2017),

$$\begin{aligned}P[\{c(t)\}|c(0)]&=\int\mathcal{D}\pi\, e^{V\int_0^\tau dt[-\pi(t)\cdot d_t c(t)+\mathcal{H}(c(t),\pi(t))]}\\&=\int\mathcal{D}\pi\, e^{V\mathcal{A}[\{c(t)\},\{\pi(t)\}]}.\end{aligned} \tag{105}$$

In Eq. (105) π is an auxiliary variable to integrate out in order to pass from the Poissonian generating function of the transitions $e^{V\int_0^\tau dt\mathcal{H}(c,\pi)}$ to the probability distribution of the trajectories (Gaveau, Moreau, and Toth, 1999; Lefevre and Biroli, 2007). Equation (105) can be formally obtained by applying a time slicing to the solution of Eq. (103)—that is, $p(c,t)=e^{V\int_0^\tau dt\mathcal{H}(c,-V^{-1}\partial_c)}p(c,0)$, with a time-ordered exponential—analogously to the derivation of the quantum path integral representation of the Schrödinger equation.[7] Because of the appearance of V in the exponential, the functional integral in Eq. (105) is dominated for large V by the trajectories that maximize the action functional (Dykman *et al.*, 1994; Smith, 2011; Lazarescu *et al.*, 2019),

$$\mathcal{A}=\int_0^\tau dt[-\pi(t)\cdot d_t c(t)+\sum_\rho r_\rho(c(t))(e^{\Delta_\rho\cdot\pi(t)}-1)], \tag{106}$$

supplemented by the appropriate boundary conditions (Lazarescu *et al.*, 2019). Namely, the solutions of the Hamiltonian equations

$$\begin{aligned}d_t c&=\partial_\pi\mathcal{H}(c,\pi)=\sum_\rho\Delta_\rho r_\rho(c)e^{\Delta_\rho\cdot\pi},\\d_t\pi&=-\partial_c\mathcal{H}(c,\pi)=-\sum_\rho\partial_c r_\rho(c)(e^{\Delta_\rho\cdot\pi}-1)\end{aligned} \tag{107}$$

are the most likely paths. When inserted into Eq. (106), they give their exponentially small probability

$$P[\{c(t)\}|c(0)]p(c(0),0)\asymp e^{V(\mathcal{A}[\{c(t),\pi(t)\}]-I(c(0),0))}. \tag{108}$$

While small fluctuations can be described by Langevin dynamics (whose range of validity is discussed in Sec. IV.C), large deviations from the average dynamics [Eq. (45)] are correctly described only by Eq. (107). In particular, an important class of solutions is that of fluctuating trajectories, called instantons (Coleman, 1988), that connect in a long (formally infinite) time the attractor x^* to an arbitrary state c in the same basin. These trajectories, starting at a stable fixed point[8] $c(0)=x^*_\gamma$, are characterized by $\pi(0)=0$ and thus $\mathcal{H}(c(t),\pi(t))=0$ for all t since $\mathcal{H}$ is a constant of motion in the absence of explicit time dependence of the transition rates r_ρ. It follows from Eq. (52) that $\pi=\partial_c I_{\rm ss}$ on the manifold $\mathcal{H}=0$. Hence, instantons are solutions of

$$d_t c(t)=\sum_\rho\Delta_\rho r_\rho(c(t))e^{\Delta_\rho\cdot\partial_c I_{\rm ss}(c(t))}=-F^\dagger(c(t)). \tag{109}$$

Namely, they are the time reversal of the dual-dynamics trajectories $x^\dagger(t)$ introduced in Eq. (53).

As a consequence, the long-time transition probability from x^*_γ to c [that is, the local stationary probability in the basin of attraction γ, $p^{(\gamma)}_{\rm ss}(c)$] is related at the leading order to the difference of the local quasipotential (Bouchet and Reygner, 2016),

$$\begin{aligned}\lim_{t\to\infty}P(c(t)=c|c(0)=x^*)=p^{(\gamma)}_{\rm ss}(c)&\asymp e^{-V\int_{c(0)=x^*}^{c(\infty)=c}dt\pi(t)\cdot d_t c(t)}\\&=e^{-V[I^{(\gamma)}_{\rm ss}(c)-I^{(\gamma)}_{\rm ss}(x^*_\gamma)]}.\end{aligned} \tag{110}$$

We note that the integral in Eq. (110) can be multivalued. This means that a given state c can correspond to different values of π on the instanton. This Hamiltonian trajectory generates folds, called caustics, when projected onto the state space (Graham and Tél, 1985; Maier and Stein, 1993; Luchinsky, McClintock, and Dykman, 1998; Bouchet, Gawredzki, and Nardini, 2016). In this case $I^\gamma_{\rm ss}(c)$ is obtained by taking the minimum value over π of the integral in Eq. (110).[9] Since this minimizer can jump from one branch of the instanton to another when we move away from c in different directions of the state space, the local quasipotential is generally not differentiable at such points (unless the dynamics is detailed balance), a phenomenon called the Lagrangian phase transition (Bertini *et al.*, 2010).

B. Fluctuating thermodynamics

In this subsection we formulate the second law along single fluctuating trajectories and use it to derive a bound on the variation of the rate function. To do so, we first present the asymptotic dynamics that describe the evolution of the states and the single transitions jointly. Because of Eq. (28), the transition flux is expected to asymptotically scale linearly with V, i.e., $J_\rho(t)=Vj_\rho(t)+o(V)$, with $j_\rho(t)$ independent of V.

[7] More rigorously, one can see Eq. (106) as the action associated with the Hamilton-Jacobi equation defined by Eq. (32).

[8] In infinite time, the most likely trajectory starting from any point of the attractor displays an initial relaxation to the local stable fixed point in which the velocity is null. This deterministic relaxation nullifies the action; thus, it can be neglected and the initial condition can be directly placed into the fixed point.

[9] A caustic, in analogy with geometrical, optics is then the set of states c with multiple minimizers.

Therefore, dividing both sides of Eq. (1) by V, we obtain the asymptotic stochastic evolution of the state vector,

$$d_t c(t) = \sum_\rho \Delta_\rho j_\rho(t). \tag{111}$$

Since the flux $j_\rho(t)$ can be described using a Poissonian distribution conditioned on the present state $c(t)$ with the average $r_\rho(c(t))$, the average value of Eq. (111) coincides with Eq. (42) for the mean concentration obtained from the asymptotic form of the master equation (103).

When one uses the scaling of the flux J_ρ and that of the probability distribution [Eq. (31)], the scaled entropy production rate [Eq. (8)] takes the asymptotic form

$$\dot\sigma(t) = \sum_\rho j_\rho(t)\sigma_\rho(c(t)) + d_t I(c(t),t). \tag{112}$$

The decomposition in Eq. (17) becomes

$$\dot\sigma(t) = \dot\sigma_{\rm nc}(t) + \dot\sigma_{\rm d}(t) + d_t(I-\phi)(c(t),t). \tag{113}$$

Namely, it displays the scaled dissipation rate due to nonconservative forces $\dot\sigma_{\rm nc}(t) \coloneqq \sum_\rho j_\rho(t) a_\rho$ and the scaled dissipation rate needed to parametrically drive the reference equilibrium, $\dot\sigma_{\rm d}(t) \coloneqq -\partial_t \phi(c,t)|_{c=c(t)}$, plus the total time derivative of the scaled stochastic Massieu potential $I(c,t)-\phi(c,t)$. Note the presence of the scaled variation of self-information on the right-hand sides of Eqs. (112) and (113). While the scaled variation vanishes on average, it is nonzero along macroscopic fluctuating trajectories such that

$$\lim_{V\to\infty} \frac{1}{V} S_{\rm syst}(n(t),t) = I(c(t),t) + s_{\rm int}(c(t)). \tag{114}$$

The decomposition in Eq. (18) becomes

$$\dot\sigma(t) = \sum_\rho j_\rho(t)\sigma_\rho^{\rm ad} + \dot\sigma_{\rm na} \tag{115}$$

using the scaled adiabatic entropy production of each transition [Eq. (41)] and the scaled nonadiabatic entropy production rate

$$\dot\sigma_{\rm na}(t) \coloneqq d_t[I(c(t),t) - I_{\rm ss}^t(c(t))] + \partial_t I_{\rm ss}^t(c)|_{c=c(t)}. \tag{116}$$

Again, for autonomous systems at stationarity, $I(c,t) = I_{\rm ss}(c) = I_{\rm ss}^t(c)$, so Eq. (116) is identically zero and the scaled adiabatic entropy production rate

$$\dot\sigma_{\rm ad}(t) = \sum_\rho j_\rho(t)\sigma_\rho^{\rm ad}(t) \tag{117}$$

equals $\dot\sigma(t)$. For nonautonomous detailed balance dynamics, $I_{\rm ss}^t(c) = \phi(c,t) + \text{const}$, so Eq. (117) is identically zero for all ρ and the scaled nonadiabatic entropy production rate $\dot\sigma_{\rm na}(t)$ equals $\dot\sigma(t)$. The adiabatic-nonadiabatic decomposition [Eq. (115)] can be used to provide a strengthening of the second law of thermodynamics. This follows from averaging Eq. (116) and taking the limit $V\to\infty$ combined with $\langle\dot\sigma_{\rm na}\rangle \geq 0$ and $\langle\dot\sigma_{\rm ad}\rangle \geq 0$, which yield

$$\lim_{V\to\infty} \langle\dot\sigma(x(t))\rangle \geq -d_t I_{\rm ss}^t(x(t)) + \partial_t I_{\rm ss}^t(c)|_{c=x(t)} \geq 0. \tag{118}$$

In particular, for autonomous relaxation dynamics the equality $I_{\rm ss}^t = I_{\rm ss}$ simplifies Eq. (118) to (J. N. Freitas and Esposito, 2022)

$$\lim_{V\to\infty} \langle\dot\sigma(x(t))\rangle \geq -d_t I_{\rm ss}(x(t)) \geq 0, \tag{119}$$

where the last inequality is the Lyapunov property [Eq. (48)]. Equation (119) is the nonlinear extension of Eq. (101) and was first given by Gaveau, Moreau, and Toth (1998) for reaction-diffusion systems. Note that $I_{\rm ss}$ is replaced by the local quasipotential $I_{\rm ss}^{(\gamma)}$ if the initial condition of the dynamics is localized on a single basin of attraction γ, a fact that is used in Sec. IV.H. The first inequality in Eq. (119) becomes tight when a_ρ is infinitesimal (Falasco and Esposito, 2021; J. N. Freitas and Esposito, 2022). In that limit the quasipotential is still determined by thermodynamics. Indeed, a first order expansion in a_ρ of Eq. (34) gives within each basin γ

$$I_{\rm ss}^{(\gamma)}(c) = \phi(c) + \sigma_{\rm nc}^{(0)}(c, x_\gamma^{\rm eq}), \tag{120}$$

where

$$\sigma_{\rm nc}^{(0)}(c, x_\gamma^{\rm eq}) \coloneqq \int_{x(0)=c}^{x(\infty)=x_\gamma^{\rm eq}} dt \sum_\rho r_\rho^{(0)}(x(t)) a_\rho \tag{121}$$

is the dissipation of nonconservative forces along the solution of detailed balance deterministic dynamics

$$d_t x(t) = \sum_\rho \Delta_\rho r_\rho^{(0)}(x(t)) \tag{122}$$

connecting $x(0)=c$ to the equilibrium fixed point $x(t\to\infty) = x_\gamma^{\rm eq}$ (Falasco and Esposito, 2021; Freitas, Falasco, and Esposito, 2021). Note that Eq. (120) is valid for any c in the basin of attraction γ, not only one close to x_γ^*. The linear response equation (120) yields the large-deviation form of the McLennan-Zubarev probability distribution function (McLennan, 1959; Zubarev, 1994; Maes and Netočný, 2010; Colangeli, Maes, and Wynants, 2011) by replacing the average of the near-equilibrium dissipation over all trajectories with its most likely value.

By relating the macroscopic entropy production during relaxation to steady state macroscopic fluctuations, Eqs. (118) and (119) can thus be seen as generalized fluctuation-dissipation relations. Standard fluctuation-dissipation relations are recovered using a parabolic approximation of $I_{\rm ss}^{(\gamma)}(c)$ around an equilibrium fixed point (Freitas, Falasco, and Esposito, 2021) that is equivalent to the alternative derivation based on the Langevin approximation given in Sec. IV.C. Finally, the nonadiabatic entropy production provides a second (upper) bound valid for rare fluctuations (an instanton) that is derived in Appendix A and used in Sec. IV.H.

C. Gaussian fluctuations

When comparing Eqs. (107) and (45), we recognize that the solution $\pi(t)=0$, giving $\mathcal{A}=0$, corresponds to the deterministic trajectories. This suggests that small fluctuations around the deterministic behavior are characterized by small values of $\pi(t)$. In particular, Gaussian fluctuations around each deterministic solution can be obtained by expanding Eq. (106) around $\pi(t)=0$ and $c(t)=x(t)$ to quadratic order in $\pi(t)$ and $\varrho(t) \coloneqq c(t)-x(t)$, respectively,

$$\mathcal{A}_{\mathrm{G}}=\int_0^\tau dt[-\pi\cdot d_t\varrho+\varrho\cdot\partial_c F(x)\cdot\pi+\pi\cdot D(x)\cdot\pi]. \quad (123)$$

Equation (123) holds only for times much shorter than the escape time from a basin of attraction, which is discussed in Sec. IV.H. It is equivalent to the first order in Van Kampen's system-size expansion of Eq. (30) (van Kampen, 2007), which is known as the linear noise approximation (Thomas and Grima, 2015). Equation (123) contains the scaled generator

$$\mathcal{H}_{\mathrm{FPE}}(\varrho,\pi)=\varrho\cdot\partial_c F(x)\cdot\pi+\pi\cdot D(x)\cdot\pi, \quad (124)$$

which depends parametrically on time via $x(t)$ and corresponds to the Fokker-Planck equation

$$\partial_t p(\varrho,t)=-\partial_\varrho\cdot\left[\varrho\cdot\partial_c F(x)p(\varrho,t)-\frac{D(x)}{V}\partial_\varrho p(\varrho,t)\right]. \quad (125)$$

The associated linear Langevin equation with Gaussian additive noise η reads

$$d_t\varrho(t)=\varrho(t)\cdot\partial_c F(x(t))+\frac{1}{\sqrt{V}}\eta(t). \quad (126)$$

In Eq. (126) η is delta correlated, where the mean zero and covariance matrix $2D(x(t))$ is as defined in Eq. (81) and $\partial_c F$ is the Jacobian matrix of the deterministic drift F given in Eq. (46). Equation (126) also amounts to a quadratic approximation of the rate function as

$$I(\varrho,t)=\tfrac{1}{2}\varrho\cdot\partial_c^2 I(x(t))\cdot\varrho+O(\varrho^3), \quad (127)$$

where the scaled covariance matrix $\mathcal{C}=(\partial_c^2 I)^{-1}$ is obtained by multiplying Eq. (126) by $\varrho(t)$ and averaging over η,

$$\frac{d\mathcal{C}}{dt}(t)=\partial_c F^T(x(t))\cdot\mathcal{C}(t)+\mathcal{C}(t)\cdot\partial_c F(x(t))+2D(x(t)), \quad (128)$$

where $\partial_c F^T$ is the transpose of $\partial_c F$ (Tomita and Tomita, 1974). When the expansion is carried out around a limit cycle $x(t)=x^*(t)$, Eq. (126) allows one to study transversal and longitudinal Gaussian fluctuations (Dykman, Chu, and Ross, 1993; Vance and Ross, 1996; Boland, Galla, and McKane, 2008; Sheth *et al.*, 2018). The latter are unsuppressed; i.e., free diffusion takes place along the limit cycle with the effective diffusion coefficient proportional to $\tau_{\mathrm{p}}'/2V$, with τ_{p}' the period variation of the Hamiltonian orbit upon a small perturbation of $\mathcal{H}_{\mathrm{FPE}}$ (Gaspard, 2002a, 2002b). These fluctuations are stochastic Goldstone modes since they cause the decay in time of correlation functions and ultimately restore the time-translation invariance of the microscopic dynamics, which is spontaneously broken in the limit $V\to\infty$ (Smith and Morowitz, 2016). Recently, the relation between the number of coherent oscillations and the thermodynamic force (Remlein, Weissmann, and Seifert, 2022)—or the entropy production (Marsland, Cui, and Horowitz, 2019)—was studied.

When the expansion is performed around a stable fixed point x_γ^*, Eq. (128) simplifies to the steady state fluctuation-dissipation theorem (Keizer, 1978; Dykman *et al.*, 1994; Prost, Joanny, and Parrondo, 2009),

$$\partial_c F^T(x_\gamma^*)\cdot\mathcal{C}_{\mathrm{ss}}+\mathcal{C}_{\mathrm{ss}}\cdot\partial_c F(x_\gamma^*)=-2D(x_\gamma^*), \quad (129)$$

also known as the Lyapunov equation, with $\mathcal{C}_{\mathrm{ss}}=(\partial_c^2 I_{\mathrm{ss}})^{-1}(x_\gamma^*)$. Multiplying Eq. (129) by $\mathcal{C}_{\mathrm{ss}}^{-1}$ and taking the trace, we obtain

$$\lambda_\gamma=D(x_\gamma^*):\mathcal{C}_{\mathrm{ss}}^{-1}, \quad (130)$$

which connects the volume contraction rate [Eq. (47)] on the attractor, $\lambda_\gamma \coloneqq -\partial_c\cdot F(x_\gamma^*)$, to the state and noise covariance.

Close to detailed balance dynamics, Eq. (126) can be recast using Eqs. (95) and (93) as

$$d_t\varrho(t)=\varrho(t)\cdot\partial_c F^{(0)}(x^{\mathrm{eq}})+\frac{1}{\sqrt{V}}\eta(t), \quad (131)$$

which adds to Eq. (96) small fluctuations driven by the Gaussian noise η with covariance equal to $2D^{(0)}$. For $a_\rho=0$ (i.e., $x^*=x^{\mathrm{eq}}$), Eq. (131) corresponds to the linear theory of fluctuations introduced by Onsager and Machlup (1953), and Eq. (129), using Eq. (93), reduces to $\mathcal{C}_{\mathrm{ss}}^{-1}=\partial_c^2\phi(x^{\mathrm{eq}})$.

D. Truncation of the Kramers-Moyal expansion

We stress that an expansion of Eq. (106) that is quadratic in $\pi(t)$ but retains nonlinearities in $c(t)$ is equivalent to an uncontrolled truncation of the full Kramers-Moyal expansion of the master equation (van Kampen, 1961). Note that the derivation of Eq. (32) hinges on the Taylor expansion of the rate function as

$$p(c-V^{-1}\Delta_\rho,t)=p(c,t)e^{\Delta_\rho\cdot\partial_c I(c,t)+O(V^{-1})}, \quad (132)$$

which is generally different from a direct expansion of the probability density,

$$p(c-V^{-1}\Delta_\rho,t)\approx\left[1-\frac{\Delta_\rho}{V}\cdot\partial_c+\frac{1}{2V^2}(\Delta_\rho\cdot\partial_c)^2\right]p(c,t). \quad (133)$$

Equation (133) wrongly assumes that $p(c,t)$ remains a smooth function as V approaches infinity and reduces Eq. (103) to the Fokker-Planck equation

$$\partial_t p(c,t)\approx-\partial_c\cdot\left\{F(c)p(c,t)-\frac{1}{V}\partial_c\cdot[D(c)p(c,t)]\right\}. \quad (134)$$

Albeit generally incorrect, this approximation is often used. Equation (134) becomes accurate if Δ_ρ or $\partial_c I(c,t)$ is infinitesimal—namely, when a certain continuous limit exists (as in Sec. V.A) or when only Gaussian fluctuations are considered, as in Sec. IV.C. The latter case corresponds to the linearization around a deterministic solution x of the drift field and the diffusion matrix in Eq. (134), which yields Eq. (125).

Equation (134) corresponds to the Ito nonlinear Langevin equation (Gillespie, 2000; Vastola and Holmes, 2020)

$$d_t c(t) = F(c(t)) + \frac{1}{\sqrt{V}}\eta(t), \tag{135}$$

with multiplicative Gaussian noise $\eta(t)$ that has the covariance $2D(c(t))$. In general, Eq. (135) does not correctly capture the fluctuations of $c(t)$ beyond the Gaussian level. Indeed, as already discussed for some specific models (Hänggi and Jung, 1988; Gaveau, Moreau, and Toth, 1997; Vellela and Qian, 2009; Gopal, Esposito, and Freitas, 2022), Eq. (135) mistakes the rate function $I_{\rm ss}$ away from x^*_γ and x_ν. The discrepancy can be made explicit for one-step processes in one dimension, i.e., $\Delta_{\pm\rho} = \pm 1$ and $N = 1$, whose exact- and diffusion-approximated rate function can be obtained analytically. For such systems Eq. (34) reads

$$\sum_{\rho>0} r_\rho(c)(e^{d_c I_{\rm ss}(c)} - 1) = \sum_{\rho>0} r_{-\rho}(c)(1 - e^{-d_c I_{\rm ss}(c)}), \tag{136}$$

which is solved by

$$d_c I_{\rm ss}(c) = \ln \frac{\sum_{\rho>0} r_{-\rho}(c)}{\sum_{\rho>0} r_\rho(c)}, \tag{137}$$

while the expansion of Eq. (136) to second order in $d_c I_{\rm ss}$ [corresponding to Eq. (135)] has the solution

$$d_c I_{\rm NLE}(c) = \frac{\sum_{\rho>0}[r_{-\rho}(c) - r_\rho(c)]}{(1/2)\sum_{\rho>0}[r_\rho(c) + r_{-\rho}(c)]} = -\frac{F(c)}{D(c)}, \tag{138}$$

as can be directly verified by substitution. The subscript NLE denotes quantities corresponding to the nonlinear Langevin equation (135). Hence, for this simple model it is easy to see that $I_{\rm NLE}(c) \neq I_{\rm ss}(c)$ unless c is infinitesimally close to x^*_γ or x_ν. Indeed, in a neighborhood of the fixed points where $F = \varepsilon \to 0$, it holds that $\sum_{\rho>0} r_{-\rho} = \sum_{\rho>0} r_\rho + \varepsilon$ and thus $d_c I_{\rm ss} = \varepsilon/(\sum_{\rho>0} r_\rho) = d_c I_{\rm NLE}$ at first order in ε. The use of Eq. (137) is exemplified in Secs. VII.A and VII.B.1.

E. Informational entropy production of Langevin equations

The nonlinear Langevin approximation of Sec. IV.D is also thermodynamically inconsistent in addition to being incorrect to describe fluctuations beyond the Gaussian level. Here we derive the apparent entropy production associated with Eq. (135) and show that its mean value differs from Eq. (61). In particular, it vanishes in any stationary state. In Sec. IV.I we also explicitly show that Eq. (135) breaks the fluctuation theorem for currents. As discussed in Sec. V.A, the nonlinear Langevin approximation of an underlying jump process is accurate only in a continuous limit that restores the validity of the Einstein relation.

Given a nonlinear Langevin equation of the type of Eq. (135), we can write the associated path probability $P[\{c(t)\}|c(0)]$ starting with the conditional Gaussian weight of the noise $P[\{\eta(t)\}|c(t)] \propto e^{-(1/4)\int_0^\tau dt \eta(t)\cdot D^{-1}(c(t))\cdot\eta(t)}$ and implementing a change of variables $\eta(t) \mapsto c(t)$ (Wiegel, 1986; Zinn-Justin, 2002),

$$P[\{c(t)\}|c(0)] \asymp e^{-(V/4)\int_0^\tau dt [d_t c - F(c)]\cdot D^{-1}(c)\cdot[d_t c - F(c)]}. \tag{139}$$

In Eq. (139) we disregarded the functional Jacobian $|\delta\eta/\delta c|$ that is subexponential in V. This is equivalent to the statement that the choice of the stochastic calculus to handle Eq. (135) is irrelevant at leading order in V. In addition, the dependence on time is explicitly not written to avoid clutter. Note that the exponent in Eq. (139) can be made linear in $d_t c - F$ by means of a Hubbard-Stratonovich transformation (Negele, 2018), i.e., by introducing the auxiliary Gaussian field $\pi(t)$ such that

$$P[\{c(t)\}|c(0)] \asymp \int \mathcal{D}\pi\, e^{-V\int_0^\tau dt [\pi\cdot D\cdot\pi - i\pi\cdot(d_t c - F)]}, \tag{140}$$

with $\mathcal{D}\pi$ the appropriately normalized measure.

The path probability associated with a time-reversed trajectory satisfying Eq. (135) is obtained by swopping the sign of the time derivative in Eq. (139),

$$\bar{P}[\{c(t)\}|c(0)] \asymp e^{-V(1/4)\int_0^\tau dt [d_t c + F]\cdot D^{-1}\cdot[d_t c + F]}. \tag{141}$$

The scaled entropy production estimated on the basis of Eq. (135) is thus given by the log ratio between forward and time-reversed path probabilities, Eqs. (139) and (141). When one uses Eq. (31) for the initial and final probability densities (with the truncation of Sec. IV.D), the log ratio reads

$$\sigma_{\rm NLE} \coloneqq \frac{1}{V}\ln\frac{P[\{c(t)\}|c(0)]}{\bar{P}[\{c(t)\}|c(t)]} + I_{\rm NLE}(c(\tau),\tau) - I_{\rm NLE}(c(0),0). \tag{142}$$

Equation (142) is only an apparent entropy production inferred solely from the dynamics in configuration space. We explained in Sec. IV the shortcomings of the boundary term in Eq. (142). We now show that the informational entropy flow, the first line of Eq. (142), is also flawed. Using Eq. (139), we obtain for the rate of Eq. (142)

$$\dot{\sigma}_{\rm NLE} = d_t c(t)\cdot D^{-1}(c(t))\cdot F(c(t)) + d_t I_{\rm NLE}(c(t),t). \tag{143}$$

Taking its average and replacing $d_t c$ by means of Eq. (135), we arrive at

$$\lim_{V\to\infty}\langle\dot{\sigma}_{\rm NLE}\rangle = F(x(t))\cdot D^{-1}(x(t))\cdot F(x(t)), \tag{144}$$

recalling that $\langle\eta(t)\cdot D^{-1}(c(t))\cdot F(c(t))\rangle = O(V^0)$. Equation (144) is the Kullback-Leibler divergence between forward and backward probability densities of path solutions

of Eq. (135); i.e., it is the diffusive approximation of Eq. (22). Correlations between fluctuations are at least of the order of $O(V^{-1})$ and thus do not appear in the macroscopic limit. Hence, Eq. (144) is also the mean entropy production rate of the linear Langevin equation desribed in Sec. IV.C once F is linearized around a stable state.

In any stationary state the apparent entropy production rate vanishes identically,

$$\lim_{V\to\infty}\langle\dot\sigma_{\rm NLE}\rangle = F(x^*)\cdot D^{-1}(x^*)\cdot F(x^*) = 0, \tag{145}$$

since $F(x^*)=0$ by definition of a fixed point. Namely, the macroscopic entropy production predicted by a Langevin dynamics misses altogether the contribution needed to sustain a time-independent attractor, i.e., the quantity $\langle\dot\sigma_\gamma\rangle$ defined in Sec. VI. In particular, if we consider small deviations from a stable fixed point, Eq. (144) becomes

$$\begin{aligned}\lim_{V\to\infty}\langle\dot\sigma_{\rm NLE}\rangle = (x-x^*_\gamma)\cdot\partial_c F(x^*_\gamma)\cdot D^{-1}(x^*_\gamma)\\ \cdot\partial_c F^T(x^*_\gamma)\cdot(x-x^*_\gamma),\end{aligned} \tag{146}$$

which reduces to the first term of Eq.(101) close to detailed balance dynamics. Therefore, $\langle\dot\sigma_{\rm NLE}\rangle$ misses the adiabatic component and thus underestimates the thermodynamic entropy production rate. We emphasize that the entropy production has the same formal structure for linear and nonlinear Langevin equations, in the sense that it is a quadratic form of the forces: the Langevin equation linearizes the fluxes in the forces. For the linear Langevin equation, the force is further linearized in the displacement of the state c from its fixed point.

F. Nonreciprocity

In conservative mechanical systems that follow Newton's third law of action and reaction, interactions between different degrees of freedom are said to be reciprocal. This holds true when they are brought into contact with thermal reservoirs in such a way that their stochastic dynamics remain detailed balanced. Nonreciprocity arises in the presence of dissipative processes, be them nongradient forces or effective time-delayed interactions (Ivlev *et al.*, 2015; Steffenoni, Kroy, and Falasco, 2016; Loos and Klapp, 2020; Fruchart *et al.*, 2021; Dinelli *et al.*, 2023). In stochastic systems characterized by the deterministic asymptotic dynamics in Eq. (45), nonreciprocity can be defined by means of the Jacobian matrix

$$\lim_{V\to\infty}\frac{\partial\dot c}{\partial c}(t) = \partial_c F(x(t)), \tag{147}$$

which measures the variation rate of a degree of freedom to perturbations in a different one. The trace of Eq. (147) gives the variation rate of phase-space volumes introduced in Eq. (47). To evaluate Eq. (147) in a stable fixed point, we use the decomposition in Eq. (75). We simplify the gradient part of the drift as

$$\begin{aligned}\partial_c\mathcal{F}(x^*) &= \mathcal{M}(x^*)\cdot\partial_c^2 I_{\rm ss}(x^*) + \partial_c\mathcal{M}(x^*)\cdot\partial_c I_{\rm ss}(x^*)\\ &= D(x^*)\cdot\partial_c^2 I_{\rm ss}(x^*),\end{aligned} \tag{148}$$

while for the dissipative part we employ the property in Eq. (77) to write $\partial_c v_{\rm ss}(x^*) =: \varpi = \mathcal{N}(x^*)\cdot\mathcal{C}_{\rm ss}^{-1}$. The matrix ϖ has purely imaginary eigenvalues, referred to as cycling frequencies, that have been proposed as empirical quantities to measure irreversibility (Battle *et al.*, 2016; Mura, Gradziuk, and Broedersz, 2018). We thus obtain

$$\partial_c F(x^*) = -D(x^*)\cdot\mathcal{C}_{\rm ss}^{-1} + \varpi. \tag{149}$$

Taking the trace, we regain the relation for the phase-space contraction rate [Eq. (130)]. Factoring out the kinetic matrix that sets the timescale of the interactions, we can define the macroscopic response matrix as

$$\mathfrak{R} \equiv D^{-1}(x^*)\cdot\partial_c F(x^*) = -\mathcal{C}_{\rm ss}^{-1} + D^{-1}(x^*)\cdot\varpi. \tag{150}$$

For detailed balance dynamics $\varpi = 0$, which implies that $\mathfrak{R}$ is symmetric,

$$\mathfrak{R} \underset{a_\rho=0}{=} -\partial_c^2\phi(x^{\rm eq}). \tag{151}$$

Hence, we can extract a measure of nonreciprocity of the coupling between 2 degrees of freedom from the antisymmetric part of Eq. (150),

$$\mathfrak{R} - \mathfrak{R}^T = D^{-1}(x^*)\cdot\varpi - \varpi^T\cdot D^{-1}(x^*). \tag{152}$$

If multiple fixed points exist, Eq. (152) is valid for each attractor for t much smaller than the escape time from its basin.

G. Irreversibility of relaxation and instanton

Under the condition of detailed balance $a_\rho = 0$, the instantons $c(t)$ that solve Eq. (107) are the time reversal of the deterministic trajectory solutions of Eq. (45),

$$d_t c(t) \underset{a_\rho=0}{=} -d_t x(t). \tag{153}$$

Equation (153) readily follows from the equality $r_\rho^\dagger = r_\rho$, which is valid for detailed balance systems. This result is ultimately a consequence of the symmetry

$$\mathcal{H}(c,\pi) \underset{a_\rho=0}{=} \mathcal{H}(c,-\pi+\partial_c\phi), \tag{154}$$

which holds in the presence of detailed balance (Dykman *et al.*, 1994) and is responsible for the validity of Eq. (120) (Falasco and Esposito, 2021). Its generalization leads to the fluctuation theorems discussed in Sec. IV.I.

Instead, when the dynamics is not detailed balanced, $a_\rho \neq 0$, the adiabatic entropy production quantifies the time asymmetry between relaxational and instantonic trajectories. Equation (153) is replaced by

$$\begin{aligned}d_t c(t) &= \sum_\rho \Delta_\rho r_\rho(c(t)) e^{\Delta_\rho\cdot\pi(t)} = -F^\dagger(c(t))\\ &= -\sum_\rho \Delta_\rho r_\rho(c(t)) e^{-\sigma_\rho^{\rm ad}(t)} = -d_t x(t) + O(\sigma_\rho^{\rm ad}),\end{aligned} \tag{155}$$

where we use $\pi(t) = \partial_c I_{\rm ss}(c(t))$ on the manifold $\mathcal{H} = 0$, the dual drift [Eq. (51)], the relation

$$r_\rho^\dagger(c) = r_\rho(c) e^{-\sigma_\rho^{\rm ad}(c)} \tag{156}$$

valid for autonomous dynamics, and the relabeling of the transitions $\rho \mapsto -\rho$. We mention two important aspects of the instanton dynamics. First, in the case of Gaussian noise, the time-reversed dual dynamics that defines the instanton is a simple transformation of the drift field that flips the sign of the gradient part (Bertini *et al.*, 2015; Chernyak, Chertkov, and Jarzynski, 2006), i.e., $-D(c)\cdot\partial_c I_{\rm ss}(c) \mapsto D(c)\cdot\partial_c I_{\rm ss}(c)$, without changing the probability velocity $v_{\rm ss}(c)$. Away from the diffusive limit, the dual dynamics has to be implemented at the level of single transition rates, i.e., $r_\rho \mapsto r_\rho^\dagger$, rather than directly on quantities defined in configuration space. Second, the dual transition rates $r_\rho^\dagger$ do not generally have the same functional form of the transition rate r_ρ unless detailed balance holds; cf. Eq. (156). This means that trajectories akin to the most likely fluctuations cannot be generated in the deterministic system only by tuning the nonconservative forces; new transitions belonging to different physical classes are instead required. See Sec. VII.A.1 for an example.

H. Thermodynamic constraints on transition rates between attractors

The distribution of exit locations from an attractor asymptotically peaks on the saddle points[10] dividing two basins (Day, 1990; Maier and Stein, 1997; Luchinsky *et al.*, 1999). Therefore, when the end point c of an instanton coincides with a saddle point x_ν on the separatrix dividing the basin of attraction of x_γ^* and $x_{\gamma'}^*$, Eq. (110) is the macroscopic transition rate κ_ν from the attractor γ to γ' through the saddle point ν (see Appendix B),

$$\kappa_\nu \asymp e^{-V[I_{\rm ss}^{(\gamma)}(x_\nu) - I_{\rm ss}^{(\gamma)}(x_\gamma^*)]}. \tag{157}$$

Since exit times from each attractor are exponentially distributed in the large V limit (Day, 1983; Freidlin and Wentzell, 1998; Bovier *et al.*, 2002), the inverse of the transition rate coincides with the mean first passage time $1/\kappa_\nu := \inf\{t \geq 0 : c(0) = x_\gamma^*, c(t) = x_\nu\}$. Hereafter, $\kappa_{-\nu}$ is used to indicate the rate of the opposite transition, namely, from $x_{\gamma'}^*$ to x_γ^* through the same saddle ν. If one used the quasipotential $I_{\rm NLE}$ obtained by the nonlinear Langevin equation in Eqs. (110) and (157), the transition probability and the escape rate from the attractor would be misestimated with an exponential error (Bressloff and Newby, 2014; Assaf and Meerson, 2017).

For detailed balance dynamics $I_{\rm ss}$ is equal to ϕ up to a constant, as shown in Sec. IV.B. Hence, Eq. (157) takes the form of an Arrhenius rate (Arrhenius, 1889; Hänggi, Talkner, and Borkovec, 1990), with the large parameter V playing the role of the (small) inverse temperature,

$$\kappa_\nu^{\rm eq} \asymp e^{-V[\phi(x_\nu) - \phi(x_\gamma^*)]}. \tag{158}$$

For later convenience we have defined an Arrhenius rate $\kappa_\nu^{\rm eq}$ with respect to the fixed and saddle points of the nonequilibrium dynamics. In fact, $\kappa_\nu^{\rm eq} \neq \lim_{a_\rho \to 0} \kappa_\nu$ since $x_\gamma^* \neq x^{\rm eq}$ and x_ν may even be absent for $a_\rho = 0$. In Secs. VII.A and VII.B.1, we give examples of such metastable states created by continuous dissipation in chemical reaction networks and electronic circuits. Note that the Eyring-Kramers formula (Eyring, 1935; Kramers, 1940; Landauer and Swanson, 1961; Langer, 1969) for the transition rate is an extension of Eq. (158) that includes subexponential prefactors.

Close to detailed balance, i.e., at linear order in a_ρ, the quasipotential is given by Eq. (120), and thus the jump dynamics between attractors inherits the local detailed balance property (Falasco and Esposito, 2021), namely,

$$\lim_{V\to\infty} \frac{1}{V} \ln \frac{\kappa_\nu}{\kappa_{-\nu}} = \phi(x_\gamma^{\rm eq}) - \phi(x_{\gamma'}^{\rm eq}) + \sigma_\nu^{(0)}, \tag{159}$$

where $\sigma_\nu^{(0)} := -\sigma_{\rm nc}^{(0)}(x_\nu, x_\gamma^{\rm eq}) + \sigma_{\rm nc}^{(0)}(x_\nu, x_{\gamma'}^{\rm eq})$ becomes the dissipation of nonconservative forces along the equilibrium instanton from $x_\gamma^{\rm eq}$ to x_ν [the time-reversed solution of Eq. (122); see Eq. (153)] plus the dissipation in the deterministic relaxation from x_ν to $x_{\gamma'}^{\rm eq}$. We show in Sec. VI that Eq. (159) allows us to retrieve standard stochastic thermodynamics when the latter is formulated for the jump dynamics on macroscopic attractors.

Thermodynamics constrains the macroscopic transition rate κ_ν from the attractor γ to γ' through the saddle point ν in terms of the entropy $\sigma_{\gamma\to\nu}$ ($\sigma_{\nu\to\gamma}$) produced along the instanton (relaxation) (see Fig. 3),

$$-\sigma_{\nu\to\gamma} \leq \lim_{V\to\infty} \frac{1}{V} \ln \kappa_\nu \leq \sigma_{\gamma\to\nu}. \tag{160}$$

We first derive the lower bound in Eq. (160). Integrating Eq. (119) along a relaxation trajectory from a neighborhood of the saddle x_ν to a neighborhood of the fixed point[11] x_γ^* and using Eq. (157), we obtain

$$\lim_{V\to\infty} \frac{1}{V} \ln \kappa_\nu \geq -\sigma_{\nu\to\gamma}. \tag{161}$$

The bound in Eq. (161) is the conceptual analog of Falasco and Esposito (2020) and Neri (2022) for state observables, i.e., a recently discovered speed limit that is an upper bound on the rate of processes defined for current observables. In general, splitting the entropy produced in the relaxation

$$\sigma_{\nu\to\gamma} = \phi(x_\nu) - \phi(x_\gamma^*) + \sigma_{\rm nc}^{\nu\to\gamma} \tag{162}$$

into the equilibrium part, i.e., the variation of the Massieu potential, and the dissipation of the nonconservative forces along the relaxation trajectory, i.e.,

$$\sigma_{\rm nc}^{\nu\to\gamma} := \int_{x(0)=x_\nu}^{x(\infty)=x_\gamma^*} dt \sum_\rho a_\rho r_\rho(x(t)), \tag{163}$$

[10] Or close to them, in the case of saddles with flat stable directions.

[11] See Appendix A for a discussion about the exact choice of the trajectory end points.

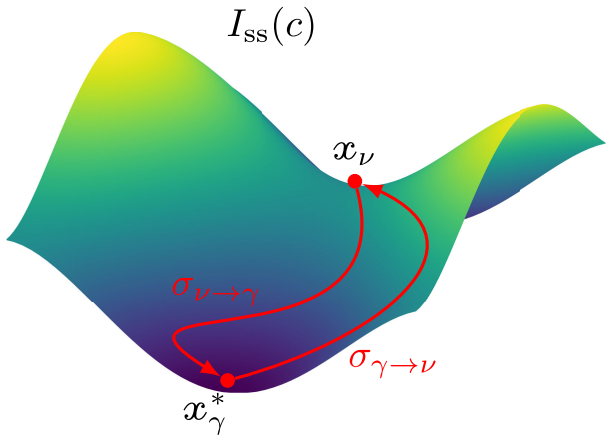

FIG. 3. Schematic representation, for a system without detailed balance, of relaxation and instanton trajectories connecting the local minimum x^*_γ of the rate function $I_{\rm ss}$ and a saddle point x_ν.

we can rephrase the bound in Eq. (161) in terms of the Arrhenius transition rate [Eq. (158)],

$$\frac{\kappa_\nu}{\kappa_\nu^{\rm eq}} \geq e^{-V\sigma_{\rm nc}^{\nu\to\gamma}}. \tag{164}$$

The additional upper bound in Eq. (160) can be obtained in a similar fashion. The derivation, which is given in Appendix A, is based on averaging the entropy production decomposition [Eq. (115)] by conditioning the initial and final points of the trajectories of infinite duration, and showing that the adiabatic entropy production remains non-negative along these paths.

For detailed balance dynamics $\sigma_{\nu\to\gamma} = -\sigma_{\gamma\to\nu} > 0$; the sign comes from the positivity of the mean entropy production [Eq. (119)], as these entropy productions are simply the difference in the Massieu potentials between the saddle point and the stable fixed point. Therefore, the upper and lower bounds in Eq. (160) converge to each other in this limit. Moreover, at linear order in a_ρ, the quasipotential is given by Eq. (120); thus, Eq. (160) holds again in the form of equality. In this case we can read Eq. (160) as a maximum entropy production principle: the attractor with the largest lifetime is the one with the largest relaxation (or smallest instantonic) entropy production. This statement remains true for all systems in which relaxation and instantonic entropy productions are close to each other. However, note that $\sigma_{\gamma\to\nu}$ need not be negative far from equilibrium, which means that the right-hand side of Eq. (160) can be a loose bound.

We can also isolate the equilibrium contribution to the entropy production of the instanton as in Eq. (162),

$$\sigma_{\gamma\to\nu} = \phi(x^*_\gamma) - \phi(x_\nu) + \sigma_{\rm nc}^{\gamma\to\nu}, \tag{165}$$

to recast the upper bound in Eq. (160) as

$$\frac{\kappa_\nu}{\kappa_\nu^{\rm eq}} \leq e^{V\sigma_{\rm nc}^{\gamma\to\nu}}. \tag{166}$$

Equation (166) is an exact result (asymptotically in V) and thus improves a similar but approximated result obtained by neglecting changes in the system's dynamical activity (Kuznets-Speck and Limmer, 2021). The main differences are that $\sigma_{\rm nc}^{\gamma\to\nu}$ was replaced by Kuznets-Speck and Limmer (2021) by one-half of the dissipation caused by nonconservative forces along the entire trajectory connecting the two basins of attractions, and the Arrhenius rate in Eq. (166) is calculated with respect to nonequilibrium fixed points.

Finally, we note that these bounds can be tightened by considering the macroscopic limit of the information-theoretic entropy production in Eq. (68). If the jump vectors $\tilde{\Delta}_\rho$ are linearly independent, the condition $F(x^*) = 0$ implies that $\tilde{r}_\rho(x^*) - \tilde{r}_{-\rho}(x^*) = 0$ for all ρ, and the function in Eq. (68) is zero on the fixed point x^* (J. N. Freitas and Esposito, 2022). Therefore, replacing σ with $\tilde{\sigma}$ in Eq. (160) we obtain tighter bounds, although they are no longer connected to thermodynamics. See Sec. VII.B.1 for an application of these bounds to a model of an electronic circuit.

The ability to obtain exact solutions of Eqs. (45) and (107) underlies the practical applicability of the bounds in Eq. (160). While relaxation trajectories are relatively easy to find via a direct numerical integration of an initial value problem, instantons require more advanced approaches in view of the boundary value problem that defines them. One typically employs the shooting method (Press *et al.*, 2007; Keller, 2018) for low-dimensional systems. Alternatively, one resorts to the minimum action method (Weinan and Vanden-Eijnden, 2004; Grafke, Schäfer, and Vanden-Eijnden, 2017; Kikuchi *et al.*, 2020; Zakine and Vanden-Eijnden, 2023), which is a fictitious-time gradient descent on the negative of the action in Eq. (106) in the trajectory space satisfying the appropriate boundary conditions.

I. Macroscopic time-integrated observables and fluctuation theorems

The trajectory description of Secs. IV.A and IV.B can be complemented with an analysis of the full statistics of thermodynamic observables (Esposito, Harbola, and Mukamel, 2007; Chetrite and Gawedzki, 2008; Garrahan *et al.*, 2009; Speck, Engel, and Seifert, 2012; Hurtado *et al.*, 2014). For observables that are time-integrated functionals of the trajectory $\mathcal{X}$ of the form

$$\mathcal{O}[\mathcal{X}] = \int_0^\tau dt \underbrace{\sum_\rho J_\rho(t)\mathcal{O}_\rho(n(t))}_{\dot{\mathcal{O}}(t)}, \tag{167}$$

we are interested in the generating function $G_{\mathcal{O}}(z,t) \coloneqq \langle e^{z\mathcal{O}[\mathcal{X}]}\rangle$, which gives all the moments upon differentiation with respect to z, i.e., $\partial_z^m G_{\mathcal{O}}(z,\tau)|_{z=0} = \langle \mathcal{O}^m\rangle$. Toward this aim, it is customary to start with the time evolution equation of the joint distribution $P(n,\mathcal{O},t)$ of the occupation number n and the observable $\mathcal{O}$,

$$\partial_t P(n,\mathcal{O},t) = \sum_\rho [R_\rho(n-\Delta_\rho)P(n-\Delta_\rho,\mathcal{O}-\mathcal{O}_\rho,t) - R_\rho(n)P(n,\mathcal{O},t)]. \tag{168}$$

For extensive observables, i.e., such that $\lim_{V\to\infty}\mathcal{O}_\rho(n)=\mathscr{o}_\rho(c)$, we can perform a large-scale expansion analogous to that worked out for the master equation in Sec. III.A. The resulting evolution equation for the joint probability of the intensive variables c and the scaled observable $\lim_{V\to\infty}\mathcal{O}[\mathcal{X}]/V=\mathscr{o}[\mathcal{X}]$ reads

$$\partial_t p(c,\mathscr{o},t)=V\sum_\rho\left[r_\rho\left(c-\frac{\Delta_\rho}{V}\right)p\left(c-\frac{\Delta_\rho}{V},\mathscr{o}-\frac{\mathscr{o}_\rho}{V},t\right)-r_\rho(c)p(c,\mathscr{o},t)\right]. \tag{169}$$

Equation (169) admits a solution of the large deviations form

$$p(c,\mathscr{o},t)\asymp e^{-VY(c,\mathscr{o},t)} \tag{170}$$

and suggests defining the scaled cumulant generating function

$$K_{\mathscr{o}}(z,t)\coloneqq\lim_{V\to\infty}\frac{1}{V}\ln G_{\mathcal{O}}(z,t), \tag{171}$$

which encodes all the relevant statistics in the macroscopic limit. It can be obtained in the following way. Multiplying Eq. (169) by $e^{Vz\mathscr{o}}$ and integrating over $\mathscr{o}$ yields a master equation for $G_{\mathcal{O}}(c,z,t)\coloneqq\langle\delta(c(t)-c)e^{Vz\mathscr{o}[\mathcal{X}]}\rangle$, which is the generating function of $\mathcal{O}$ conditioned on the macroscopic state c at time t,

$$\partial_t G_{\mathcal{O}}(c,z,t)=V\mathcal{H}_z(c,-V^{-1}\partial_c)G_{\mathcal{O}}(c,z,t). \tag{172}$$

The latter is expressed in terms of the "tilted" operator

$$\mathcal{H}_z(c,-V^{-1}\partial_c)\coloneqq\sum_\rho(e^{z\mathscr{o}_\rho-V^{-1}\Delta_\rho\cdot\partial_c}-1)r_\rho(c), \tag{173}$$

which reduces to the generator of the stochastic dynamics in Eq. (104) for $z=0$ since $G_{\mathcal{O}}(c,z,t)|_{z=0}=p(c,t)$. As in Sec. IV.A, we can obtain the unconditioned generating function as the functional integral

$$G_{\mathcal{O}}(z,\tau)=\int\mathcal{D}c\int\mathcal{D}\pi\, e^{V\{\mathcal{A}_z[\{c(t),\pi(t)\}]-I(c(0),0)\}}, \tag{174}$$

which at leading order in V can be evaluated via the Laplace method,

$$G_{\mathcal{O}}(z,\tau)\asymp e^{V\max_{c(t),\pi(t)}\{\mathcal{A}_z[\{c(t),\pi(t)\}]-I(c(0),0)\}}. \tag{175}$$

Namely, we are left to maximize the tilted (or biased) action

$$\mathcal{A}_z=\int_0^\tau dt[-\pi(t)\cdot d_t c(t)+\mathcal{H}_z(c(t),\pi(t))] \tag{176}$$

with respect to $c(t)$ and $\pi(t)$, that is, to find the solutions of the Hamiltonian equations

$$d_t c=\partial_\pi\mathcal{H}_z(c,\pi),\qquad d_t\pi=-\partial_c\mathcal{H}_z(c,\pi), \tag{177}$$

with the appropriate boundary conditions. These read $\pi(0)=\partial_c I(c(0),0)$ and $\pi(\tau)=0$ (Lazarescu *et al.*, 2019) for trajectories drawn from the unconstrained ensemble with an initial distribution $p(c(0),t)\asymp e^{-VI(c(0),0)}$. Finally, the contracted rate function of the observable $\mathcal{O}$ is obtained via the Legendre-Fenchel transform

$$Y(\mathscr{o},\tau)\coloneqq\sup_z\{K_{\mathscr{o}}(z,\tau)-z\mathscr{o}\}. \tag{178}$$

Note that if $K_{\mathscr{o}}(z,\tau)$ has nondifferentiable points, the rate function has a nonconvex part, but Eq. (178) returns only its convex envelope.

From Eq. (176) one can directly extract the mean value of the observable along trajectories conditioned on the boundaries, $\langle\dot{\mathscr{o}}\rangle=\partial_z\mathcal{H}_z|_{z=0}(c(t),\pi(t))$, with $c(t)$ and $\pi(t)$ the solution of Eq. (177) at $z=0$, which is Eq. (107). In particular, following a derivation that is analogous to that of Sec. IV.G, we find that

$$\mathscr{o}_{\gamma\to\nu}=\int dt\sum_\rho\mathscr{o}_\rho r_\rho(c(t))e^{\Delta_\rho\cdot\partial_c I_{\rm ss}(c(t))}=\pm\int dt\sum_\rho\mathscr{o}_\rho r^\dagger_\rho(c(t))=\pm\mathscr{o}_{\nu\to\gamma}+O(\sigma^{\rm ad}_\rho), \tag{179}$$

where the positive (negative) sign is for observables $\mathscr{o}_\rho=\mathscr{o}_{-\rho}$ ($\mathscr{o}_\rho=-\mathscr{o}_{-\rho}$).

1. Entropy production at steady state

Choosing $\mathscr{o}_\rho(c)=\sigma_\rho(c)$, as defined in Eq. (29), and adding the boundary terms $q[I(c(\tau),\tau)-I(c(0),0)]$ to the action in Eq. (174), we obtain the scaled cumulant generating function of the entropy production [Eq. (112)],

$$K_\sigma(z,\tau)=\max_{c(t),\pi(t)}\{\mathcal{A}_z[\{c(t),\pi(t)\}]+zI(c(\tau),\tau)-(z+1)I(c(0),0)]\}. \tag{180}$$

If we restrict to a stationary state, i.e., $\mathcal{H}_z$ has no explicit time dependence and $I(c,\tau)=I(c,0)=I_{\rm ss}(c)$, the scaled cumulant generating function satisfies the symmetry

$$K_\sigma(z,\tau)=K_\sigma(-z-1,\tau). \tag{181}$$

This follows from the local detailed balance property in Eq. (29), which ensures the validity of the Lebowitz-Spohn symmetry of the tilted operator (Kurchan, 1998; Lebowitz and Spohn, 1999)

$$\mathcal{H}_z(c,\pi)=\sum_\rho r_{-\rho}(c)(e^{-\Delta_\rho\cdot\pi-z\sigma_\rho(c)}-1)=\sum_\rho r_\rho(c)(e^{-\Delta_\rho\cdot\pi-(z+1)\sigma_\rho(c)}-1)=\mathcal{H}_{-z-1}(c,-\pi). \tag{182}$$

Stationarity implies that the generating function can also be obtained by integrating over the time-reversed trajectories of

$c(t)$ and $\pi(t)$, defined by the change of variable $\pi \mapsto -\pi$ and $t \mapsto \tau - t$, which maps the tilted action as $\mathcal{A}_z[\{c(t),\pi(t)\}] \mapsto \mathcal{A}_{-z-1}[\{c(t),\pi(t)\}]$ thanks to Eq. (182). Hence, by the Laplace approximation the scaled cumulant generating function is recast as

$$K_\sigma(z,\tau) = \max_{\{c(t),\pi(t)\}} \{\mathcal{A}_{-z-1}[\{c(t),\pi(t)\}] + zI_{\rm ss}(c(0)) - (z+1)I_{\rm ss}(c(\tau))]\}. \tag{183}$$

Comparing Eq. (183) with Eq. (180) evaluated at stationarity, i.e., setting $I = I_{\rm ss}$, we arrive at the announced symmetry in Eq. (181).

By a Legendre-Fenchel transform of $K_\sigma(z,\tau)$ that gives the convex envelop of the rate function of the entropy production in Eq. (178), the symmetry in Eq. (181) results in finite time in the fluctuation theorem

$$Y(\sigma,\tau) - Y(-\sigma,\tau) = \sigma. \tag{184}$$

Finally, one can directly verify that the diffusion-type approximation of the generating function, obtained by expanding the tilted action in Eq. (176) to second order in $\pi(t)$, does preserve the symmetry in Eq. (182) and the fluctuation theorem in Eq. (184) provided that the functional dependence on q is left untouched. This means that preserving the fluctuation relation requires one to identify the entropy production at the mesoscopic level, i.e., by resolving the entropy production associated with each transition.

2. Transition currents at steady state

Choosing $o_{\pm\rho} = \pm 1$ and the counting field $z_\rho = -z_{-\rho}$, we obtain the scaled cumulant generating function $K_\iota(z,\tau)$ of all the time-integrated currents with the reservoirs, each of which reads $\iota_\rho[\mathcal{X}] \coloneqq \int_0^\tau dt I_\rho(t)$. We assume that the initial state $c(0)$ is sampled from the stationary probability density function $p_{\rm ss}(c)$. Thanks to the symmetry

$$\begin{aligned}\mathcal{H}_z(c,\pi) &= \sum_\rho r_{-\rho}(c)(e^{-\Delta_\rho\cdot\pi - z_\rho} - 1)\\ &= \sum_\rho r_\rho(c)(e^{-\Delta_\rho\cdot\pi - z_\rho - \sigma_\rho(c,t)} - 1)\\ &= \mathcal{H}_{-z-a}(c, -\pi + \partial_c\phi),\end{aligned} \tag{185}$$

which is obtained using Eq. (29), the tilted action is mapped as $\mathcal{A}_z[\{c(t),\pi(t)\}] \mapsto \mathcal{A}_{-z-a}[\{c(t),\pi(t)\}] + o(\tau)$ by the change of variables $\pi \mapsto -\pi + \partial_c\phi$ and the time reversal $t \mapsto \tau - t$. Therefore, the time- and size-scaled cumulant generating function $K_j(z) \coloneqq \lim_{\tau\to\infty} K_\iota(z,\tau)/\tau$ satisfies the symmetry

$$K_\iota(z) = K_\iota(-z-a), \tag{186}$$

where a is the vector of transition forces a_ρ. One can verify that the symmetry in Eq. (185), and thus that in Eq. (186), is generally broken when $\mathcal{H}_z(c,\pi)$ is expanded at second order in π, i.e., when the Langevin approximation in Eq. (135) is employed. Since the symmetry of the full action holds only asymptotically, the fluctuation theorem for the currents is valid for $\tau \to \infty$. Namely,

$$Y(\iota) - Y(-\iota) = \sum_{\rho>0} a_\rho \iota_\rho, \tag{187}$$

with the long-time large-V rate function of the currents corresponding to the probability $p(\iota,t) \asymp e^{-Vt Y(\iota)}$.

For systems with multiple deterministic fixed points x^*_γ, there are generally multiple q-dependent vectors $\big(c(t),\pi(t)\big)$ that maximize Eq. (185) as $z \to 0$. When z departs from zero, Eq. (185) attains a different value on each of these optimal solutions. Hence, the function $\partial_z K_j(z)$ has a jump discontinuity at $z = 0$, which reflects the coexistence of macroscopic states with different mean currents. Accordingly, Legendre-Fenchel transforming $K_j(z)$ gives only the convex envelope of the rate function. This phenomenon is called a dynamical phase transition (Garrahan *et al.*, 2007, 2009; Hurtado and Garrido, 2011; Espigares, Garrido, and Hurtado, 2013; Gingrich, Vaikuntanathan, and Geissler, 2014; Nyawo and Touchette, 2016) given the formal analogy with equilibrium phase transitions in which the free energy develops singularities. Its generality was shown by Lazarescu *et al.* (2019) for chemical reaction networks but extends to all systems displaying multiple stable fixed points in the macroscopic limit.

Without spelling out the derivation, which is analogous to that of Herpich, Shayanfard, and Esposito (2020), we note that Eq. (185) implies a finite-time symmetry for the scaled cumulant generating function of nonautonomous systems initially in thermal equilibrium with only one reservoir.

Mind that the validity of such detailed fluctuation theorems hinges on the initial and final probability distributions having support on the same attractors; otherwise, absolute irreversibility should be taken into account (Murashita, Funo, and Ueda, 2014; Buffoni and Campisi, 2022).

3. Fluctuation theorems from dual dynamics

Other detailed fluctuation theorems can be obtained invoking additional symmetries of a suitably tilted Hamiltonian. In particular, one can leverage the equality

$$\begin{aligned}\mathcal{H}_z(c,\pi) &= \sum_\rho r_\rho(e^{\Delta_\rho\cdot\pi + z\sigma^{\rm ad}_\rho} - 1)\\ &= \sum_\rho r^\dagger_\rho(e^{\Delta_\rho\cdot\pi + (z+1)\sigma^{\rm ad}_\rho} - 1)\\ &= \mathcal{H}^\dagger_{-z-1}(c,\pi),\end{aligned} \tag{188}$$

which follows from the facts that the escape rate of the dual dynamics is the same as that of the original dynamics, $\sum_\rho r_\rho = \sum_\rho r^\dagger_\rho$, and that $(\sigma^{\rm ad}_\rho)^\dagger = -\sigma^{\rm ad}_\rho$ changes sign under the dual transformation. From Eq. (188) we obtain the fluctuation relation that links the rate functions of the adiabatic entropy production in the original dynamics Y and in the dual one $Y^\dagger$,

$$Y(\sigma_{\rm ad},\tau) - Y^\dagger(-\sigma_{\rm ad},\tau) = \sigma_{\rm ad}. \tag{189}$$

Equation (189) also follows, in the large deviations formulation, from the log ratio of path probabilities of states and jumps (Sun, 2006), which is reported in Eq. (A2). Analogously, a fluctuation theorem for the nonadiabatic entropy production [Eq. (116)] can be derived by combining the dual dynamics with the time reversal (Rao and Esposito, 2018c). The positivity of the mean adiabatic and nonadiabatic entropy production readily follows from these symmetry relations.

V. MACROSCOPIC FIELD THEORY

A. Continuous-space limit: Dynamics

We now elaborate on the structure of the system dividing the transitions ρ into two sets, named R and C. The label R denotes a transition that keeps a discrete character (akin to chemical reactions), while C indicates jumps that become infinitesimal in size (such as continuous drift or diffusion in real space). Correspondingly, we enforce a bipartite structure by splitting the entries of the vector c, denoted as $c_{\alpha,x}$, so that transitions belonging to R (C) act only on the label α (x). For concreteness, we can think of α as a label for different particle species and x as a d-dimensional vector for the discrete space coordinate. Within this picture we assume that with each pair of first neighbors (x,x') we associate pairs of transitions $\pm\rho^{\alpha}_{(x,x')}\in C$ (with each pair acting on a single label α for simplicity), whose rates are written as $r^{\alpha}_{(x,x')}$ and $r^{\alpha}_{(x',x)}$, respectively.

We look for the continuous-space limit of Eq. (106) when a macroscopic scale Ω, such as the volume of the entire system, is large with respect to the mesoscopic scale V in which the variable $c_{\alpha,x}$ is defined. To this aim we introduce a continuous variable $r=x\epsilon$ with $\epsilon^d=V/\Omega$ such that $c_{\alpha,x}\to c_\alpha(r)$ and $\pi_{\alpha,x}\to\pi_\alpha(r)$ become smooth fields as $\epsilon\to 0$. With the rewriting $V\sum_x=\Omega\sum_x(V/\Omega)\to\Omega\int dr$, the action in Eq. (106) takes the form

$$V\mathcal{A}=\Omega\int_0^\tau dt\int dr\{-\boldsymbol{\pi}(r,t)\cdot d_t\mathbf{c}(r,t)+\mathcal{H}_R(\mathbf{c}(r,t),\boldsymbol{\pi}(r,t))+\mathcal{H}_C(\mathbf{c}(r,t),\boldsymbol{\pi}(r,t))]\}. \quad (190)$$

In Eq. (190) we have isolated the generator of transitions $\rho\in R$,

$$\mathcal{H}_R(c,\pi):=\sum_{\rho\in R}r_\rho(c)(e^{\Delta_\rho\cdot\pi}-1), \quad (191)$$

which maintains the form of the moment generating function of a Poisson noise, and the generator of transitions $\rho\in C$,

$$\mathcal{H}_C(c,\pi):=\lim_{\epsilon\to 0}\sum_{\alpha,x'}[r^{\alpha}_{+\rho}(c)(e^{\Delta_{+\rho}\cdot\pi}-1)+r^{\alpha}_{-\rho}(c)(e^{\Delta_{-\rho}\cdot\pi}-1)], \quad (192)$$

where $+\rho=(x,x')$, $-\rho=(x',x)$, and $\Delta_{\pm\rho}$ is a discrete gradient acting as, for example, $\Delta_{\pm\rho}\cdot\pi=\pm(\pi_{\alpha,x}-\pi_{\alpha,x'})$. To avoid clutter, we employ the same dot symbol to denote the scalar product in the reduced space of α, for example, $\boldsymbol{\pi}(r)\cdot d_t\mathbf{c}(r)=\sum_\alpha\pi_\alpha(r)d_tc_\alpha(r)$, and also in the physical space coordinatized by r.

To evaluate the limit in Eq. (192), we use the following expressions for the discrete gradient of functions,

$$\Delta_{\pm\rho}\cdot\pi=\pm[\epsilon\widehat{\boldsymbol{\nabla}}\pi(r)+\tfrac{1}{2}\epsilon^2\widehat{\boldsymbol{\nabla}}^2\pi(r)]+O(\epsilon^3),$$
$$\Delta_{\pm\rho}\cdot\partial_c\phi(c)=\pm\epsilon\widehat{\boldsymbol{\nabla}}\frac{\delta}{\delta c(r)}\phi[c(r)]+O(\epsilon^2), \quad (193)$$

which yield the expansion of the transition rates[12]

$$r^{\alpha}_{\pm\rho}(c)=\epsilon^{-2}[\chi_\alpha(c(r))+O(\epsilon)]\times\left[1\mp\frac{\epsilon}{2}\widehat{\boldsymbol{\nabla}}\frac{\delta\phi}{\delta c_\alpha(r)}\pm\frac{\epsilon}{2}e_{x,x'}f_\alpha(r)+O(\epsilon^2)\right], \quad (194)$$

where we write $\widehat{\boldsymbol{\nabla}}:=e_{x,x'}\cdot\boldsymbol{\nabla}$, with $e_{x,x'}$ the unit vector pointing from x to x'. In Eq. (194) the mobility matrix $\chi(c)$ (diagonal with entries χ_α) and the nonconservative force vector $f(r)$, as well as the thermodynamic functional $\phi(\{c_{x,\alpha}\})\to\phi[c(r)]$, are independent of ϵ. The scaling $\gamma_\rho(c_{x,\alpha})=\epsilon^{-2}\chi_\alpha(c(r))+O(\epsilon^{-1})$ of the kinetic part of the rates is imposed to ensure a proper diffusive limit on the same timescales of transitions $\rho\in R$. In addition, we required the nonconservative force $a_\rho=\epsilon e_{x,x'}f_\alpha(r)+O(\epsilon^2)$ to be small on the macroscopic scale, a condition called weak asymmetry in the lattice gas literature.

Therefore, when contributions of $O(\epsilon^2)$ and higher are neglected, Eqs. (193) and (194) reduce the generator $\mathcal{H}_C$ to

$$\mathcal{H}_C(c,\pi)=\boldsymbol{\nabla}\boldsymbol{\pi}\cdot\chi(c)\cdot\left[\left(-\boldsymbol{\nabla}\frac{\delta\phi}{\delta c}+f\right)+\boldsymbol{\nabla}\boldsymbol{\pi}\right], \quad (195)$$

which has the structure (quadratic in π) of the cumulant generating function of a Gaussian noise field. If the set R is empty, Eq. (195) is the generator of the full dynamics corresponding to the functional Langevin equation,

$$\partial_t c(r,t)=-\boldsymbol{\nabla}\cdot\left(j[c]+\frac{1}{\sqrt{\Omega}}\xi(r,t)\right),$$
$$j[c]:=\chi\cdot\left(-\boldsymbol{\nabla}\frac{\delta\phi}{\delta c}+f\right), \quad (196)$$

where $\xi(r,t)$ is zero mean and Gaussian, with correlations $\langle\xi(r,t)\xi(r',t')\rangle=2\chi(c(r,t))\delta(r-r')\delta(t-t')$. This can be seen by performing the Gaussian integral over π and recognizing that the resulting action is the standard one corresponding to the Langevin equation (196); cf. Eq. (140) for the finite-dimensional case. A few comments are in order. To begin, the stochastic partial differential equation (196) is ill defined (Konarovskyi, Lehmann, and von Renesse, 2020), and has to be interpreted as a formal restatement of the large

[12]We omit the explicit form of terms of the order of ϵ and ϵ^2, which are symmetric, as they cancel in the sum of Eq. (192).

deviations principle given by the action in Eq. (190). Alternatively, it can be viewed as an effective low-wave-number field theory, which is equivalent to restoring a minimal distance, i.e., the underlying lattice constant ϵ. In adddition, Eq. (196) is a continuous-space limit of the underlying lattice model, not a hydrodynamic equation for a macroscopic field obtained by locally integrating (i.e., coarse graining) the variables $c_{\alpha,x}$ (Spohn, 2012).

Equation (196) is at the basis of the macroscopic fluctuation theory (Bertini *et al.*, 2015), in which the diffusion flux is recast as the Fick law,

$$\chi_\alpha(c)\boldsymbol{\nabla}\frac{\delta\phi}{\delta c_\alpha} = D_\alpha(c)\boldsymbol{\nabla}c, \tag{197}$$

with the diffusivity obeying the Einstein relation

$$D_\alpha = \chi_\alpha \partial^2_{c_\alpha}\phi. \tag{198}$$

Equation (198) is a form of the fluctuation-dissipation relation that replaces in continuous space the detailed balance relation. In fact, the continuous-space limit reduces the initial local detailed balance assumption to a condition of local equilibrium: since the transitions $\rho \in C$ are associated with points in physical space, the reservoirs responsible for them must be accordingly distributed in space, thus creating a continuum background of local equilibria.

A particularly well-known instance of Eq. (196) is the Dean-Kawasaki equation, which describes the density of identical particles interacting through a two-body potential $U(r-r')$ (Dean, 1996; Kawasaki, 1998). It is obtained by setting

$$\phi[c] = \frac{1}{T}u[c] - s_{\mathrm{int}}[c], \tag{199}$$

with the scaled internal energy and entropy

$$\begin{aligned} u[c] &= \tfrac{1}{2}\int dr \int dr' c(r)U(r-r')c(r'), \\ s_{\mathrm{int}}[c] &= -\int drc(r)[\ln c(r) - 1], \end{aligned} \tag{200}$$

as well as $\chi(c) \propto c$. While it was originally derived starting with the overdamped Langevin equations for the coordinates of an ensemble of identical particles, here it follows from the continuous limit of a Markov jump process on the lattice with transition rates satisfying the aforementioned scaling (Lefevre and Biroli, 2007). For $f = 0$ the average value of Eq. (196) reduces to the central equation of dynamic density functional theory (Marconi and Tarazona, 1999).

Another important class is that of simple exclusion processes obtained using Eq. (199) with the free energy of an ideal binary mixture,

$$\begin{aligned} u[c] &= 0, \\ s_{\mathrm{int}}[c] &= -\int dr\{c(r)\ln c(r) + [1-c(r)]\ln[1-c(r)]\}, \end{aligned} \tag{201}$$

and the mobility $\chi(c) \propto c(1-c)$ (Lefevre and Biroli, 2007; Tailleur, Kurchan, and Lecomte, 2007; Bertini *et al.*, 2015).

The full action in Eq. (190) shows that for large Ω the most likely trajectories dominate the statistical averages. In particular, the probability density function of the stochastic field $c(r,t)$ acquires the large deviations form

$$p[c(r),t] \asymp e^{-\Omega I[c(r),t]}, \tag{202}$$

with the rate functional I. Analogous considerations on the macroscopic dynamics discussed previously for the finite-dimensional case apply here to the field theoretical description (Bertini *et al.*, 2015). In particular, when the set R is empty, the functional analog of the Hamilton-Jacobi equation (32) can be obtained from the Fokker-Planck equation associated with Eq. (196) (Zinn-Justin, 2002),

$$\partial_t p = \int dr \frac{\delta}{\delta c(r)}\left[-p\boldsymbol{\nabla}\cdot j + \frac{1}{\Omega}\frac{\delta(\chi p)}{\delta c(r)}\right] =: -\int dr \frac{\delta \mathbf{j}}{\delta c(r)}. \tag{203}$$

We have introduced the probability current $\mathbf{j}[c]$, as we did in Sec. III.E for the finite-dimensional case. It should not be confused with $j[c]$, which is the current of the physical field $c(r,t)$.

Plugging the large-deviation ansatz for $p[c]$ [Eq. (202)] into Eq. (203), we obtain the Hamilton-Jacobi equation

$$-\partial_t I[c(r),t] = \int dr \mathcal{H}_C\left(c(r), \frac{\delta I}{\delta c(r)}\right), \tag{204}$$

whose stationary limit (when it exists) gives

$$\int dr \mathcal{H}_C\left(c(r), \frac{\delta I_{\mathrm{ss}}}{\delta c(r)}\right) = 0. \tag{205}$$

The instanton dynamics outlined in Sec. IV.A remains formally unaltered (Elgart and Kamenev, 2004).

Moreover, one recognizes that the stationary probability velocity in the macroscopic limit [corresponding to the definition in Eq. (70) for the finite-dimensional case],

$$\lim_{V\to\infty}\lim_{t\to\infty}\frac{\mathbf{j}[c]}{p[c]} = -\boldsymbol{\nabla}\cdot\left[j(c) + \chi(c)\cdot\boldsymbol{\nabla}\frac{\delta I_{\mathrm{ss}}}{\delta c}\right] = -\boldsymbol{\nabla}\cdot j_A(c), \tag{206}$$

is the negative divergence of the nonconservative part of the macroscopic physical current j. This generalizes Eq. (70) to field theories and gives the orthogonal decomposition [cf. Eq. (71)] for the physical current

$$j = -\chi\cdot\boldsymbol{\nabla}\frac{\delta I_{\mathrm{ss}}}{\delta c} + j_A, \tag{207}$$

with $\int dr j_A\cdot\boldsymbol{\nabla}(\delta I_{\mathrm{ss}}/\delta c) = 0$. A similar decomposition holds for nonautonomous dynamics, except that I_{ss} is replaced by I^t_{ss}, the solution of Eq. (205) with driving frozen at its instantaneous value at time t.

In the most general case, i.e., when the set R is not empty, the macroscopic noiseless equation reads

$$\partial_t x(r,t) = -\nabla \cdot j + \sum_{\rho \in R} \Delta_\rho r_\rho(x(r,t)), \tag{208}$$

which is the general form of a reaction-diffusion-advection equation of interacting (Aslyamov *et al.*, 2023) and driven (or active) particles; see the example in Sec. VII.C. The last term in (208) makes the stochastic field c not conserved, i.e., in general $d_t \int dr c(r,t) = \int dr \sum_{\rho \in R} \Delta_\rho r_\rho(c(r,t)) \neq 0$. However, there might exist globally conserved quantities $c \cdot \ell$, with ℓ the left null vector(s) of the matrix Δ_ρ, namely, $\ell \cdot \Delta_\rho = 0$ for all $\rho \in R$ (Falasco, Rao, and Esposito, 2018; Rao and Esposito, 2018b; Avanzini, Falasco, and Esposito, 2019). Note that the decompositions in Eqs. (71) and (207) are still valid, but the orthogonal conditions are replaced by the single property $\int dr [v_{\rm ss} - \nabla \cdot j_A](\delta I_{\rm ss}/\delta c) = 0$.

Extending the Gaussian theory of Sec. IV.C to the infinite-dimensional case, we can linearize the stochastic dynamics around the solutions $x(r,t)$ of the deterministic equation (208) setting $\varrho(r,t) = c(r,t) - x(r,t)$. This amounts to a parabolic approximation of the rate functional $I[\varrho,t] = -(1/2)\int dr \int dr' \varrho(r) \cdot \mathcal{C}^{-1}(r,r',t) \cdot \varrho(r') + O(\varrho^3)$ and gives an equation for the covariance matrix $\mathcal{C}$ that is analogous to Eq. (128) and the Lyapunov equation (129) (under stationary conditions). This approach was employed to derive analytic expressions for the correlation length of noisy Turing patterns (Vance and Ross, 1999), but a connection to thermodynamics has not been deeply explored; see Rana and Barato (2020), however.

B. Continuous-space limit: Entropy production

The continuous-space limit can be implemented in the deterministic limit of the microscopic expression of the entropy production in Eq. (61). For transitions $\rho \in C$ the difference between the transition rates and nonconservative forces read, at leading order in ϵ, respectively,

$$\begin{aligned} r_\rho(c) - r_{-\rho}(c) &\to \epsilon^{-2}\chi(c) \cdot \epsilon \left[-\nabla \frac{\delta \phi}{\delta c} + f\right] = \frac{1}{\epsilon} j[c], \\ \Delta_\rho \partial_c \phi + a_\rho &\to \epsilon \left[-\nabla \frac{\delta \phi}{\delta c} + f\right] = \epsilon \chi(c)^{-1} \cdot j[c], \end{aligned} \tag{209}$$

where $j[c]$ is the hydrodynamic current defined in Eq. (196). Plugging Eq. (209) into Eq. (61), we get

$$\begin{aligned} \lim_{\Omega \to \infty} \frac{1}{\Omega} \langle \dot{\Sigma} \rangle = &\int dr j[x] \cdot \chi(x(r,t))^{-1} \cdot j[x] \\ &+ \int dr \sum_{\rho \in R} r_\rho(x(r,t)) \sigma_\rho(x(r,t)), \end{aligned} \tag{210}$$

where the first term corresponds to the entropy production associated with the Langevin equation (196). The second term in Eq. (210), due to transitions unaffected by this limit, is different from the informational entropy production associated with the Langevin equation; see Sec. IV.E. The thermodynamic inconsistencies arising from an incorrect application of the Langevin approximation have been observed for various specific model systems (Brillouin, 1950; Horowitz, 2015; Ceccato and Frezzato, 2018). In Eq. (210) we have shown that such inconsistency extends to field theories that try to infer the entropy production solely on the basis of the dynamics in state space. This means that in field theories of active matter all internal processes must be resolved in general, including the chemical reactions necessary for self-propulsion. In addition, we remark that the second line in Eq. (210) differs from the entropy production obtained by linearizing the dynamics of transitions $\rho \in R$ (Markovich *et al.*, 2021) unless they are close to detailed balance (i.e., $a_{\rho \in R} \to 0$).

The first term in Eq. (210) can be decomposed as in Eq. (113) using Eq. (196) and integrating by parts,

$$\lim_{\Omega \to \infty} \frac{1}{\Omega} \langle \dot{\Sigma} \rangle = -d_t \phi[x(r,t),t] + \partial_t \phi[c,t]|_{c=x(r,t)} + \dot{\sigma}_{\rm nc}. \tag{211}$$

On the right-hand side of Eq. (211), the first two terms are the total variation in time of the thermodynamic potential plus the dissipation of driving (zero only for autonomous dynamics), while the third is the total dissipation due to nonconservative forces acting in the discrete and continuous space,

$$\dot{\sigma}_{\rm nc} = \int dr \left[\sum_{\rho \in R} r_\rho(x(r,t)) a_\rho(x(r,t)) + j[x] \cdot f(r)\right]. \tag{212}$$

In Eq. (212) we have assumed that the flow $j \cdot \delta\phi/\delta c$ at the boundaries is zero. However, different boundary conditions can be imposed by a specific scaling of a set of transitions $\rho \in R$ located at the boundaries (Bertini *et al.*, 2015).

When the set R is empty, one can show that the orthogonal decomposition in Eq. (207) naturally induces a splitting of the entropy production into the nonadiabiatic component [corresponding to the "excess work" of Bertini *et al.* (2013) for autonomous relaxation],

$$\begin{aligned} \lim_{\Omega \to \infty} \frac{1}{\Omega} \langle \dot{\Sigma}_{\rm na} \rangle &= -d_t I_t[x(r,t)] + \partial_t I^t_{\rm ss}[c]|_{c=x(r,t)} \\ &= \int dr \nabla \frac{\delta I_t}{\delta x} \cdot \chi(x) \cdot \nabla \frac{\delta I_t}{\delta x} \geq 0, \end{aligned} \tag{213}$$

and the adiabatic component,

$$\begin{aligned} \lim_{\Omega \to \infty} \frac{1}{\Omega} \langle \dot{\Sigma}_{\rm ad} \rangle &= \lim_{\Omega \to \infty} \frac{1}{\Omega} (\langle \dot{\Sigma} \rangle - \langle \dot{\Sigma}_{\rm na} \rangle) \\ &= \int dr j_A[x] \cdot \chi(x)^{-1} \cdot j_A[x] \geq 0. \end{aligned} \tag{214}$$

Equations (213) and (214), being quadratic forms, are both non-negative. We can combine Eqs. (211) and (214) to eliminate the entropy production rate,

$$\begin{aligned} \dot{\sigma}_{\rm nc} + \partial_t \phi[c,t]|_{c=x(r,t)} - \lim_{\Omega \to \infty} \frac{1}{\Omega} \langle \dot{\Sigma}_{\rm ad} \rangle &= d_t \phi[x] + \lim_{\Omega \to \infty} \frac{1}{\Omega} \langle \dot{\Sigma}_{\rm na} \rangle \\ &\geq d_t \phi[x]. \end{aligned} \tag{215}$$

In Eq. (215), for systems with reservoirs at the same temperature T, the first line is the "renormalized work" rate (times the factor T) and the last line is the nonequilibrium Clausius inequality as defined by macroscopic fluctuation theory (Bertini *et al.*, 2013). The renormalized work counts only the energy needed in a transformation, discarding the energy that keeps the system away from equilibrium. In the context of stochastic thermodynamics, different definitions have been proposed for such a quantity (Hatano and Sasa, 2001; Maes and Netočný, 2014), inspired by the early phenomenological approaches to nonequilibrium thermodynamics (Oono and Paniconi, 1998; Sasa and Tasaki, 2006). Note that Eq. (215) is not peculiar to the continuous-space limit but can be equally written for the intensive quantities appearing in Eqs. (113), (67), and (66).

VI. EMERGENT STOCHASTIC THERMODYNAMICS

The picture appearing in Sec. IV is that of a stochastic dynamics asymptotically characterized by two distinct regimes: relatively fast relaxation in a basin [Eq. (45)] followed by small Gaussian fluctuations on the attractor [Eq. (126)] and rare large fluctuations corresponding to jumps between nearby attractors along transition trajectories, i.e., the sum of instanton and noiseless relaxation paths. Hence, it is natural to asymptotically describe the stochastic dynamics as a Markov jump process on the space of the various attractors (see Fig. 1), with transition rates given by Eq. (157) at leading order in V (Qian *et al.*, 2016; Smith, 2020). This description is valid when the macroscopic dynamics [Eq. (45)] have isolated fixed points and sufficiently regular time-dependent attractors and is far from a bifurcation; see Sec. VII.C for an example in which this condition is not met (Graham, 1987; Freidlin and Wentzell, 1998). For simplicity, we restrict to autonomous dynamics in the following.

For large V the probability density of states can be approximated as

$$p(c,\tau) \asymp e^{-VI(c,\tau)} \to \sum_\gamma \mathscr{p}_\gamma(\tau)\delta_V(c-x_\gamma^*), \tag{216}$$

where $\delta_V(c-x_\gamma^*)$ is a strongly peaked function with support on the ball $\mathcal{B}_\gamma$ with radius[13] $O(V^{-1/2})$, which is centered on x_γ^* (whose boundary is denoted as $\partial\mathcal{B}_\gamma$). This is normalized such that $\mathscr{p}_\gamma(\tau) \coloneqq \int_{\mathcal{B}_\gamma} dc\, p(c,\tau)$ and tends to a Dirac delta as $V\to\infty$.

The probability of finding the system in the neighborhood of the attractor γ at time τ, i.e., $\mathscr{p}_\gamma(\tau)$, is determined by the master equation

$$d_\tau \mathscr{p}_\gamma(\tau) = \sum_\nu \delta_{\circ(\nu)\gamma}[\kappa_{-\nu}\mathscr{p}_{\circ(-\nu)}(\tau) - \kappa_\nu \mathscr{p}_\gamma(\tau)], \tag{217}$$

where $\circ(\nu)$ denotes the origin of the transition ν.

Time-integrated observables of the form of Eq. (167) are split by summing the intrabasin and interbasin contributions as

$$\mathcal{O}[\mathcal{X}] = \sum_\gamma \int_0^\tau dt\, \dot{\mathcal{O}}(t)\Theta_\gamma(t) + \sum_\nu \int_0^\tau dt\, \dot{\mathcal{O}}(t)\Theta_\nu(t) + \varepsilon[\mathcal{X}]. \tag{218}$$

In Eq. (218) $\Theta_\gamma(t)=1$ if $n(t)\in\mathcal{B}_\gamma$ and $\Theta_\gamma(t)=0$ otherwise, while $\Theta_{+\nu}(t)=1$ [$\Theta_{-\nu}(t)=1$] if $n(t)$ belongs to a tube of width $V^{-1/2}$ centered on a transition trajectory going from $\partial\mathcal{B}_\gamma$ to $\partial\mathcal{B}_{\gamma'}$ (a transition trajectory going from $\partial\mathcal{B}_{\gamma'}$ to $\partial\mathcal{B}_\gamma$) and $\Theta_{+\nu}(t)=0$ otherwise. The functional $\varepsilon[\mathcal{X}]$ accounts for trajectories exiting and reentering the same ball, incomplete transition attempts, and transitions between different balls happening far from the transition path. Since they become exponentially unlikely in the macroscopic limit, we neglect $\varepsilon[\mathcal{X}]$ in the following. Therefore, for large V and for τ much larger than the typical relaxation times within each basin, we can recast the macroscopic rate of the scaled observable [Eq. (218)] as

$$\frac{\mathcal{O}[\mathcal{X}]}{V\tau} =: \dot{o} = \sum_\gamma \dot{o}_\gamma \mathcal{P}_\gamma(\tau) + \sum_\nu o_\nu \mathcal{I}_\nu(\tau), \tag{219}$$

where $\dot{o}_\gamma$, o_ν, $\mathcal{P}_\gamma$, and $\mathcal{I}_\nu$ are independent stochastic variables defined in the following.

The observable $\mathcal{P}_\gamma(\tau) \coloneqq (1/\tau)\int_0^\tau dt\Theta_\gamma(t)$ is the empirical density on the attractor γ satisfying $\langle\mathcal{P}_\gamma\rangle = \mathscr{p}_\gamma$. The number of transitions between attractors γ and γ' through x_ν divided by the time span τ is given by $\mathcal{I}_\nu(\tau)$, which asymptotically approaches a conditional Poisson distribution with intensity κ_ν given by Eq. (157) (Day, 1983; Graham, 1987; Freidlin and Wentzell, 1998). In other words, it is the empirical flux through the saddle ν satisfying $\langle\mathcal{I}_\nu\rangle = \kappa_\nu \mathscr{p}_{\circ(\nu)}$. Note that the sum over ν, in Eq. (219) and hereafter, counts transitions in the two directions.

The observable

$$\dot{o}_\gamma \coloneqq \frac{1}{V}\frac{\int_0^\tau dt\dot{\mathcal{O}}(t)\Theta_\gamma(t)}{\int_0^\tau dt\Theta_\gamma(t)} \tag{220}$$

is the time-independent rate of $o[\mathcal{X}]$ inside the attractor γ, i.e., in an infinitesimal neighborhood of x_γ^*. Its scaled cumulant generating function can be obtained by the scaled tilted action [Eq. (176)] evaluated on the constant optimal trajectories $\{\bar{c},\bar{\pi}\}$, i.e., the solutions of the time-independent version of Eq. (177) such that $\bar{c}=x_\gamma^*$ and $\bar{\pi}=0$ as $z\to 0$,

$$K_{\dot{o}_\gamma}(z) = \mathcal{H}_z(\bar{c},\bar{\pi}). \tag{221}$$

In practice, one may want to approximate the statistics of Eq. (221) at the Gaussian level by retaining only terms of the order of $\mathcal{O}(z^2)$ in $\mathcal{A}_z$ (Nguyen and Seifert, 2020).

The observable o_ν is the contribution of $o[\mathcal{X}]$ along the transition path through x_ν,

$$o_\nu \coloneqq \frac{1}{V}\int_0^{\tau_\nu^{\mathrm{tr}}} dt\dot{\mathcal{O}}(t)\Theta_\nu(t). \tag{222}$$

[13]The fact that Gaussian fluctuations are of the order of $O(V^{-1/2})$ can be seen in Sec. IV.C.

Its scaled cumulant generating function can be approximated by the tilted action [Eq. (176)] evaluated on the optimal trajectories $\{\bar{c}(t), \bar{\pi}(t)\}$, i.e., the solutions of Eq. (177) such that $\bar{c}(0) \in \partial\mathcal{B}_\gamma$ and $\bar{c}(\tau_\nu^{\rm tr}) \in \partial\mathcal{B}_{\gamma'}$ as $z \to 0$,

$$K_{\mathscr{o}_\nu}(z, \tau_\nu^{\rm tr}) = \mathcal{A}_z[\{\bar{c}(t), \bar{\pi}(t)\}]. \tag{223}$$

The duration $\tau_\nu^{\rm tr}$ of this trajectory is a stochastic variable itself, whose mean differs from the mean escape time $1/\kappa_\nu$ from a basin of attraction: $\tau_\nu^{\rm tr}$ refers to the transition time of those rare trajectories that have just exited $\mathcal{B}_\gamma$. Thus, it does not account for the exponentially long dwelling time in the neighborhood of a fixed point—which on the contrary enters $1/\kappa_\nu$. To our knowledge, its probability distribution has been evaluated only for detailed balance systems with Gaussian noise. In this case the most probable value of $\tau_\nu^{\rm tr}$ and its mean $\langle \tau_\nu^{\rm tr} \rangle$ grow as the logarithm of the inverse noise strength and coincide in the limit of vanishing noise (Caroli, Caroli, and Roulet, 1979, 1981; Caroli *et al.*, 1980; Malinin and Chernyak, 2010). Even though we are not aware of similar results for systems with nonconservative forces and non-Gaussian noise, one can speculate about replacing $\tau_\nu^{\rm tr}$ in Eq. (223) with its mean value, as measured in computer simulations or experiments. Not only the statistics of transition times but also those of (thermo) dynamic observables conditioned on transition paths remain a subject to be explored in systems lacking detailed balance.

In particular, we can write the mean entropy production rate on the network of attractors as

$$\langle \dot{\sigma} \rangle = \sum_\gamma \langle \dot{\sigma}_\gamma \rangle \mathscr{p}_\gamma + \sum_{\nu>0} (\langle \sigma_\nu \rangle \kappa_\nu \mathscr{p}_{\circ(\nu)} + \langle \sigma_{-\nu} \rangle \kappa_{-\nu} \mathscr{p}_{\circ(-\nu)}) - d_\tau \sum_\gamma \mathscr{p}_\gamma \frac{\ln \mathscr{p}_\gamma}{V}, \tag{224}$$

where the last term is obtained using the expression for the probability density [Eq. (216)] in the Shannon entropy [Eq. (56)]. Equation (224) has three important differences with respect to its definition on the mesoscopic dynamics. (i) The existence of a mean state entropy production rate,

$$\langle \dot{\sigma}_\gamma \rangle = \sum_{\rho>0} [r_\rho(x_\gamma^*) - r_{-\rho}(x_\gamma^*)] \ln \frac{r_\rho(x_\gamma^*)}{r_{-\rho}(x_\gamma^*)} \geq 0, \tag{225}$$

which is independent of the macroscopic transitions, stemming from the continuous dissipation needed to sustain the attractors. (ii) The mean entropy production associated with a macroscopic transition $\langle \sigma_\nu \rangle$ that is not given by the log ratio of macroscopic transition rates $\kappa_{\pm\nu}$. Indeed, as shown in Sec. IV, the transition rates do not generally obey the local detailed balance condition, unless the system is close to equilibrium; see Eq. (159). (iii) The presence of all fluxes in Eq. (224), which cannot be written in terms of currents, since in general $\sigma_{-\nu} \neq -\sigma_\nu$. This is because the breaking of time reversibility in the underling mesoscopic dynamics implies that the transition path between γ and γ' is not equal to the time-reversed transition path between γ' and γ. Even when these paths are the same, such as in the low-dimensional systems of Secs. VII.A.1 and VII.B.1, $\sigma_{-\nu}$ need not equal $-\sigma_\nu$, because of Eq. (179).

At linear order in a_ρ around detailed balance, Eq. (224) reduces to the standard expression of traditional stochastic thermodynamics [Eq. (8)]. In this limit we find that $\langle \dot{\sigma}_\gamma \rangle = \sum_\rho r_\rho^{(0)}(x_{\rm eq}) a_\rho = 0$, the transition entropy production σ_ν changes sign under path reversal because of Eq. (153), and the transition rates satisfy local detailed balance [Eq. (159)].

Finally, we observe that the constant α_γ introduced in Eq. (55) as the relative weight of the attractor γ is related to the stationary probability $\mathscr{p}_\gamma^{\rm ss}$ solution of Eq. (217) as $\alpha_\gamma = -(1/V) \ln \mathscr{p}_\gamma^{\rm ss}$. In the Freidlin-Wentzell theory (Freidlin and Wentzell, 1998), $\mathscr{p}_\gamma^{\rm ss}$ is calculated by the matrix-tree theorem for Markov chains (Zia and Schmittmann, 2007; Polettini, 2015; Çetiner and Gunawardena, 2022; Dal Cengio, Lecomte, and Polettini, 2023), retaining only the leading spanning tree monomial in the limit $V \to \infty$ (Maes and Netočný, 2013).

VII. APPLICATIONS

We now exemplify the general theory of the previous sections in three prototypical classes of model systems, namely, networks of chemical reactions, nonlinear electronic circuits, and driven interacting units.

A. Chemical reaction networks

We consider chemical species in a volume V of solvent in equilibrium at temperature T. Mass transport (for example, by diffusion or advection) is taken to be fast enough to homogenize the local distribution of chemicals on the typical timescales of the reactions. All the internal (for example, vibrational or rotational) degrees of the chemicals are assumed to be at equilibrium such that the only relevant dynamical variables are the number of particles n_i of the dynamical species labeled by i. In a closed system chemical reactions exclusively involve the N chemical species. In open systems they also involve N_Y chemostatted species, whose concentrations c_y are externally prescribed (Rao and Esposito, 2016).

We first consider closed systems and assume that chemical reactions are well described via a Markov jump process with transitions $\rho \in R$. The associated transition rates read (Gillespie, 1992; Schmiedl and Seifert, 2007)

$$R_\rho(n) = V k_\rho \prod_{i=1}^N \frac{1}{V^{\nu_\rho^i}} \frac{n_i!}{(n_i - \nu_\rho^i)!}, \tag{226}$$

where the stoichiometric coefficient ν_ρ^i ($\nu_{-\rho}^i$) is the number of reactants (products) of species i involved in the reaction ρ. The entries of the jump matrix are given by $\Delta_\rho^i = \nu_{-\rho}^i - \nu_\rho^i$. Equation (226) is known as mass-action kinetics and holds for elementary reactions between diluted chemicals (Avanzini *et al.*, 2021). The reaction constants k_ρ are independent of V and satisfy

$$T \log \frac{k_\rho}{k_{-\rho}} = -\sum_{i=1}^N \Delta_\rho^i \mu_i^\circ, \tag{227}$$

where μ_i° is the standard chemical potential of the dynamical chemical species i, including the contribution of the solvent. The mesoscopic local detailed balance [Eq. (5)] holds in the form

$$T\Sigma_\rho(n) = -\Phi_{\rm can}(n+\Delta_\rho) + \Phi_{\rm can}(n) \tag{228}$$

with the "canonical" Gibbs free energy of a mixture of N ideal gasses,

$$\Phi_{\rm can}(n) = \mu^\circ \cdot n + T \ln n!. \tag{229}$$

The system is closed; namely, no matter is exchanged with the environment. The system dynamics is detailed balance since Eq. (228) does not display nonconservative forces: $a_\rho = 0$. Moreover, the quantities $L(n) \coloneqq \ell \cdot n$ are conserved, with the vectors ℓ defined by $\ell \cdot \Delta_\rho = 0$ for all ρ. The conservation follows from multiplying Eq. (1) by ℓ. For instance, the number of atoms of each chemical element and the charges are conserved. The system relaxes to the Gibbs distribution

$$P_{\rm eq}(n) \propto e^{-\Phi_{\rm can}(n)/T} \delta(L(n) - L), \tag{230}$$

which is constrained by the value of the conserved quantities fixed by the initial conditions.

We now turn to open systems where chemostats are present, i.e., $N_Y \geq 1$ chemical species (labeled as y) have a large copy number controlled by external reservoirs, while N species continue to evolve stochastically. The transition rates [Eq. (226)] become

$$R_\rho(n) = V k_\rho \prod_{y=1}^{N_Y} c_y^{\nu_\rho^y} \prod_{i=1}^{N} \frac{1}{V^{\nu_\rho^i}} \frac{n_i!}{(n_i - \nu_\rho^i)!}, \tag{231}$$

where $c_y = n_y/V$ is the externally controlled concentration of chemostatted species y. The local detailed balance of the open system reads

$$T\Sigma_\rho(n) = -\Phi_{\rm can}(n+\Delta_\rho) + \Phi_{\rm can}(n) - \sum_{y=1}^{N_Y} \Delta_\rho^y \mu_y, \tag{232}$$

where the last sum represents the free energy exchanged with the reservoirs with $\mu_y = \mu_y^\circ + RT \ln c_y$, the chemical potential of the chemostats.

We obtain the Massieu potential $\Phi(n)$ that appears in Eq. (5) by subtracting the free-energy contribution of the exchanged matter. The "semigrandcanonical" Gibbs free energy reads

$$\Phi(n) = \Phi_{\rm can}(n) - \tilde{\mu} \cdot n, \tag{233}$$

where $\tilde{\mu}_i$ is the chemical potential of the part of species i that is exchanged with the chemostats. This is obtained by means of the quantities $L(n)$ that are no longer conserved when the system is opened. The nonconservative forces a_ρ can be given in terms of the projection of cycle affinities $\mathcal{A}_{\rm nc}^k = \sum_\rho C_\rho^k \sum_{y=1}^{N_Y} \Delta_\rho^y \mu_y$ on the transition ρ,

$$a_\rho = \sum_k \mathcal{A}_{\rm nc}^k \mathbb{X}_\rho^k, \tag{234}$$

where $\mathbb{X}_\rho^k$ counts how many times the reaction ρ takes place in the cycle k. A cycle[14] is a sequence of transitions C_ρ, defined by $\sum_\rho \Delta_\rho^i C_\rho = 0$ for all $i = \{1, \ldots, N\}$, that leave the dynamical species unchanged overall but results in exchange of matter between reservoirs.

In the macroscopic limit $V \to \infty$, the concentration $c_i = n_i/V$ of the species i stay finite. From Eq. (226) it is straightforward to derive that the macroscopic transition rates [Eq. (27)] are the polynomials

$$r_\rho(c) = k_\rho \prod_{j=1}^{N} c_j^{\nu_\rho^j}. \tag{235}$$

Moreover, the Massieu potential [Eq. (236)] is extensive as required by Eq. (26), and its density is obtained by applying Stirling's approximation,

$$\phi(c) = \mu^\circ \cdot c + T \sum_{i=1}^{N} (c_i \log c_i - c_i) - \tilde{\mu} \cdot c. \tag{236}$$

At infinite volume V, the deterministic dynamics [Eq. (45)] is the chemical rate equation (Kurtz, 1972; Anderson and Kurtz, 2011)

$$d_t c = \sum_\rho \Delta_\rho k_\rho \prod_{j=1}^{N} c_j^{\nu_\rho^j}. \tag{237}$$

Since Eq. (236) has a single minimum for a given value of conserved quantities, a macroscopic chemical reaction network at detailed balance can only have a single stable fixed point (Snarski, 2021). To create multiple attractors, it is necessary either to consider interactions [i.e., to go beyond the mass-action kinetics (Avanzini *et al.*, 2021)] that make Eq. (236) nonconvex or to introduce nonconservative forces that induce a quasipotential $I_{\rm ss}$ with multiple minima. Nonconservative forces can also create more complex time-dependent attractors, such as limit cycles (Boland, Galla, and McKane, 2008) and chaos (Epstein and Pojman, 1998; Gaspard, 2020). In the following we provide examples for dissipative multistability and periodic attractors.

1. Dissipative metastability: The Schlögel model

We consider the Schlögel model (Schlögl, 1972; Vellela and Qian, 2009; Lazarescu *et al.*, 2019), an autocatalytic chemical system displaying bistability far from equilibrium. It consists of the following set of chemical reactions:

$$2\mathsf{X} + \mathsf{A} \underset{k_{-1}}{\overset{k_{+1}}{\rightleftharpoons}} 3\mathsf{X}, \qquad \mathsf{B} \underset{k_{-2}}{\overset{k_{+2}}{\rightleftharpoons}} \mathsf{X}. \tag{238}$$

In Eq. (238) species A and B are chemostatted reservoirs with constant concentration a and b, respectively. The only degree

[14]Only emergent cycles enter Eq. (234), i.e., those that appear when the system is chemostatted.

of freedom is the number n of molecules of species X. The mesoscopic reaction rate [Eq. (226)] reads

$$R_1(n) = \frac{k_{+1}}{V} an(n-1), \qquad R_2 = k_{+2} b,$$
$$R_{-1}(n) = \frac{k_{-1}}{V^2} n(n-1)(n-2), \qquad R_{-2}(n) = k_{-2} n. \tag{239}$$

and in the macroscopic limit $V \to \infty$ it gives for Eq. (235)

$$r_1(c) = k_{+1} a c^2, \qquad r_{-1}(c) = k_{-1} c^3,$$
$$r_2 = k_{+2} b, \qquad r_{-2}(c) = k_{-2} c. \tag{240}$$

The chemical rate equation [Eq. (237)] reads

$$d_t x = r_1(x) - r_{-1}(x) + r_2 - r_{-2}(x). \tag{241}$$

The only cycle affinity $\mathcal{A}_{\mathrm{nc}} = \mu_A - \mu_B =: \Delta\mu$ is the chemical potential difference of the two reservoirs and corresponds to the log ratio of rates along a cycle

$$\Delta\mu = \ln \frac{r_1(c) r_{-2}(c)}{r_{-1}(c) r_2} = \ln \frac{a k_1 k_{-2}}{b k_{-1} k_2}. \tag{242}$$

If we set $k_{+1} a = 1 = k_{+2} b$ by choosing appropriate units for time and concentrations, Eq. (242) gives the parametrization of the rate constant $k_{-1} = k_{-2} e^{-\Delta\mu}$ in terms of k_{-2} and $\Delta\mu$. Detailed balance is realized for $\Delta\mu = 0$ such that both currents vanish $r_1(x^{\mathrm{eq}}) - r_{-1}(x^{\mathrm{eq}}) = 0 = r_2 - r_{-2}(x^{\mathrm{eq}})$. This condition yields the equilibrium fixed point $x^{\mathrm{eq}} = 1/k_{-2}$.

Since the model is a one-step jump process in one dimension, the exact quasipotential I_{ss} is obtained by integrating Eq. (137),

$$I_{\mathrm{ss}}(c) = c \log\left(\frac{c(1 + e^{-\Delta\mu} c^2)}{x^{\mathrm{eq}}(1 + c^2)}\right) - c + \mathrm{const}$$
$$+ 2 e^{\Delta\mu/2} \arctan\left(e^{-\Delta\mu/2} c\right) - 2 \arctan(c), \tag{243}$$

where the constant is the normalization ensuring that $\min_\gamma I_{\mathrm{ss}}(x_\gamma^*) = 0$. For $\Delta\mu = 0$ the first line in Eq. (243) is the free energy [Eq. (236)]. The rate function is nonconvex for $\Delta\mu \geq \ln 9$ and can display two local minima, $x_1^* < x_2^*$ only for $k_{-2} \geq \sqrt{3}$, which correspond to the two stable fixed points of Eq. (241). The appearance of metastability at the stochastic level corresponds to a saddle node or a supercritical pitchfork bifurcation at the deterministic level, depending on how the parameters k_{-2} and $\Delta\mu$ are varied (Remlein and Seifert, 2024). At large V the transition times between the two metastable states are determined by the quasipotential barrier height $\Delta I_{\mathrm{ss}} := I_{\mathrm{ss}}(x_\nu) - I_{\mathrm{ss}}(x^*)$, according to Eq. (157). We compare the exact expression [Eq. (243)] with the approximated quasipotential [Eq. (138)] obtained by truncating the master equation into a chemical Fokker-Planck equation [Eq. (134)]. Figure 4 displays the difference in barrier height between the two expressions,

$$\delta := \Delta I_{\mathrm{ss}} - \Delta I_{\mathrm{FPE}}, \tag{244}$$

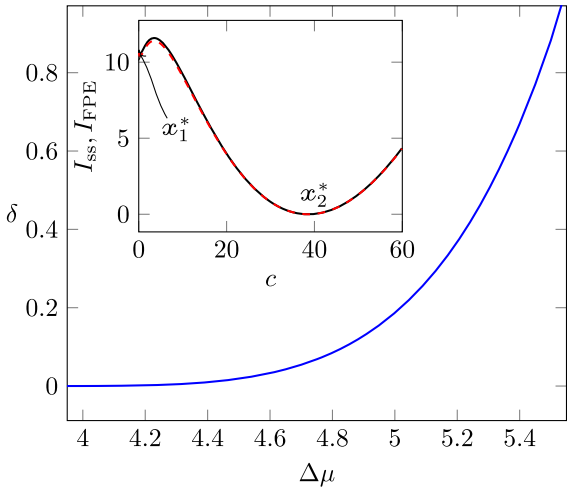

FIG. 4. Difference in the barrier height [Eq. (244)] for a fixed point $x_2^* > x_1^*$ as a function of the chemical potential difference $\Delta\mu$ for $k_{-2} = 3.5$. Bistability is present above the critical value $\Delta\tilde{\mu} \simeq 3.85$. Inset: the quasipotential I_{ss} given by Eq. (243) (the solid line) and its approximation I_{NLE} (the dashed line) for $k_{-2} = 3.5$ and $\Delta\mu = 5$.

with $\Delta\mu$ varied at fixed k_{-2}. The chemical Fokker-Planck equation is accurate close to the bifurcation, while it systematically underestimates the barrier height away from it (Gaveau and Schulman, 1998). Note that a difference $\delta \simeq 0.2$ for $V \simeq 30$ would result in a transition rate that is around 400 times larger than κ_ν.

Since the system is one dimensional, the stationary probability current [Eq. (69)] must be zero everywhere in order to vanish at infinity and to have zero derivative. Therefore, $v_{\mathrm{ss}}(c) = 0$ for all c, and the deterministic drift $F(c) = -\mathcal{M}(c)\partial_c I_{\mathrm{ss}}$ is composed only of the gradient part with mobility [Eq. (73)], $\mathcal{M} = (\tilde{r}_1 - \tilde{r}_{-1})/\ln(\tilde{r}_1/\tilde{r}_{-1})$, a monotonically growing function of c. Here $\tilde{r}_1 = r_1 + r_2$ and $\tilde{r}_{-1} = r_{-1} + r_{-2}$ are the lumped rates that enter the information-theoretic entropy production rate [Eq. (68)],

$$\dot{\sigma}_{\mathrm{info}}(c) = \underbrace{[\tilde{r}_1(c) - \tilde{r}_{-1}(c)]}_{F(c)} \underbrace{\ln \frac{\tilde{r}_1(c)}{\tilde{r}_{-1}(c)}}_{-\partial_c I_{\mathrm{ss}}(c)}. \tag{245}$$

Hence, the dynamics in configuration space appears to be reversible,[15] and one can check by direct substitution of Eq. (137) into Eq. (109) that relaxation and instanton dynamics are time reversals of each other,

$$d_t c(t) = \tilde{r}_1 e^{\partial_c I_{\mathrm{ss}}} - \tilde{r}_{-1} e^{-\partial_c I_{\mathrm{ss}}} = -(r_1 - r_{-1})$$
$$= -d_t x(t). \tag{246}$$

However, the underlying chemical reactions are not in equilibrium, as witnessed by the fact that the dual rates,

[15] One can also write the drift field as the derivative of a function $F(c) = -d_c h(c)$ such that $d_t h(x(t)) = -F^2(x(t)) \leq 0$, which has no connection to the quasipotential.

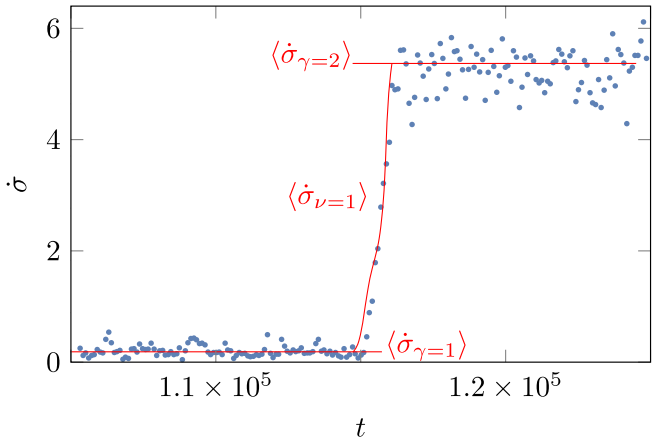

FIG. 5. Instantaneous entropy production rate [Eq. (112)] along a stochastic trajectory [obtained via the Gillespie algorithm (Gillespie, 1977) with $\Delta\mu = 2.84$, $k_{-2} = 2.07$, and $V = 10^2$], starting in the basin of attraction of x_1^* and ending in that of x_2^*. The solid lines are the constant values of the macroscopic mean entropy production in the two fixed points [Eq. (225)] and the mean entropy production rate along the transition trajectory [Eq. (249)].

$$r_1^\dagger = \frac{c^4 + c^2}{e^{\Delta\mu} + c^2}, \qquad r_{-1}^\dagger = \frac{e^{-\Delta\mu}c^5 + c^3}{x^{\mathrm{eq}}(x^2+1)},$$
$$r_2^\dagger = \frac{e^{\Delta\mu}(c^2+1)}{e^{\Delta\mu} + c^2}, \qquad r_{-2}^\dagger = \frac{e^{-\Delta\mu}c^3 + c}{x^{\mathrm{eq}}(c^2+1)}, \tag{247}$$

equal the physical rates r_ρ only at $\Delta\mu = 0$. Note that for $\Delta\mu \neq 0$ they do not follow the mass-action law [Eq. (235)].

Since bistability is created only far from equilibrium, $\sigma_{\gamma\to\nu}$ and $|\sigma_{\nu\to\gamma}|$ are large, thus making the bound [Eq. (160)] loose. Nevertheless, the bound turns into an equality if the thermodynamic entropy production is replaced by Eq. (245), which equals the time derivative (negative time derivative) of the rate function [Eq. (243)] along the instanton (the relaxation) thanks to Eq. (246),

$$\dot{\sigma}_{\mathrm{info}} = d_t I(c(t)) = -d_t I(x(t)). \tag{248}$$

For long times the system can be described by a two-state Markov jump processes with transition rates $\kappa_{\pm1}$ (Vellela and Qian, 2009). The entropy production [Eq. (112)] of the underlying dynamics is compared in Fig. 5 with the internal entropy production of the metastable states [Eq. (225)] and the entropy production rate calculated along the transition path from a neighborhood of x_1^* to a neighborhood of x_2^* in time $\langle\tau^{\mathrm{tr}}\rangle$,

$$\langle\dot{\sigma}_\nu(t)\rangle = \sum_\rho r_\rho(c(t))e^{\Delta_\rho\cdot\pi(t)}\ln\frac{r_\rho(c(t))}{r_{-\rho}(c(t))}. \tag{249}$$

In Eq. (249) $c(t)$ and $\pi(t)$ are solutions of Eq. (107) on the manifold $\mathcal{H}(c(t),\pi(t)) = E$ implicitly determined by

$$\langle\tau^{\mathrm{tr}}\rangle = \int_0^{\langle\tau^{\mathrm{tr}}\rangle} dt = \int_{\mathcal{D}} \frac{dc}{\dot{c}(c,\pi(c,E))}, \tag{250}$$

with the integration domain $\mathcal{D} = [x_1^* + 1/\sqrt{\Omega}, x_2^* - 1/\sqrt{\Omega}]$. We note that, since there is no exact formula for $\langle\tau_{\mathrm{tr}}\rangle$, its value is estimated using an expression valid for detailed balance dynamics (Malinin and Chernyak, 2010) and replacing the height of the energy barrier with that of the quasipotential.

2. Entropy production in a limit cycle: Brusselator model

We consider the Brusselator model, a prototypical model displaying a limit cycle far from equilibrium (Prigogine and Lefever, 1968; Lefever, Nicolis, and Borckmans, 1988; Andrieux and Gaspard, 2008; Nguyen and Seifert, 2020). It is an autocatalytic chemical reaction network,

$$\mathsf{Y}_1 \underset{k_{-1}}{\overset{k_{+1}}{\rightleftharpoons}} \mathsf{X}_1, \qquad \mathsf{X}_1 + \mathsf{Y}_2 \underset{k_{-2}}{\overset{k_{+2}}{\rightleftharpoons}} \mathsf{X}_2 + \mathsf{Y}_3, \tag{251}$$

$$2\mathsf{X}_1 + \mathsf{X}_2 \underset{k_{-3}}{\overset{k_{+3}}{\rightleftharpoons}} 3\mathsf{X}_1, \qquad \mathsf{X}_1 \underset{k_{-4}}{\overset{k_{+4}}{\rightleftharpoons}} \mathsf{Y}_4, \tag{252}$$

made up of two dynamical species X_1 and X_2 and four chemostatted species Y_y (with concentrations denoted c_{Y_y}). The model has two emergent cycles $C^1 = (1,0,0,1)$ and $C^2 = (0,1,1,0)$ with corresponding cycle affinities $\mathcal{A}^1_{\mathrm{nc}} = \log(k_1k_4c_{\mathsf{Y}_1}/k_{-1}k_{-4}c_{\mathsf{Y}_4})$ and $\mathcal{A}^2_{\mathrm{nc}} = \log(k_2k_3c_{\mathsf{Y}_2}/k_{-2}k_{-3}c_{\mathsf{Y}_3})$. The dynamics is detailed balance when the chemical potentials of all c_{Y_i} are equal, so the cycle affinities are zero.

Choosing the concentration of Y_1 as a control parameter, the deterministic rate equation (237) displays a supercritical Hopf bifurcation, namely, a transition from a single stable fixed point to a stable limit cycle with period t_{p}. This is seen from a linear stability analysis of the deterministic rate equations,

$$d_t x_1 = r_1 - r_{-1} - r_2 + r_{-2} + r_3 - r_{-3} - r_4 + r_{-4},$$
$$d_t x_2 = r_2 - r_{-2} - r_3 + r_{-3}, \tag{253}$$

with macroscopic scaled rates

$$r_1 = k_1c_{\mathsf{Y}_1}, \qquad r_{-1} = k_{-1}c_1,$$
$$r_2 = k_2c_1c_{\mathsf{Y}_2}, \qquad r_{-2} = k_{-2}c_2c_{\mathsf{Y}_3},$$
$$r_3 = k_3c_1^2c_2, \qquad r_{-3} = k_{-3}c_1^3,$$
$$r_4 = k_4c_1, \qquad r_{-4} = k_{-4}c_{\mathsf{Y}_4}. \tag{254}$$

The eigenvalues of the Jacobian of the drift field evaluated at the fixed point $\partial_c F(x^*)$ are a complex pair that develops a positive real part above some critical value $\tilde{c}_{\mathsf{Y}_1}$ and a stable periodic trajectory appears. Here we point out the failure of the Langevin approximation in the description of the system thermodynamics. The macroscopic entropy production rate associated with the chemical Langevin equation (144) time averaged over a period reads

$$\overline{\dot{\sigma}_{\mathrm{NLE}}} := \frac{1}{t_{\mathrm{p}}}\int_0^{t_{\mathrm{p}}} dt \lim_{V\to\infty}\langle\dot{\sigma}_{\mathrm{NLE}}\rangle$$
$$= \frac{1}{t_{\mathrm{p}}}\int_0^{t_{\mathrm{p}}} dt F(x^*(t))\cdot D^{-1}(x^*(t))\cdot F(x^*(t)), \tag{255}$$

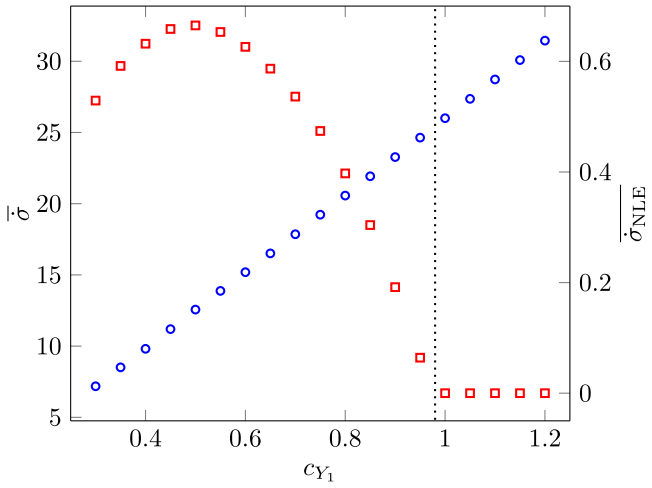

FIG. 6. Mean scaled entropy production rate averaged over one period in the infinite system-size limit: the exact expression corresponding to Eq. (61) (circles) and the approximation based on Eq. (144) given by the nonlinear Langevin equation (squares). The vertical dashed line shows the critical value $\tilde{c}_{\mathsf{Y}_1} \simeq 0.97$ for the onset of the supercritical Hopf bifurcation. The parameters are $k_1 = 1.00, k_2 c_{\mathsf{Y}_2} = 3.00, k_3 = 1.00, k_4 = 1.00, k_{-1} = 0.01, k_{-2} c_{\mathsf{Y}_3} = 0.01, k_{-3} = 0.01$, and $k_{-4} c_{\mathsf{Y}_4} = 0.01$.

with $x^*(t) = x^*(t + t_{\mathrm{p}})$ the periodic solution of Eq. (253). In Fig. 6 we show, by numerically integrating the rate equation (237), that the exact period-averaged entropy production rate

$$\bar{\dot{\sigma}} := \frac{1}{t_{\mathrm{p}}} \int_0^{t_{\mathrm{p}}} dt \lim_{V\to\infty} \langle \dot{\sigma} \rangle = \frac{1}{t_{\mathrm{p}}} \int_0^{t_{\mathrm{p}}} dt \sum_{\rho>0} [r_\rho(x^*(t)) - r_{-\rho}(x^*(t))] \ln \frac{r_\rho(x^*(t))}{r_{-\rho}(x^*(t))} \tag{256}$$

is largely underestimated by the approximation in Eq. (255), and even its qualitative behavior as a function of c_{Y_1} is incorrect. In particular, the latter is identically zero for $c_{\mathsf{Y}_1} > \tilde{c}_{\mathsf{Y}_1}$, i.e., in the absence of a limit cycle, since the drift F is by definition null on the fixed point, as shown in general in Eq. (145). Note that the Langevin approach is often used to estimate the energetic cost of biochemical oscillations (Xiao, Hou, and Xin, 2008; Cao, Jiang, and Hou, 2020).

B. Electronic systems

We consider an arrangement of ideal conductors whose state is determined by the charge vector q and electrostatic potential vector V (Freitas, Delvenne, and Esposito, 2021). The potentials are measured with respect to some reference (ground) potential and are linearly related to the charges, $q = C \cdot V$, through the capacitance matrix C. The internal energy of the system is thus

$$E = \tfrac{1}{2} q \cdot V. \tag{257}$$

The system is open when N_{Y} conductors have fixed potentials imposed by external voltage sources so that the state is specified by N charges. Elementary charges with value q_e are transported between pairs of conductors by two-terminal devices. Each of these channels is modeled as a bidirectional Poisson process labeled with $\pm\rho$ with rate $R_{\pm\rho}(q)$, which changes the system state as $q \to q \pm q_e \Delta_\rho$. This allows one to describe many relevant devices, such as tunnel junctions, diodes, MOS transistors in subthreshold operation (Freitas, Delvenne, and Esposito, 2021). The matrix with entries Δ_ρ^i encoding the circuit network is the analog of the stoichiometric matrix of chemical reactions in Sec. VII.A. Its left (right) null vectors identify the conserved quantities (the cycles). The stochastic dynamics is given by Eq. (1), with $nq_e = q$ and $q_e J_\rho$ the electric current on each channel device. Heat conduction is assumed to be large enough that the temperature in each conductor is constant and equal to T [i.e., there is no self-heating (Semenov, Vassighi, and Sachdev, 2006)].

A closed circuit satisfies the detailed balance condition

$$T \ln \frac{R_\rho(q)}{R_{-\rho}(q + q_e \Delta_\rho)} = -E(q + q_e \Delta_\rho) + E(q), \tag{258}$$

with the quadratic energy [Eq. (257)] (because $S_{\mathrm{int}} = 0$), and relaxes to the equilibrium distribution at fixed value of the conserved quantities $L(q)$,

$$P_{\mathrm{eq}}(q) \propto e^{-E(q)/T} \delta(L(q) - L). \tag{259}$$

For open circuits the Massieu potential is obtained by subtracting from the electrostatic energy the contribution exchanged with the regulated conductors,

$$\Phi(q) = E(q) - \tilde{V} \cdot q, \tag{260}$$

with an appropriate voltage vector $\tilde{V}$ that is constructed from the quantities $L(q)$ that are no longer conserved when the system is opened. In analogy with chemical reaction networks, the forces a_ρ are differences between the voltages of regulated conductors in the connected components of the channel ρ (Freitas, Delvenne, and Esposito, 2021).

The explicit form of the transition rates can be obtained from the I-V curve that gives the macroscopic average electric current $\langle I \rangle(V)$ through a two-terminal device as a function of the applied voltage V across it. In the case of a constant voltage V, the mean current

$$\langle I \rangle(V) = q_e (R_+ - R_-) \tag{261}$$

and the local detailed balance

$$T \ln \frac{R_+}{R_-} = q_e V \tag{262}$$

are two independent equations that allow one to determine $R_\pm$. In the general case of a device embedded in a circuit, the transition rates $R_{\pm\rho}$ are obtained by replacing the constant V in Eqs. (261) and (262) with the average of the voltage difference

before and after the transition $q \to q \pm q_e \Delta_\rho$ (Freitas, Delvenne, and Esposito, 2021). In closed circuits choices aside from this midpoint rule would lead to a stationary probability density that differs from the equilibrium [Eq. (259)], thus entailing the possibility to indefinitely extract energy; see the Brillouin paradox (Brillouin, 1950).

We focus on those devices in which the characteristic capacitance $C \to \infty$ and the transition rates $R_{\pm\rho}$ (and thus the charges $q \to \infty$) scale with the system size. Hence, in the macroscopic limit we consider the elementary voltage $v_e = q_e/C \to 0$ to be negligible in comparison to all other voltage scales of the circuit and equal to the inverse of the large parameter $V \equiv 1/v_e \to \infty$.

Open electronic circuits under detailed balance conditions cannot be used to store information or to generate signals with specific frequencies. These are prevented by the facts that the Massieu potential [Eq. (260)] has a unique minimum $x_{\rm eq} = 0$ and that the spectrum of the generator of the (overdamped) dynamics is real (see Sec. III.C), respectively. Multistability and oscillations require nonconservative forces created by voltage differences. In practice, they can be realized by connecting two inverters, i.e., NOT gates, in a loop [a static random access memory (SRAM) cell (Rezaei *et al.*, 2020)] and an odd number of inverters in a chain [a ring oscillator (Hajimiri, Limotyrakis, and Lee, 1999)], respectively.

1. Dissipative logical states: CMOS SRAM cell

Low-power SRAM cells are usually implemented by connecting two CMOS inverters. Each inverter is composed of a pMOS and a nMOS transistor (see Fig. 7) and is powered by a voltage bias $2V_{dd}$. Each pMOS (nMOS) transistor can be modeled as a conduction channel between the drain and source terminals, with the associated transition rates $R^p_\pm$ ($R^n_\pm$) (Freitas, Delvenne, and Esposito, 2021). The voltages v_1 and v_2 at the output of each inverter are the 2 independent degrees of freedom, given by $v = nq_e/C$, with n the number vector of charges and C the capacitance characterizing the device. Following the general procedure introduced in Sec. VII.B based on the I-V curve and the local detailed balance, with the Massieu potential $\Phi(v_1, v_2) = C(v_1^2 + v_2^2)/2 + CV_{\rm dd}^2$ one obtains

$$R^p_+(v_1, v_2) = (I_0/q_e)e^{(V_{\rm dd} - V_{\rm th} - v_2)/({\rm n}V_{\rm T})},$$
$$R^p_-(v_1, v_2) = R^p_+(v_1, v_2)e^{-(V_{\rm dd} - v_1)/V_{\rm T} - v_e/(2V_{\rm T})}, \tag{263}$$

and $R^n_\pm(v_1, v_2) = R^p_\pm(-v_1, -v_2)$ (Freitas, Proesmans, and Esposito, 2022), where I_0, $V_{\rm th}$, and n are parameters characterizing the transistor. The nonconservative work of the transitions is $a_{\pm\rho} = \pm q_e V_{\rm dd}$.

The macroscopic limit is obtained as $v_e \to 0$, with the bias voltage $V_{\rm dd}$ and the thermal voltage $V_{\rm T} = k_{\rm B}T/q_e$ kept finite. The corresponding macroscopic transition rates read

$$r^p_+(v_1, v_2) = (I_0/C)e^{(V_{\rm dd} - V_{\rm th} - v_2)/({\rm n}V_{\rm T})},$$
$$r^p_-(v_1, v_2) = r^p_+(v_1, v_2)e^{-(V_{\rm dd} - v_1)/V_{\rm T}} \tag{264}$$

and yield the deterministic dynamics of voltages

$$d_t \upsilon_1 = I_p(\upsilon_1, \upsilon_2) - I_n(\upsilon_1, \upsilon_2),$$
$$d_t \upsilon_2 = I_p(\upsilon_2, \upsilon_1) - I_n(\upsilon_2, \upsilon_1) \tag{265}$$

in terms of the difference of currents between the two transistors, $I_{p/n}(\upsilon_1, \upsilon_2) = r^{p/n}_+(\upsilon_1, \upsilon_2) - r^{p/n}_-(\upsilon_1, \upsilon_2)$. Equations (265) admit a single stable fix point $\upsilon^*_1 = \upsilon^*_2 = 0$ for a small bias $V_{\rm dd} \le V_{\rm T} \ln 2$ and two stable (symmetric) fixed points $\pm\upsilon^* = \pm(\upsilon_{\rm bit}, -\upsilon_{\rm bit})$, with $(n = 1)$

$$\upsilon_{\rm bit} = V_{\rm dd} + V_{\rm T} \ln\left(\tfrac{1}{2} + \sqrt{1/4 - e^{-2V_{\rm dd}/V_{\rm T}}}\right) \tag{266}$$

separated by a saddle in the origin for $V_{\rm dd} > V_{\rm T} \ln 2$. These explicit formulas hold for $n = 1$, although more lengthy expressions can be derived for $n \neq 1$. The pitchfork bifurcation undergone by the dynamical system in Eq. (265) at the critical value $\tilde{V}_{\rm dd} := V_{\rm T} \ln 2$ corresponds to the emergence of bistability in the deterministic dynamics and makes the system usable as a volatile memory. Initializing the voltages in a given basin of attraction allows one to store 1 bit of information for a mean time equal to the inverse of the escape rate $\kappa \asymp e^{-[I_{\rm ss}(0) - I_{\rm ss}(\upsilon^*)]/v_e}$. The energy dissipated to maintain

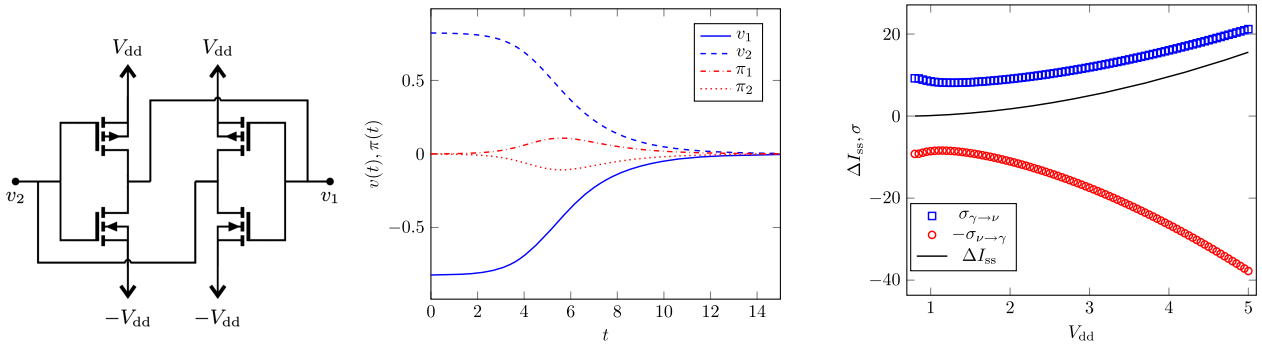

FIG. 7. Left panel: circuit diagram of a CMOS SRAM cell. Center panel: instanton obtained via the minimum action method (Zakine and Vanden-Eijnden, 2023) evolves at $v_1 = -v_2$ and $\pi_1 = -\pi_2$. The parameter values are $(I_0/C)e^{-V_{\rm th}/V_{\rm T}}$, $n = 1$, $V_{\rm T} = 1$, and $V_{\rm dd} = 0.9$. Right panel: the height of the quasipotential barrier obtained from Eq. (268) (solid line) as a function of $V_{\rm dd}$ and its upper and lower bounds, i.e., entropy production of the instanton (squares) and negative entropy production of the relaxation (circles), respectively. The latter ones are obtained according to Eq. (272) with a small parameter $\epsilon = 0.02$.

such a logical state is $T\langle\sigma_{\pm1}\rangle$, where the mean entropy production rate [Eq. (225)] reads

$$\langle\dot{\sigma}_{\gamma=\pm1}\rangle = V_{\rm dd} q_e \sum_\rho \langle j_\rho\rangle = 4V_{\rm dd} I_0 e^{-V_{\rm th}/V_{\rm T}}. \quad (267)$$

The quasipotential cannot be obtained analytically. Nevertheless, if only rare fluctuations leading to memory losses are of interest, we can restrict the analysis to the linear space $c = (v_1 - v_2)/2$. Owing to the symmetry of the rates, relaxation and instanton trajectories that connect the fixed points to the saddle lie entirely on the reaction coordinate c at $v_1 + v_2 = 0$; see Fig. 7. The determination of $I_{\rm ss}(c)$ reduces to a one-dimensional problem that is analogous to the one in Sec. VII.A.1. Writing Eq. (34) in terms of the new variable c and setting $v_1 = -v_2$, $\pi_1 = -\pi_2 = \partial_c I_{\rm ss}(c)$ gives Eq. (136), whose integral is

$$I_{\rm ss}(c) = \frac{c^2}{V_{\rm T}} + \frac{n}{V_{\rm T}(n+2)}[L(-c, V_{\rm dd}) - L(c, -V_{\rm dd}) + L(c, V_{\rm dd}) - L(-c, -V_{\rm dd})] + \text{const}, \quad (268)$$

with $L(c, V_{\rm dd}) = \mathrm{Li}_2(-\exp([V_{\rm dd} + c(1+2/n)]/V_{\rm T})$ and $\mathrm{Li}_2(\cdot)$ the polylogarithm function of second order. Equation (268) was derived by Freitas, Proesmans, and Esposito (2022) and is reported here in an equivalent form that explicitly shows the symmetry $I_{\rm ss}(c) = I_{\rm ss}(-c)$.

For $V_{\rm dd} \to 0$ Eq. (268) reduces to the macroscopic Massieu potential on the subspace $v_1 = -v_2$,

$$\phi(c) \coloneqq \lim_{v_e\to 0} v_e \Phi(c, -c) = \frac{c^2}{V_{\rm T}}. \quad (269)$$

The quasipotential barrier takes the simple expression

$$I_{\rm ss}(0) - I_{\rm ss}(v_{\rm bit}) \simeq \frac{2}{2+n}\frac{V_{\rm dd}^2}{V_{\rm T}} \quad (270)$$

in the far-from-equilibrium regime $V_{\rm dd} \gg \tilde{V}_{\rm dd}$ and leads to the error rate due to thermal noise

$$-\lim_{v_e\to 0} v_e \ln\kappa \propto \langle\dot{\sigma}_{\gamma=\pm1}\rangle^2. \quad (271)$$

The stability of the electronic memory grows proportionally to the square of the macroscopic dissipation of the device. This direct relation between the two quantities is made possible by the fact that the macroscopic current $I_0 e^{-V_{\rm th}/V_{\rm T}}$ is constant in the bistable regime.

As for the Schlögl model in Sec. VII.A.1, relaxation and instanton dynamics along c are related by time reversal and share the same local speed $\dot{c}(c)$. Yet, the corresponding local entropy production rates differ, leading in general to

$$\sigma_{\nu\to\gamma} = \int_{\mathcal{D}} dc \frac{\dot{\sigma}_{\nu\to\gamma}(c)}{\dot{c}(c)} \neq -\int_{\mathcal{D}} dc \frac{\dot{\sigma}_{\gamma\to\nu}(c)}{\dot{c}(c)} = -\sigma_{\gamma\to\nu} \quad (272)$$

when the integration over the domain $\mathcal{D} = [1/\sqrt{\Omega}, v_{\rm bit} - 1/\sqrt{\Omega}]$ is performed. Modulus equality is achieved only at linear order in $V_{\rm dd}$,

$$\frac{\dot{\sigma}_{\nu\to\gamma}(c)}{\dot{c}(c)} = -\frac{2c}{V_{\rm T}} + \frac{2V_{\rm dd}}{V_{\rm T}}\tanh\left(\frac{(n+2)c}{2nV_{\rm T}}\right) + O(V_{\rm dd}^2), \quad (273)$$

whose integral gives the near-equilibrium approximation [Eq. (120)] of the rate function (Freitas, Falasco, and Esposito, 2021). Since bistability does not appear at vanishing bias, the thermodynamic bounds [Eq. (160)] are loose due to large values of the adiabatic entropy production; see Fig. 7. Nevertheless, the bounds in Eq. (160) turn into an equality by replacing the thermodynamic entropy production by the coarse-grained quantity in Eq. (245) along c with the lumped rates $\tilde{r}_\pm(v_1, v_2) = r^p_\pm(v_1, v_2) + r^n_\mp(v_1, v_2)$ (J. N. Freitas and Esposito, 2022). Note that close to the bifurcation point the quasipotential barrier vanishes and the regions of typical fluctuations around the fixed point overlap. The escape rate between attractors is dominated by subexponential terms that are neglected in Eq. (157) and Eq. (160) becomes obsolete; see Sec. VII.C for a discussion of the attractor stability in this regime.

C. Driven Potts models

We consider a system that consists of $V \equiv M$ all-to-all interacting identical units subject to the same nonconservative force a and identically coupled to a thermal bath of temperature T. Each unit is made of $N \equiv q$ identical states on a ring coupled to their nearest neighbors.[16] Owing to the mean-field nature of the interactions between units, all configurations with the same number n_i of units in states $i = 1, \ldots, q$ are equivalent. The internal entropy of the system resulting from such a degeneracy is (Herpich *et al.*, 2020)

$$S_{\rm int}(n) = \ln\frac{M!}{\prod_{i=1}^q n_i!}, \quad (274)$$

and the energy accounts for the interactions between all units in the same state i,

$$U = \frac{1}{2M}\sum_{i=1}^q u_i n_i(n_i - 1), \quad (275)$$

where the prefactor $1/M$ makes the mean-field energy extensive, according to Kac's prescription (Kac, Uhlenbeck, and Hemmer, 1963). The system has q forward and q backward mesoscopic transitions, with each connecting two successive single-unit states. The stochastic transitions $\rho = \pm i$ change the populations of nearby states i and $i+1$ as $(n_i, n_{i+1}) \to (n_i \mp 1, n_{i+1} \pm 1)$, that is, $\Delta^i_\rho = -\delta_{\rho,i} + \delta_{-\rho,i} + \delta_{\rho,i-1} - \delta_{-\rho,i-1} = -\Delta^i_{-\rho}$, where i and ρ are modulo q.

[16]We use the letter q to denote the number of accessible mesoscopic states, as is customary for the Potts model (Wu, 1982).

In the limit $M \to \infty$ we obtain the scaled internal entropy (using Stirling's approximation)

$$s_{\mathrm{int}}(c) = -\prod_{i=1}^{q} c_i \ln c_i, \tag{276}$$

which constitutes the macroscopic system entropy [Eq. (58)], and the scaled energy

$$u(c) = \frac{1}{2}\sum_{i=1}^{q} u_i c_i^2 \tag{277}$$

in terms of the occupation densities $c := n/M$. Hence, the macroscopic entropy production in Eq. (29) for transitions $|\rho| = i$ between single-unit states i and $i+1$ takes the form

$$\sigma_\rho(c) = \mp\left[(\partial_{c_{i+1}} - \partial_{c_i})\phi(c)\right] \pm a, \tag{278}$$

where $\phi(c) = u(c)/T - s_{\mathrm{int}}(c)$ is the scaled Helmholtz free energy divided by the temperature T, as introduced in Eq. (6), and the nonconservative part $a_{\pm\rho} = \pm a$ favors unidirectional rotation along the single-unit states. With attractive interactions $u_i = -\mathcal{J} > 0$ equal for all states i, this class of systems includes the driven Curie-Weiss model, i.e., the mean-field Ising model ($q = 2$)—in which $c_1 - c_2 = m$ is the magnetization—and the ferromagnetic mean-field Potts model ($q \geq 3$). In all cases the state of a unit can be identified with a spin orientation; see Fig. 8.

A possible choice of single-unit transition rates that respects the local detailed balance is the so-called Arrhenius form, which is characterized by an exponential form and a global timescale $1/\gamma$ (Meibohm and Esposito, 2024b). In this case the scaled macroscopic transition rates [Eq. (27)] for transitions $\rho = i$ ($\rho = 1 - i$) between single-unit states i and $i+1$ ($i-1$) reads

$$r_\rho(c) = \gamma c_i e^{(1/2)\{[(1\mp\xi)/T](u_{i\pm1}c_{i\pm1} - u_i c_i) \pm a\}}, \tag{279}$$

with $-1 \leq \xi \leq 1$. Note that the logarithm of $r_i(c)/r_{-i}(c)$ precisely equals Eq. (278), with the change of internal entropy

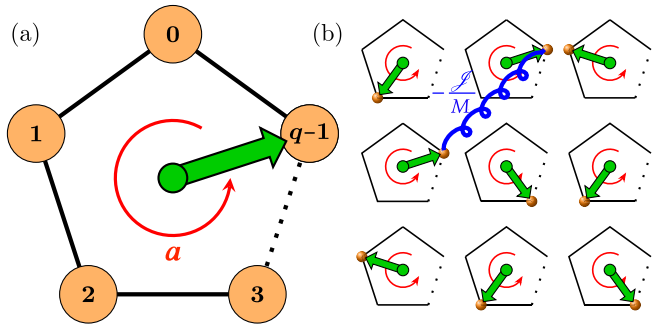

FIG. 8. Sketch of the driven Potts model. (a) A single unit is composed of q states identified by a single spin configuration. Counterclockwise transitions are favored by a nonconservative thermodynamic force $a > 0$. (b) Interactions entering the transition rates in Eq. (279) that are between the same states i of all M units.

s_{int} given by $\ln(c_i/c_{i+1})$. Extensions have been studied that include a constant energy bias for each state i, interactions between different single-unit states, and couplings to baths at different temperatures (Herpich *et al.*, 2020).

In the detailed balance Curie-Weiss model in contact with a single thermal bath ($q = 2$ and $a_\rho = 0$), the emergence of a dynamical phase transition was observed upon an instantaneous disordering quench from low to high temperature, i.e., the appearance at the critical time t_c of a kink in the time-dependent rate function of the magnetization $I(m,t)$ (Meibohm and Esposito, 2022). This corresponds to a sudden change in the optimal fluctuations driven by the competition in Eq. (108) between the statistical weights of a trajectory and those of its initial condition, which are $\mathcal{A}$, as given in Eq. (106), and $I(m(0),0)$, respectively. An analogous dynamical phase transition occurs in the time-dependent rate function of the exchanged heat, similarly due to a change of dominance in the most likely trajectories (Meibohm and Esposito, 2023). For the Curie-Weiss model in contact with two different thermal baths (i.e., two sets of transitions [Eq. (279)], where each is associated with a bath at a different temperature), a different dynamical phase transition appears as a kink in the steady state cumulant generating function of the exchanged heat (Herpich *et al.*, 2020). In this case, as we described in Sec. IV.I.2, the singularity stems from the competition between the multiple stationary solutions of the tilted Hamiltonian equations (177) and represents a signature of the bistability of the system in the current statistics.

The driven Potts model ($q \geq 3$) has been extensively studied, for example, as a model for synchronization in work-to-work converters (Herpich, Thingna, and Esposito, 2018; Herpich and Esposito, 2019). The deterministic dynamics can be thoroughly examined. As $T/\mathcal{J} \to \infty$, the system becomes effectively detailed balance and the dynamics is entropy dominated with a single stable, disordered fixed point $x^* = (1/q, \ldots, 1/q)$. Conversely, as $T/\mathcal{J} \to 0$, the system is energy dominated with q stable, ordered fixed points characterized by all units in the same state, i.e., $x^*_{\gamma=1} = (1, 0, \ldots, 0)$, and $x^*_{\gamma>1}$ is obtained by cyclic permutations of the elements of the vector $x^*_{\gamma=1}$. Above a critical coupling strength $\mathcal{J}_c$, the disordered fixed point becomes unstable. For $|a| \to 0$, regardless of the choice of transition rate [for example, ξ in Eq. (279)], $\mathcal{J}_c \to qT$ and the macroscopic system settles in one ordered fixed point. When detailed balance is broken, $\mathcal{J}_c$ depends on the specific class of transition rates in Eq. (279), and for $\mathcal{J} > \mathcal{J}_c$ the system can display time-dependent attractors $x^*_\gamma(t)$ corresponding to the synchronized motion of all the units. The macroscopic deterministic dynamics close to the bifurcation can be exactly solved by transforming to Fourier modes $\hat{c}_k := \sum_{j=0}^{q-1} c_j e^{i2\pi jk/q}$ and deriving normal form equations for their amplitude $\varkappa_k$ and phase φ_k (Meibohm and Esposito, 2024a,2024b). The emerging phase diagram, as a function of q and the dynamical class [for example, ξ in (279)], is extremely rich. One finds regions with a finite number of active modes $|S_a| = 1, 2, \ldots$, i.e., modes k such that $\varkappa_k > 0$. In the region $|S_a| = 1$ several single-mode oscillating states can be simultaneously stable. For $|S_a| \geq 2$ a unique multimode oscillating state exists, which

is generally a quasiperiodic attractor since the different modes show frequencies with irrational ratios.

The coexisting limit cycles at $|S_a| = 1$ become metastable at large but finite M. In particular, close to the bifurcation the system switches between them thanks to typical fluctuations, not via rare instantons. Indeed, the quasipotential barrier separating the stochastic limit cycles vanishes, $\Delta I_{ss} \to 0$, and the escape rate is dominated by the subexponential prefactor neglected in Eq. (157). The lifetime of such competing states is decided by the phase-space contraction rate λ defined in Eq. (47), whose magnitude corresponds to the macroscopic limit of the inflow rate [Eq. (25)] averaged over the attractor. In general, this connection between the Lyapunov stability of the deterministic dynamics and the typical fluctuations is given by Eq. (130). Close to the bifurcation point, one can prove the stability-dissipation relation (Meibohm and Esposito, 2024a, 2024b)

$$\Delta\dot{\sigma} \propto \Delta\lambda, \tag{280}$$

where $\Delta\langle\mathcal{O}\rangle \coloneqq \lim_{N\to\infty}(\langle\mathcal{O}\rangle - \langle\mathcal{O}\rangle_{\mathcal{J}=0})/\langle\mathcal{O}\rangle_{\mathcal{J}=0}$ stands for the normalized variation of the average values of the observable $\mathcal{O}$ between interacting and noninteracting (i.e., $\mathcal{J} = 0$) conditions. The macroscopic mean $\lim_{N\to\infty}\langle\mathcal{O}\rangle$ is generally different for each attractor. Therefore, Eq. (280) implies that the least dissipative attractor is the most stable one. This constitutes the first derivation of a minimum entropy production principle that is valid far from equilibrium. Note that the entropy production rate entering Eq. (280) is a thermodynamic quantity linked to the microscopic energetics of the system by the local detailed balance [Eq. (29)], not an abstract definition of dissipation based on information theory arguments (Daems and Nicolis, 1999).

The aforementioned Potts model can be embedded in a d-dimensional physical space. To this end, we consider a lattice in which each node contains a large number of q-state units described in the macroscopic limit by a local density $c_{i,x}$; see Sec. V.A. Units not only can change their internal state, i.e., rotate the spin, but also can jump to nearby lattice sites with rates belonging to the sets R and C, respectively. The scaled entropy production rate reads

$$\sigma_\rho(\{c_{i,x}\}) = \mp\,[(\partial_{c_{i+1,x}} - \partial_{c_{i,x}})\phi] \pm a^{\mathrm{rot}} \tag{281}$$

for transitions $\rho \in R$ between states i and $i+1$ and

$$\sigma_\rho(\{c_{i,x}\}) = -[(\partial_{c_{i,x'}} - \partial_{c_{i,x}})\phi] + a^{\mathrm{tra}}_\rho \tag{282}$$

for transitions $\rho \in C$ from the site x to the neighboring site x'. Detailed balance is broken by the nonconservative contributions $\pm a^{\mathrm{rot}}$ and a^{tra}_ρ that force the spin to rotate and to drift in space, respectively. By choosing a^{tra}_ρ to be constant in magnitude and aligned with the local spin direction, one obtains a toy model for self-propelled particles. In the following we restrict ourselves to the case of active Ising spins, i.e., $q = 2$, but the discussion can be generalized to $q > 2$.

Taking the continuous limit by sending the lattice spacing ϵ to zero as detailed in Sec. V.A, one gets a stochastic field theory for $c_{i,x} \to c_i(r,t)$,

$$\partial_t c_i = -\boldsymbol{\nabla}\cdot\underbrace{\left[\gamma c_i\left(-\boldsymbol{\nabla}\frac{\delta u}{\delta c_i} + f_i\right) - \gamma T\boldsymbol{\nabla}c_i + \xi_i\right]}_{j_i[c]} + I_i. \tag{283}$$

In Eq. (283) ξ_i are independent zero-mean Gaussian white noise fields with the variance $2\gamma T c_i/\Omega$ and Ω the system size, $I_1 = -I_2$ is a white noise field with the Skellam distribution (Skellam, 1946) being the difference between Poissonian jumps in and out of the single-unit state i [for example, with the rates in Eq. (279)], and a constant drift vector $f \equiv f_1 = -f_2$ that derives from the continuous limit of a^{tra}_ρ. Note that $\chi = \gamma c\mathbb{I}$ is the mobility matrix and that the diffusive flux $-\gamma T\boldsymbol{\nabla}c$ stems from the entropic term $-\chi\cdot\boldsymbol{\nabla}\delta s_{\mathrm{int}}/\delta c$. Summing and subtracting the two equations in Eq. (283), one can obtain closed stochastic equations for the local magnetization $m(r,t) \coloneqq c_1(r,t) - c_2(r,t)$ and the local density of spins $c_{\mathrm{tot}}(r,t) \coloneqq c_1(r,t) + c_2(r,t)$.

The macroscopic entropy production follows directly from the general expression derived in Sec. V.B. In particular, in a stationary state it reduces to the nonconservative contribution in Eq. (212),

$$\dot{\sigma}_{\mathrm{nc}} = \int dr[a^{\mathrm{rot}}\langle I_1\rangle + f\cdot(\langle j_1\rangle - \langle j_2\rangle)], \tag{284}$$

which displays, in order, the contribution of the single-unit rotational driving and of the active drift in space. When the explicit expressions of the currents $\langle j_i\rangle$ in Eq. (283) are used, the entropy production of translation in Eq. (284) reads

$$\begin{aligned}\dot{\sigma}_{\mathrm{nc}} &\underset{a^{\mathrm{rot}}=0}{=} \int dr f\cdot(\langle j_1\rangle - \langle j_2\rangle)\\ &= \gamma f^2 c_{\mathrm{tot}} + \gamma f\cdot\int dr\left(c_1\nabla\frac{\delta\phi}{\delta c_1} - c_2\nabla\frac{\delta\phi}{\delta c_2}\right).\end{aligned}$$

In particular, one finds that

$$\dot{\sigma}_{\mathrm{nc}} \underset{a^{\mathrm{rot}}=0}{=} \gamma f^2 c_{\mathrm{tot}} \tag{285}$$

in any homogeneous state or whenever the contribution of interfaces (between magnetized and disordered domains) is negligible compared to the bulk one. Note that Eq. (285) is the same dissipation as that of a gas of driven noninteracting particles and is thus independent of the system phase.

For $a^{\mathrm{rot}} = 0$ one obtains a thermodynamically consistent version (Agranov *et al.*, 2024) of the active Ising model ($q = 2$) (Solon and Tailleur, 2013, 2015), which was generalized to $q \geq 2$ by Mangeat *et al.* (2020) and Solon *et al.* (2022). Therein, the energy variation due to the jumps of the units in space [namely, the first term on the right-hand side of Eq. (282)] was neglected. Alternatively, one can interpret the

model of Solon and Tailleur (2013, 2015) as satisfying local detailed balance with a fine-tuned field-dependent nonconservative part $\tilde{a}^{\mathrm{tra}}_{\rho}(\{c_{i,x}\})$ that exactly counterbalances the energy variations, thus yielding a constant drift in space. Here, instead, we discuss a thermodynamic consistent model in which the translational nonconservative force on each spin is constant while the ensuing drift is affected by the interactions with nearby spins. The original model (Solon and Tailleur, 2013, 2015) predicts the emergence of flocking at sufficiently large density and small temperature, i.e., a state with $\langle m\rangle \neq 0$, which can be retrieved via the thermodynamically consistent version by adding nearest-neighbor interactions (Agranov *et al.*, 2024; Proesmans *et al.*, 2024). The model by Solon and Tailleur (2013, 2015) was used by Yu and Tu (2022) to evaluate the entropy production in Eq. (61), which was found to display a kink at the onset of flocking, in disagreement with Eq. (285). In light of the previous discussion, such apparent entropy production is an artifact caused by neglecting the energy variations of translating spins.

Finally, for active particles with internal rotation, $a^{\mathrm{rot}} \neq 0$, the entropy production cannot be inferred only from the spacial dynamics, as is often assumed in active field theories (Nardini *et al.*, 2017). Indeed, the first term on the right-hand side of Eq. (284) requires explicit knowledge of the internal current between single-unit states and reduces to the quadratic form of linear irreversible thermodynamics (Markovich *et al.*, 2021), in which $\langle I_1\rangle \propto a^{\mathrm{rot}}$ only if $a^{\mathrm{rot}} \to 0$.

VIII. DISCUSSION

A. Summary

We started with a description of an open system using a stochastic dynamics in terms of mesoscopic configurations specified by the occupation number of mesoscopic states, and we reviewed the standard procedure to build the superstructure of stochastic thermodynamics on it. In doing so, we took for granted that transitions rates between states, and thermodynamic observables associated with the states, can be expressed in terms of occupation numbers only. This means that we assumed for each mesoscopic state that the internal degrees of freedom are at equilibrium and that an equilibrium Massieu potential $\Phi(n)$ [and thus an internal entropy $S_{\mathrm{int}}(n)$] can be assigned to them that is solely a function of the occupation number of the mesostate. As a result, the entropy production can be expressed in terms of the mesoscopic transitions and the probability distribution over the mesostates; see Eqs. (8) and (9). We note that even when these conditions are satisfied, obtaining such transitions rates in practice may not always be straightforward (Prinz *et al.*, 2011).

We then imposed the necessary constraints to obtain a deterministic macroscopic dynamics and an extensive thermodynamics, namely, extensive transition rates and Massieu potentials, together with nonconservative forces a_{ρ} that are nonextensive. In the resulting entropy production, the contribution due to the system entropy stemming from the uncertainty of the mesoscopic state (i.e., the Shannon entropy) vanishes [see Eq. (57)] and only the internal entropy (if there is one) survives. For example, for systems in which the mesoscopic state i is occupied by n_i noninteracting units (such as reacting chemicals), the internal entropy is simply the Boltzmann entropy of the complexion number, $S_{\mathrm{int}}(n) = \ln(|n|!/\prod_i n_i!)$, whose scaled macroscopic limit reads $s_{\mathrm{int}}(c) = -\sum_i c_i \ln c_i$; see Sec. VII.C. This has the form of a Shannon entropy on the space of concentrations but has nothing to do with the Shannon entropy in terms of the mesoscopic probabilities, which, as just mentioned, vanishes. Accordingly, it counts the uncertainty in the microscopic configurations within the mesoscopic states i, not the randomness in the distribution of the mesoscopic state. However, be aware that an extensive Shannon entropy [Eq. (57)] can appear if a system has a number of (near) degenerate minima of the quasipotential [Eq. (55)] that scales exponentially with the size $V \to \infty$, as in the case of glasses (Castellani and Cavagna, 2005).

We emphasize that we focused only on thermal noise. We excluded systems whose dynamics remains noisy in the macroscopic limit, for example, in the presence of a quenched disorder (De Giuli and Scalliet, 2022) or any kind of extrinsic noise (Bressloff, 2017). We also specialized the discussion of the macroscopic limit to dynamics characterized only by isolated, nondegenerate fixed points. However, the theory is expected to hold more generally *mutatis mutandis* in the presence of sufficiently regular time-dependent attractors, such as the limit cycles that we mentioned in passing. The practical difficulty in this case is to determine the large fluctuations and the quasipotential.

We then considered a continuous-space limit that leads to a stochastic field theory. The conserved dynamics—called model B in the standard classification (Hohenberg and Halperin, 1977)—is the special case, extensively treated by Bertini *et al.* (2015), that we retrieved when all transitions scale diffusively. In this respect we reframe and contextualize many results of macroscopic fluctuation theory within ST. In general, we connected with fluctuating hydrodynamic theories (Landau and Lifshitz, 1959; de Groot and Mazur, 1984; de Zárate and Sengers, 2006), particularly nonlinear ones (Zubarev and Morozov, 1983), although in our treatment the intensive thermodynamic quantities characterizing the equilibrium reservoirs are not dynamically coupled to the mesoscopic variable c; for example, the temperature is unaffected by the dissipated heat. We thus achieved the goal of systematizing all well-established thermodynamics theories, from deterministic to statistical ones, within the overarching framework offered by ST; see Fig. 9.

Note that while we have *a priori* assumed the existence of a well-defined large-scale parameter that controls the thermodynamic limit, this setting may not be the only one that leads to macroscopic deterministic dynamics. The low temperature limit (with respect to a typical energy scale) is a much studied example, especially in the context of Langevin dynamics (Graham, 1987). Moreover, stochastic dynamics in continuous space converge to deterministic ones within an appropriate hydrodynamic description that averages the microscopic observables over suitably small volumes (Bertini *et al.*, 2015) without necessarily invoking that

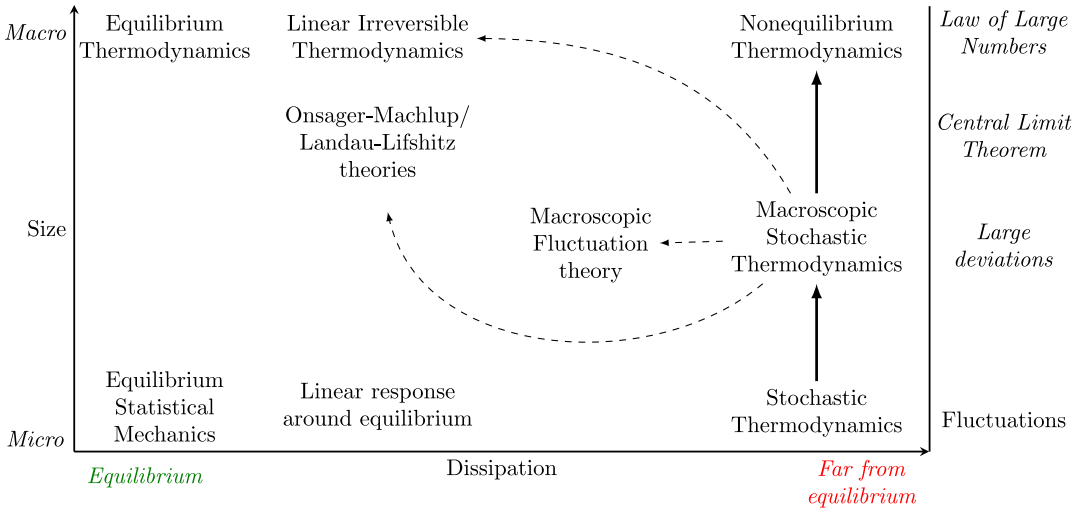

FIG. 9. Schematic classification of the thermodynamic theories in terms of the system size and distance from equilibrium. This review extends stochastic thermodynamics to macroscopic systems and recovers irreversible thermodynamics (deterministic) and Onsager-Machlup and Laundau-Lifshitz theories (Gaussian fluctuations) in the near-equilibrium regime. It also comprises macroscopic fluctuation theory, wherein forces are linearly related to fluxes but are nonlinear functions of macroscopic variables, which thus have non-Gaussian fluctuations.

the number of particles per lattice site diverges, as we effectively did in Sec. V.A.

Finally, in Sec. VI, we coarse grained the long-time dynamics as a Markov jump process over the attractors and discussed the resulting thermodynamics. The attractors provide a notion of states that emerge from the underlying dynamics and are generically out of equilibrium, thus overcoming a central starting assumption of ST. This section, together with the bounds on the macroscopic transition rates of Sec. IV.H, creates a long-sought bridge between thermodynamics and the Freidlin-Wentzell theory of large deviations (Graham and Tél, 1985; Freidlin and Wentzell, 1998). In this respect we worked at a formal level, in particular, making use of generating functions conditioned on subsets of trajectories. While conditioning the entropy production on a single basin of attraction has recently received some attention (Fiore *et al.*, 2021), conditioning on transition paths—and the underlying problem of calculating the statistics of transition times out of equilibrium—remains an issue to thoroughly explore. These tools are needed if one wants to explicitly compute the emerging observables from the underlying mesoscopic dynamics. However, this bottom-up derivation is expected to be possible only in relatively simple models. The main goal of the coarse graining in Sec. VI is to identify the structure of the emerging thermodynamics in terms of nonequilibrium states so as to guide the construction of effective models in complex systems, possibly informed by measurements of emerging observables. In Sec. VII we outlined three classes of models that comply with the general theory, namely, reaction networks of ideal chemicals, nonlinear electronic circuits, and driven Potts models.

B. Outlook

We focused on the macroscopic limit of the core structure of ST, thus providing the basis for a systematic analysis of many specific aspects connected to the nonequilibrium thermodynamic limit and for further extensions to other classes of systems.

1. Thermodynamic uncertainty relations

In the simplest formulation, the thermodynamic uncertainty relation (TUR) asserts that the ratio between the squared mean and the variance of a current integrated over a time τ is bounded from above by half the entropy produced in the time τ; see Jarzynski (2011), Barato and Seifert (2015), Gingrich, Rotskoff, and Horowitz (2017), Macieszczak, Brandner, and Garrahan (2018), Hasegawa and Van Vu (2019), Timpanaro *et al.* (2019), Dechant and Sasa (2020, 2021), Falasco, Esposito, and Delvenne (2020), Van Vu, Tuan Vo, and Hasegawa (2020), and Van Vu and Saito (2023). For the extensive observables of Sec. IV.I introduced in Eq. (167), one concludes that the TUR is valid in terms of the scaled moments, as both sides of the inequality scale as V (Koyuk and Seifert, 2022). Its explicit expression will depend on the observation timescale τ, however. For systems initially prepared in an attractor γ, as a consequence of metastability, the TUR will involve only the entropy production of the attractor γ,

$$\frac{\langle \mathscr{O} \rangle^2}{\langle \mathscr{O}^2 \rangle - \langle \mathscr{O}^2 \rangle} \leq \frac{\langle \dot{\sigma}_\gamma \rangle \tau}{2}, \tag{286}$$

if the integration time τ is much shorter than the minimum escape time $1/\kappa_\nu$. The TURs [Eq. (286)], if used for inference, provide multiple bounds to the dissipation of each attractor rather than a single bound on the entropy production of the full system. Combining Eq. (286) with the TUR evaluated at $\tau \gg 1/\kappa_\nu$, one can possibly bound the transition entropy production σ_ν.

The macroscopic limit not only decomposes the TUR into multiple bounds for the different macroscopic attractors, as given by Eq. (286), but also generates tighter constraints on single degrees of freedom. Indeed, Yoshimura and Ito (2021)

showed that the deterministic dynamics in Eq. (45) is associated with the bound[17]

$$|d_t x_i| = |F_i| \leq \sqrt{D_{ii}\dot{\sigma}_i}, \tag{287}$$

where D_{ii} is the diagonal component on the diffusion matrix in Eq. (81) and $\dot{\sigma}_i := \sum_{\rho>0:\Delta^i_\rho\neq 0}[r_\rho(x(t)) - r_{-\rho}(x(t))]\sigma_\rho(x(t))$ is the scaled macroscopic entropy production associated with variations of the ith component of the configuration vector x. Note that $\dot{\sigma}_i \leq \langle\dot{\sigma}\rangle$, which means that Eq. (287) cannot be obtained by the microscopic TUR, with the latter being a global bound in terms of the total dissipation. As a corollary, integration of Eq. (287) yields a local speed limit that replaces—with respect to its microscopic counterpart (Shiraishi, Funo, and Saito, 2018; Vo, Van Vu, and Hasegawa, 2020; Van Vu and Saito, 2023)—mesoscopic probabilities $p(n,t)$ with macroscopic configurations x. It remains to be explored how recent approaches based on the statistics of residence and return times behave in the macroscopic limit (Marsland, Cui, and Horowitz, 2019; Skinner and Dunkel, 2021a, 2021b; Harunari *et al.*, 2022; Van der Meer, Ertel, and Seifert, 2022).

2. Phase transitions

Macroscopic ST provides a unifying language to describe nonequilibrium phase transitions, not only dynamically but also from an energetic point of view. On the one hand, bifurcation theory can be employed to study the deterministic dynamics upon changing some external parameter (Strogatz, 2015), for instance, the intensive thermodynamic variables of the reservoirs or the system's kinetic factors. Nonconservative forces give rise to a far richer scenario than that encountered in equilibrium phase transitions, where only fixed points are present and their statistical weight can be changed. In the macroscopic limit bistability can emerge as a consequence of a saddle node [see Figs. 10(a) and 10(b)] or a pitchfork bifurcation [see Figs. 10(c) and 10(d)] in processes similar to equilibrium first or second order phase transitions, respectively. A critical point corresponding to a locally flat quasipotential [see Fig. 10(c)] is accompanied by diverging fluctuations so that the Langevin approach of Sec. IV.C breaks down (van Kampen, 2007). A higher order expansion of the master equation captures the critical slowing down of the mean dynamics and the different scaling in V of the fluctuations (Dekker, 1980; Remlein and Seifert, 2024). This phenomenology is akin to phase transitions in systems with detailed balance dynamics, with the quasipotential I_{ss} playing the role of the Massieu potential ϕ. A transition that has no counterpart at equilibrium is the emergence of a limit cycle, for example, through a Hopf bifurcation; see Figs. 10(e) and 10(f). In this case the minimum of the quasipotential lies on a flat manifold, on which a finite dissipative drift $v_{ss}(x^*(t))$ is present and determines the probability distribution along the cycle as $p(x^*(t)) \propto |v_{ss}(x^*(t))|^{-1}$ (Vance and Ross, 1996). On the other hand, large deviations theory is instrumental in identifying dynamical phase transitions. These are singularities in the rate function of dynamical observables either appearing at long times (see Sec. IV.I.2) (Garrahan *et al.*, 2007, 2009; Hurtado and Garrido, 2011; Espigares, Garrido, and Hurtado, 2013; Gingrich, Vaikuntanathan, and Geissler, 2014; Nyawo and Touchette, 2016) or developing at some critical finite time (see Sec. VII.C) (Meibohm and Esposito, 2022, 2023; Blom, 2023).

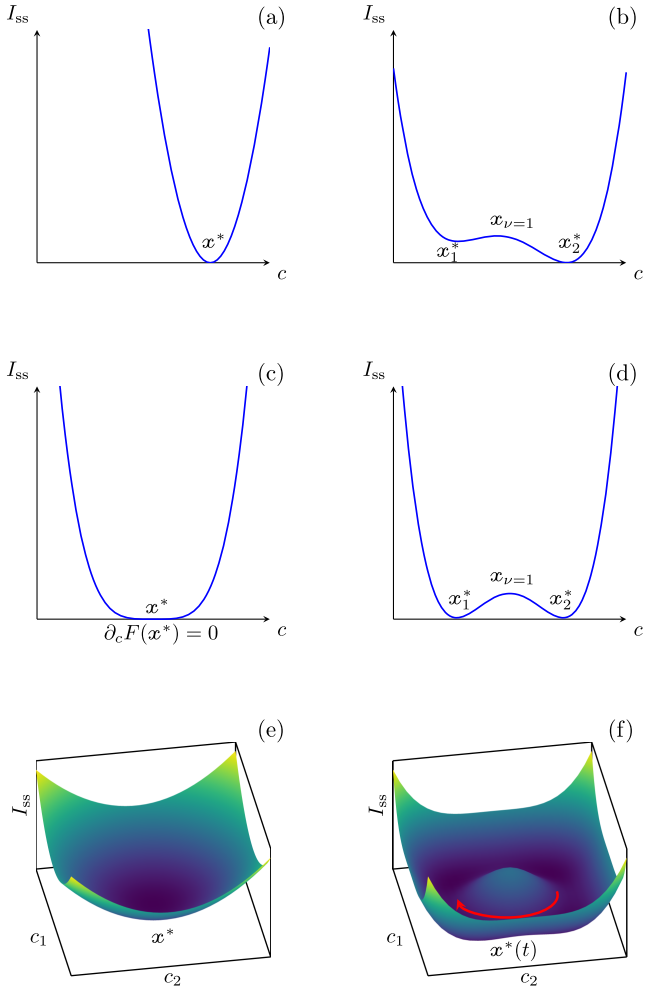

FIG. 10. Representation of the qualitative changes in the quasipotential I_{ss} at phase transitions obtained from variations of an external parameter. The corresponding bifurcations in the macroscopic dynamics [Eq. (45)] are [from (a) to (b)] saddle-node bifurcation, [from (c) to (d)] pitchfork bifurcation, and [from (e) to (f)] Hopf bifurcation in which a finite circulation is present. While the first two are analogous to first and second order phase transitions at equilibrium, respectively, the last one has a genuine dissipative character.

A significant research line concerns the possibility of characterizing the phase transitions and the phase coexistence that appear in the thermodynamic limit by means of the nonequilibrium thermodynamic quantities of the system. The entropy production rate and the Massieu potential (or their derivatives) can display singularities at the critical points, in ways that seem to depend on the specificity of the model under

[17]This result was obtained for deterministic chemical reaction networks but holds for all systems described in this review that admit Eq. (45) as macroscopic dynamics.

scrutiny (Falasco, Rao, and Esposito, 2018; Fernández Noa *et al.*, 2019; Martynec, Klapp, and Loos, 2020; Nguyen and Seifert, 2020; Rana and Barato, 2020; Fiore *et al.*, 2021). Nonequilibrium intensive quantities, such as chemical potential (Guioth and Bertin, 2018, 2019a, 2019b), pressure (Takatori, Yan, and Brady, 2014; Solon *et al.*, 2015; Joyeux and Bertin, 2016), and surface tension (Bialké *et al.*, 2015; Zakine *et al.*, 2020), have been studied to understand whether they can predict the chemical and mechanical stability, especially that of active systems. For pressure, in particular, a generalized equation of state for generic diffusive systems derived by Falasco *et al.* (2016) displays the dissipated heat alongside the standard virial terms. For some notable models, such as active Brownian particles (Solon *et al.*, 2015), this formula yields a pressure that is only a function of bulk variables—regardless of the details of confinement, as in equilibrium. We believe that the macroscopic ST outlined here can help to unify these somewhat detached research efforts.

3. Finite size effects

Within the previously described framework, interesting effects often appear at large yet finite system size. Moving beyond the asymptotic regime considered here requires one to retain subleading corrections in the thermodynamic and kinetic variables, Eqs. (29) and (28). The resulting modification of the large deviations form for probability distributions can be found by means of WKB expansions (Caroli, Caroli, and Roulet, 1979; Caroli *et al.*, 1980; Assaf and Meerson, 2017; Proesmans and Derrida, 2019). For instance, Eq. (31) is replaced by

$$p(c,t) = [A_1(c,t) + O(V^{-1})]e^{-VI(c,t)}, \tag{288}$$

with A_1 satisfying a transport equation obtained by expanding the master equation (3). In particular, the long-time limit of A_1 would allow one to compute subleading corrections to the transition rates in Eq. (157), i.e., the nonequilibrium generalization of the Kramers formula (Hänggi, Talkner, and Borkovec, 1990). To our knowledge, this has been done only for systems with Gaussian noise (Maier and Stein, 1993, 1997) where A_1 can be linked to the instanton dynamics (Bouchet and Reygner, 2016) and presents an additional contribution due to the phase-space contraction rate for systems lacking detailed balance. Moreover, subextensive terms should appear in the deterministic dynamics [Eq. (45)]. Such corrections to the drift field are often computed by adding a small fluctuation of the order of $O(V^{-1/2})$ to the deterministic solution x and averaging it. This procedure leads to the deterministic evolution

$$\dot{x} = F(x) + \frac{1}{2V}\mathrm{Cov}:\partial_c\partial_c F(x), \tag{289}$$

with the covariance $\mathrm{Cov} \coloneqq \langle (c-x)(c-x)\rangle$ computed (at the leading order) by means of Eq. (126). This modified drift may better predict the phase diagram of finite systems—for example, changing the order of phase transitions in extended systems as the active Ising model of Sec. VII.C (Solon and Tailleur, 2015)—but it is not guaranteed to respect the thermodynamic structure of the theory. Even more subtly, at large but finite V the definition of metastable states cannot be reduced to the sole notion of deterministic attractors, which should be identified by the spectral analysis of the Markov generator (Gaveau and Schulman, 1998; Kurchan, 2009).

Finally, subextensive contributions play a key role in the information flows within a system (Parrondo, Horowitz, and Sagawa, 2015). For systems with an at least bipartite structure—i.e., with two sets of transitions, each affecting only one set of states, as in Sec. V.A—it is possible to quantify the entropy exchanges via the rate of variation of mutual information between the two sets of states (Hartich, Barato, and Seifert, 2014; Horowitz and Esposito, 2014). This framework allows one to describe *inter alia* the thermodynamics of autonomous Maxwell demons, in which a part of the system creates correlations used by the rest, for example, to drive a current (Freitas and Esposito, 2021). This mechanism, as it is based on the rectification of thermal fluctuations, breaks down in the macroscopic limit that we considered. Nevertheless, it can be rescued by making the nonconservative force a_ρ extensive in V, although at the expense of a vanishing efficiency (N. Freitas and Esposito, 2022; 2023).

4. Odd-parity variables and quantum systems

We have focused on systems described only by state variables that are even under time reversal. Repeating the approach of this work with odd-parity variables, such as momenta, would lead to, for example, underdamped fluctuating hydrodynamics (Nakamura and Yoshimori, 2009; Manacorda and Puglisi, 2017). The noiseless limit of such theory was considered by Forastiere, Avanzini, and Esposito (2022), who followed the conventional approach of closing moments hierarchy based on the Boltzmann equation, while the asymptotic fluctuations should be derivable using large deviations theory (Bouchet, 2020). The theory can be extended to long-range interacting systems, such as those composed by self-gravitating particles (Chavanis, 2006, 2019), whose energy can be made extensive, albeit not additive, under Kac's prescription. How to generalize the theory to open quantum systems is another research avenue to explore.

5. Response theory

We have not discussed response theory around nonequilibrium states (Baiesi and Maes, 2013). The linear theory allows one to calculate thermodynamic susceptibilities (Boksenbojm *et al.*, 2011; Baiesi, Basu, and Maes, 2014; Falasco and Baiesi, 2016a, 2016b) and transport coefficients (Speck and Seifert, 2006, Seifert and Speck, 2010; Baiesi, Maes, and Wynants, 2011; Falasco, Esposito, and Delvenne, 2020; Chun, Gao, and Horowitz, 2021). Arguably the most general setup to highlight the connection with thermodynamics is the one based on path probabilities, which shows how purely kinetic factors—the excess dynamical activity—pair with the entropy production to produce the system's response (Baiesi, Maes, and Wynants, 2009). How the macroscopic limit affects the scaling of these two contributions remains to be seen. Thermodynamic bounds on susceptibilities have also recently appeared (Owen, Gingrich, and Horowitz, 2020; Aslyamov

and Esposito, 2023). Nonlinear response, originally developed for thermostatted dynamical systems (Evans and Morriss, 1990; Marini Bettolo Marconi *et al.*, 2008; Ruelle, 2009), has received comparatively less attention in the context of ST (Andrieux and Gaspard, 2007; Dechant and Sasa, 2020; Falasco, Esposito, and Delvenne, 2022) despite its experimental importance in dissipative mesoscopic systems, as in active microrheology (Müller *et al.*, 2020), mechanical resonators (Conti *et al.*, 2013; Geitner *et al.*, 2017), and optical microscopy (Radunz *et al.*, 2009).

6. Phenomenological laws

Sections IV.H and VI present new results that emerge as natural consequences of the macroscopic limit of ST. We speculate that they may provide links to some phenomenological laws that have been previously postulated.

On the one hand, the maximum entropy production principle of Sec. IV.H is fundamentally different from the usual statement, which goes under the same name—an empirical law with mixed success. The usual statement can be rephrased in the language of this review by the postulate that the attractor with the largest dissipation $\langle\dot\sigma_\gamma\rangle$ is the one with the smallest escape rate, i.e., the longest lifetime (Martyushev and Seleznev, 2006; Nicolis and Nicolis, 2010). The two statements can agree only under some peculiar conditions, for instance, if most of the nonconservative entropy production is localized on a small neighborhood of the stable fixed points. In this case we should have for the relaxation

$$\sigma^{\mathrm{nc}}_{\nu\to\gamma} = \int dt \sum_\rho a_\rho r_\rho(x(t)) \simeq \langle\dot\sigma_\gamma\rangle \tau^{\mathrm{rel}}_\gamma, \tag{290}$$

where $\tau^{\mathrm{rel}}_\gamma$ is the longest relaxation time of the linear dynamics in Eq. (87), i.e., the inverse absolute value of the smallest eigenvalue of $\partial_c F(x^*_\gamma)$. Similarly, we should have for the instanton

$$\sigma^{\mathrm{nc}}_{\gamma\to\nu} = \int dt \sum_\rho a_\rho r_\rho(c(t)) e^{\Delta_\rho\cdot\partial_c I_{\mathrm{ss}}(c(t))} \simeq -\langle\dot\sigma_\gamma\rangle \tau^{\mathrm{inst}}_\gamma, \tag{291}$$

where $\tau^{\mathrm{inst}}_\gamma$ is the largest timescale of the linearized instanton dynamics

$$d_t c = (c - x^*_\gamma)\cdot[\partial_c F(x^*_\gamma) + 2D(x^*_\gamma)\partial^2_c I_{\mathrm{ss}}(x^*_\gamma)], \tag{292}$$

i.e., the inverse absolute value of the smallest eigenvalue of $\partial_c F^\dagger(x^*_\gamma)$. For Eq. (160) to be tight, one needs $\tau^{\mathrm{rel}}_\gamma \simeq \tau^{\mathrm{inst}}_\gamma$, which is generally true only if $\langle\dot\sigma_\gamma\rangle \to 0$ [see Eq. (153)], i.e., close to detailed balance dynamics. This does not exclude the possibility that in some specific systems the condition $\tau^{\mathrm{rel}}_\gamma \simeq \tau^{\mathrm{inst}}_\gamma$ can be met even far from detailed balance but suggests that some fine-tuning or peculiar symmetries are present. Nevertheless, we remark that in dissipative stochastic systems a local criterion of stability, for example, the lifetime of an attractor, does not determine the global stability, for example, the stationary probability of an attractor. While detailed balance states that are surrounded by the highest energy barrier (and hence have the largest lifetime) are also the most populated in the long-time limit, dissipative states with small escape rate may have a small probability (Maes and Netočný, 2013).

On the other hand, the emergent second law [Eq. (224)], when only baths at the same temperature are present, is an energy balance that counts the energy of maintenance of γ and the energy of changing γ. Imagine a system with a large number $M \to \infty$ of metastable states coordinatized by the continuous variable $m := \gamma/M$. In the case in which $\kappa_{-\nu} \ll \kappa_\nu$ for all $\nu > 0$, the random walk along m is almost surely increasing. Equation (224) takes the general form postulated for the energetics of the resting metabolism of organisms (Lynch and Marinov, 2015), for example, with m the normalized mass of an individual and $\langle\dot\sigma_\gamma\rangle$ the resting metabolic expenditure. This analogy highlights the possibility that the emergent thermodynamics of Sec. VI can carry over to phenomenological energy balances (Yang *et al.*, 2021), thereby helping to clarify the mesoscopic origin of empirically determined laws such as the allometric scaling of $\langle\dot\sigma_\gamma\rangle$ (Ilker and Hinczewski, 2019).

ACKNOWLEDGMENTS

The authors thank D. Forastiere, N. Freitas, and J. Meibohm for the stimulating discussions. G. F. is funded by the European Union NextGenerationEU program and by the STARS@UNIPD program through the project "ThermoComplex." M. E. is supported by the ChemComplex project (Project No. C21/MS/16356329), funded by Fonds National de la Recherche Luxembourg (FNR), and by Project No. INTER/FNRS/20/15074473, funded by FNR and Fonds de la Recherche Scientifique (Belgium).

APPENDIX A: DERIVATION OF THE ENTROPIC UPPER BOUND ON THE TRANSITION RATES

For autonomous systems, we start with the decomposition into adiabatic and nonadiabatic entropy production at the level of single trajectories, multiply both sides of the time-integrated version of Eq. (115) by $\delta(c(0)-x^*_\gamma)\delta(c(t)-x_\nu)$ and take the average. Hence, among all trajectories we sample only those that start at fixed points and reach a saddle. For large t, the left-hand side can be written in terms of the entropy production of the instantonic trajectory, which is defined as

$$\begin{aligned}\sigma_{\gamma\to\nu} &:= \frac{1}{p^{(\gamma)}_{\mathrm{ss}}(x_\nu)} \lim_{t\to\infty}\lim_{V\to\infty} \langle\sigma\delta(c(0)-x^*_\gamma)\delta(c(t)-x_\nu)\rangle, \\ &= \int_{c(0)=x^*_\gamma}^{c(\infty)=x_\nu} dt \sum_\rho r_\rho(c(t))\sigma_\rho(c(t)) e^{\Delta_\rho\cdot\pi(t)},\end{aligned} \tag{A1}$$

where the second equality is from Eq. (179) and $c(t)$ and $\pi(t) = \partial_c I(c(t))$ are the solutions of Eq. (107) with boundary conditions $c(0) = x^*_\gamma$ and $c(\infty) = x_\nu$. In Eq. (A1) we divided by $p^{(\gamma)}_{\mathrm{ss}}(x_\nu)$ to eliminate the exponentially small probability of the instanton [see Eq. (110)] since we are interested only in the value of the entropy production along the trajectory, not in its statistical weight. Note that the macroscopic limit removes the

Shannon entropy of the boundary states, so $\sigma_{\gamma\to\nu}$ counts only the entropy flow of the instanton.

Next we show that the conditional mean of the adiabatic entropy production is still positive. The proof goes as follows. First, we note that

$$\sigma_{\rm ad}[\mathcal{X}] = -\frac{1}{V}\ln\frac{P^\dagger[\mathcal{X}]}{P[\mathcal{X}]}, \tag{A2}$$

where $P^\dagger[\mathcal{X}]$ denotes the path probability under the dual dynamics with transition rates $r^\dagger_\rho(c)$ given in Eq. (40). We therefore write the transition probability $P^\dagger(x_\nu,t|x^*_\gamma,0)$ from x^*_γ to x_ν under the dual dynamics as the conditional average over paths,

$$\begin{aligned}
&P^\dagger(x_\nu,t|x^*_\gamma,0)\\
&=\sum_{\mathcal{X}}P^\dagger[\mathcal{X}]\delta(c(0)-x^*_\gamma)\delta(c(t)-x_\nu)\\
&=\sum_{\mathcal{X}}P[\mathcal{X}]e^{-V\sigma_{\rm ad}[\mathcal{X}]}\delta(c(0)-x^*_\gamma)\delta(c(t)-x_\nu)\\
&\geq P(x_\nu,t|x^*_\gamma,0)e^{-[V/P(x_\nu,t|x^*_\gamma,0)]\langle\sigma_{\rm ad}\delta(c(0)-x^*_\gamma)\delta(c(t)-x_\nu)\rangle}.
\end{aligned} \tag{A3}$$

On the last line of Eq. (A3), we used Jensen's inequality applied to the normalized conditional average, $\langle\ldots\delta(c(0)-x^*_\gamma)\delta(c(t)-x_\nu)\rangle/P(x_\nu,t|x^*_\gamma,0)$, in the same spirit as Falasco and Esposito (2020). Second, we use the fact that for large V and large t the transition probability approaches the local stationary probability distribution at the saddle point x_ν,

$$\lim_{t\to\infty}P(x_\nu,t|x^*_\gamma,0)\asymp e^{-V[I^{(\gamma)}_{\rm ss}(x_\nu)-I^{(\gamma)}_{\rm ss}(x^*_\gamma)]}=p^{(\gamma)}_{\rm ss}(x_\nu). \tag{A4}$$

But since the dual dynamics preserves the steady state $p^{(\gamma)}_{\rm ss}$, we have $P^\dagger(x_\nu,t|x^*_\gamma,0)=P(x_\nu,t|x^*_\gamma,0)$ for large t. Hence, Eq. (A3) gives

$$1\geq e^{-V\sigma^{\rm ad}_{\gamma\to\nu}}, \tag{A5}$$

which implies that the adiabatic entropy production of an instantonic trajectory is non-negative,

$$\sigma^{\rm ad}_{\gamma\to\nu}:=\frac{1}{p^{(\gamma)}_{\rm ss}(x_\nu)}\lim_{t\to\infty}\lim_{V\to\infty}\langle\sigma^{\rm ad}\delta(c(0)-x^*_\gamma)\delta(c(t)-x_\nu)\rangle\geq 0. \tag{A6}$$

As in Eq. (A1), we have factored out the exponentially small probability $p^{(\gamma)}_{\rm ss}\geq 0$ of the instanton.

At this point we return to the conditional average of the entropy production decomposition in Eq. (115) and use Eqs. (A6) and (A1) to write

$$\begin{aligned}
\sigma_{\gamma\to\nu}&\geq-\int_{x(0)=x^*_\gamma}^{x(\infty)=x_\nu}d_\tau I^{(\gamma)}_{\rm ss}(x(\tau))d\tau\\
&=-I^{(\gamma)}_{\rm ss}(x_\nu)+I^{(\gamma)}_{\rm ss}(x^*_\gamma).
\end{aligned} \tag{A7}$$

Multiplying Eq. (A7) by V and exponentiating, we finally obtain the upper bound [Eq. (160)] on the transition rate κ_ν.

We conclude by pointing out that integrating the entropy production between fixed points gives a diverging quantity— (unless detailed balance holds) because relaxation (and instantonic) trajectories have an infinite duration. This is traced back to the Laplace approximation in Eq. (107), which is valid for states c at which the noise is small compared to the drift field $F(c)$. This assumption breaks down on fixed points, in which the drift field is null. One should consider boundary conditions that belong to the boundary of a ball centered on the fixed point with a radius of the order of the Gaussian fluctuations $O(V^{-1/2})$. Inside any such ball the weak-noise limit breaks down.[18] Changing the integration boundaries in this way introduces on the left-hand side of Eq. (A7) a correction of the order of $O(1/V)$ (since $\partial_c I^\gamma_{\rm ss}$ is zero on every fixed point), and hence a subexponential correction to κ_ν, but makes $\sigma_{\gamma\to\nu}$ and $\sigma_{\nu\to\gamma}$ finite by discarding the entropy produced at the fixed point. Using Eq. (22), for which all of the aforementioned derivations can be repeated, rather than the thermodynamic entropy production is an alternative approach to remove the divergence (without tuning the integration boundaries) and thus tighten the bounds.

APPENDIX B: DERIVATION OF THE EMERGING TRANSITION RATES

We now give a formal derivation of Eq. (157) along the lines of the proof developed by Bouchet and Reygner (2016) for diffusive dynamics. We consider an autonomous system initially localized in a basin of attraction γ and place absorbing boundary conditions in the neighborhood of the saddle points x_ν. For times much smaller than the escape time from the basin (which we want to determine), the system probability density $p_{\rm abs}(c,t)$ coincides with $p^{(\gamma)}_{\rm ss}(c)\asymp e^{-VI^{(\gamma)}_{\rm ss}(c)}$ for all c in the basin but on a small boundary layer of linear size $O(V^{-1/2})$ around the saddles x_ν. To quantify how probability mass gets removed, we thus introduce the survival probability, the monotonic decreasing function (Redner, 2001)

$$\mathcal{P}_{\rm surv}(t)=\int dc\, p_{\rm abs}(c,t), \tag{B1}$$

which we express in terms of the total escape rate κ from the attractor. In general, the survival probability depends on all eigenvalues of the master equation operator with absorbing boundary conditions (Freitas, Proesmans, and Esposito, 2022). But in the presence of metastability (see Sec. III.B) only the largest, $-\kappa$, contributes, unless $t\to 0$. This means that escape events are exponentially distributed in the limit $V\to\infty$, i.e., $\mathcal{P}_{\rm surv}(t)=e^{-\kappa t}$ (Day, 1983). Moreover, we assume that the saddles are well separated and thus contribute independently to the escape rate as $\kappa=\sum_\nu\kappa_\nu$.

[18] A rigorous treatment that includes subexponential corrections would require the use of a boundary layer approximation (Schuss, 2009).

The evolution of the survival probability can be deduced from the master equation

$$\partial_t p_{\rm abs}(c,t) = -\partial_c \cdot \mathbf{j}_{\rm abs}(c,t) \tag{B2}$$

with absorbing conditions $p_{\rm abs}(x_\nu,t)=0$. Integrating Eq. (B2) over the basin of attraction using Eq. (B1) and the divergence theorem, we obtain

$$\mathcal{P}_{\rm surv}(t)\sum_\nu k_\nu = \sum_\nu \mathbf{j}_{\rm abs}(x_\nu,t)\cdot\hat{e}(x_\nu)\Delta\mathcal{S}, \tag{B3}$$

where $\Delta\mathcal{S}$ is a small surface element of the boundary of the basin and $\hat{e}(x_\nu)$ is the local outward unit vector. Using the definition of the probability current $\mathbf{j}_{\rm abs}(c,t) = \langle \dot{c}(t)\delta(c(t)-c)\rangle$, we can write Eq. (B3) for $V\to\infty$ as

$$\mathbf{j}_{\rm abs}(x_\nu,t) = \dot{c}(t)p_{\rm abs}(x_\nu,t), \tag{B4}$$

with $\dot{c}(t)$ the velocity of the typical escape path near the saddle. Equation (B3) is particularly valid at times much shorter than $1/\kappa$ when $\mathcal{P}_{\rm surv}(t\ll 1/\kappa)\simeq 1$ and $p_{\rm abs}(c,t\ll 1/\kappa)\asymp p_{\rm ss}^{(\gamma)}(c)$ is indistinguishable from the local stationary probability in Eq. (110) at leading order (Bouchet and Reygner, 2016). Therefore, when subexponential contributions are discarded, Eq. (B3) reads

$$\sum_\nu k_\nu \asymp \sum_\nu e^{-V[I_{\rm ss}^{(\gamma)}(x_\nu)-I_{\rm ss}^{(\gamma)}(x_\gamma^*)]}, \tag{B5}$$

which gives Eq. (157) under the hypothesis of independent escape paths through each separate saddle point.

REFERENCES

Agranov, T., R. L. Jack, M. E. Cates, and É. Fodor, 2024, arXiv:2401.09901.

Anderson, D. F., and T. G. Kurtz, 2011, in *Design and Analysis of Biomolecular Circuits: Engineering Approaches to Systems and Synthetic Biology*, edited by H. Koeppl, G. Setti, M. di Bernardo, and D. Densmore (Springer, New York), pp. 3–44.

Andrieux, D., and P. Gaspard, 2007, J. Stat. Mech. P02006.

Andrieux, D., and P. Gaspard, 2008, J. Chem. Phys. **128**, 154506.

Arrhenius, S., 1889, Z. Phys. Chem., Stoechiom. Verwandtschaftsl. **4U**, 226.

Aslyamov, T., F. Avanzini, E. Fodor, and M. Esposito, 2023, Phys. Rev. Lett. **131**, 138301.

Aslyamov, T., and M. Esposito, 2023, arXiv:2308.04260.

Assaf, M., and B. Meerson, 2017, J. Phys. A **50**, 263001.

Auffèves, A., 2022, PRX Quantum **3**, 020101.

Avanzini, F., G. Falasco, and M. Esposito, 2019, J. Chem. Phys. **151**, 234103.

Avanzini, F., E. Penocchio, G. Falasco, and M. Esposito, 2021, J. Chem. Phys. **154**, 094114.

Baek, Y., and Y. Kafri, 2015, J. Stat. Mech. P08026.

Baiesi, M., U. Basu, and C. Maes, 2014, Eur. Phys. J. B **87**, 277.

Baiesi, M., and G. Falasco, 2015, Phys. Rev. E **92**, 042162.

Baiesi, M., and C. Maes, 2013, New J. Phys. **15**, 013004.

Baiesi, M., C. Maes, and B. Wynants, 2009, Phys. Rev. Lett. **103**, 010602.

Baiesi, M., C. Maes, and B. Wynants, 2011, Proc. R. Soc. A **467**, 2792.

Barato, A. C., and U. Seifert, 2015, Phys. Rev. Lett. **114**, 158101.

Battle, C., C. P. Broedersz, N. Fakhri, V. F. Geyer, J. Howard, C. F. Schmidt, and F. C. MacKintosh, 2016, Science **352**, 604.

Bauer, M., and F. Cornu, 2015, J. Phys. A **48**, 015008.

Bebon, R., J. F. Robinson, and T. Speck, 2024, arXiv:2401.02252.

Bechinger, C., R. Di Leonardo, and H. Löwen, C. Reichhardt, G. Volpe, and G. Volpe, 2016, Rev. Mod. Phys. **88**, 045006.

Benenti, G., G. Casati, K. Saito, and R. S. Whitney, 2017, Phys. Rep. **694**, 1.

Benettin, G., L. Galgani, A. Giorgilli, and J.-M. Strelcyn, 1980, Meccanica **15**, 9.

Bergmann, P. G., and J. L. Lebowitz, 1955, Phys. Rev. **99**, 578.

Bertini, L., A. De Sole, D. Gabrielli, G. Jona-Lasinio, and C. Landim, 2015, Rev. Mod. Phys. **87**, 593.

Bertini, L., A. De Sole, D. Gabrielli, G. Jona-Lasinio, and C. Landim, 2010, J. Stat. Mech. L11001.

Bertini, L., D. Gabrielli, G. Jona-Lasinio, and C. Landim, 2013, Phys. Rev. Lett. **110**, 020601.

Bérut, A., A. Arakelyan, A. Petrosyan, S. Ciliberto, R. Dillenschneider, and E. Lutz, 2012, Nature (London) **483**, 187.

Bialké, J., J. T. Siebert, H. Löwen, and T. Speck, 2015, Phys. Rev. Lett. **115**, 098301.

Blickle, V., T. Speck, L. Helden, U. Seifert, and C. Bechinger, 2006, Phys. Rev. Lett. **96**, 070603.

Blom, K., 2023, *Pair-Correlation Effects in Many-Body Systems: Towards a Complete Theoretical Description of Pair-Correlations in the Static and Kinetic Description of Many-Body Systems*, Springer Theses (Springer, New York), pp. 131–162.

Bo, S., and A. Celani, 2014, J. Stat. Phys. **154**, 1325.

Bo, S., and A. Celani, 2017, Phys. Rep. **670**, 1.

Boksenbojm, E., C. Maes, K. Netočný, and J. Pešek, 2011, Europhys. Lett. **96**, 40001.

Boland, R. P., T. Galla, and A. J. McKane, 2008, J. Stat. Mech. P09001.

Bouchet, F., 2020, J. Stat. Phys. **181**, 515.

Bouchet, F., K. Gawredzki, and C. Nardini, 2016, J. Stat. Phys. **163**, 1157.

Bouchet, F., and J. Reygner, 2016, Ann. Henri Poincaré **17**, 3499.

Bovier, A., M. Eckhoff, V. Gayrard, and M. Klein, 2002, Commun. Math. Phys. **228**, 219.

Bressloff, P. C., 2017, J. Phys. A **50**, 133001.

Bressloff, P. C., and J. M. Newby, 2014, Phys. Rev. E **89**, 042701.

Brillouin, L., 1950, Phys. Rev. **78**, 627.

Brown, A. I., and D. A. Sivak, 2020, Chem. Rev. **120**, 434.

Buffoni, L., and M. Campisi, 2022, J. Stat. Phys. **186**, 31.

Callen, H. B., 1991, *Thermodynamics and an Introduction to Thermostatistics* (John Wiley & Sons, New York).

Cao, Z., H. Jiang, and Z. Hou, 2020, Phys. Rev. Res. **2**, 043331.

Caroli, B., C. Caroli, and B. Roulet, 1979, J. Stat. Phys. **21**, 415.

Caroli, B., C. Caroli, and B. Roulet, 1981, J. Stat. Phys. **26**, 83.

Caroli, B., C. Caroli, B. Roulet, and J. F. Gouyet, 1980, J. Stat. Phys. **22**, 515.

Castellani, T., and A. Cavagna, 2005, J. Stat. Mech. P05012.

Ceccato, A., and D. Frezzato, 2018, J. Chem. Phys. **148**, 064114.

Çetiner, U., and J. Gunawardena, 2022, Phys. Rev. E **106**, 064128.

Chavanis, P.-H., 2006, Physica (Amsterdam) **361A**, 81.

Chavanis, P.-H., 2019, Entropy **21**, 1006.

Chernyak, V. Y., M. Chertkov, and C. Jarzynski, 2006, J. Stat. Mech. P08001.

Chetrite, R., and K. Gawedzki, 2008, Commun. Math. Phys. **282**, 469.

Chun, H.-M., Q. Gao, and J. M. Horowitz, 2021, Phys. Rev. Res. **3**, 043172.
Ciliberto, S., 2017, Phys. Rev. X **7**, 021051.
Cohen, E., and L. Rondoni, 1998, Chaos **8**, 357.
Colangeli, M., C. Maes, and B. Wynants, 2011, J. Phys. A **44**, 095001.
Coleman, S., 1988, *Aspects of Symmetry: Selected Erice Lectures* (Cambridge University Press, Cambridge, England).
Conti, L., P. De Gregorio, G. Karapetyan, C. Lazzaro, M. Pegoraro, M. Bonaldi, and L. Rondoni, 2013, J. Stat. Mech. P12003.
Daems, D., and G. Nicolis, 1999, Phys. Rev. E **59**, 4000.
Dal Cengio, S., V. Lecomte, and M. Polettini, 2023, Phys. Rev. X **13**, 021040.
Day, M. V., 1983, Stochastics **8**, 297.
Day, M. V., 1990, J. Math. Anal. Appl. **147**, 134.
Dean, D. S., 1996, J. Phys. A **29**, L613.
Dechant, A., and S.-i. Sasa, 2020, Proc. Natl. Acad. Sci. U.S.A. **117**, 6430.
Dechant, A., and S.-i. Sasa, 2021, Phys. Rev. X **11**, 041061.
De Dominicis, C., and L. Peliti, 1978, Phys. Rev. B **18**, 353.
De Giuli, E., and C. Scalliet, 2022, J. Phys. A **55**, 474002.
de Groot, S. R., and P. Mazur, 1984, *Non-Equilibrium Thermodynamics* (Dover, New York).
Dekker, H., 1980, Physica (Amsterdam) **103A**, 80.
de Zárate, J. M. O., and J. V. Sengers, 2006, *Hydrodynamic Fluctuations in Fluids and Fluid Mixtures* (Elsevier, New York).
Dinelli, A., J. O'Byrne, A. Curatolo, Y. Zhao, P. Sollich, and J. Tailleur, 2023, Nat. Commun. **14**, 7035.
Doi, M., 1976, J. Phys. A **9**, 1465.
Dorfman, J. R., 1999, in *An Introduction to Chaos in Nonequilibrium Statistical Mechanics*, Cambridge Lecture Notes in Physics Vol. 14 (Cambridge University Press, Cambridge, England).
Dykman, M., X. Chu, and J. Ross, 1993, Phys. Rev. E **48**, 1646.
Dykman, M. I., E. Mori, J. Ross, and P. M. Hunt, 1994, J. Chem. Phys. **100**, 5735.
Einstein, A., 1910, Ann. Phys. (Berlin) **338**, 1275.
Elgart, V., and A. Kamenev, 2004, Phys. Rev. E **70**, 041106.
Epstein, I. R., and J. A. Pojman, 1998, *An Introduction to Nonlinear Chemical Dynamics: Oscillations, Waves, Patterns, and Chaos* (Oxford University Press, New York).
Espigares, C. P., P. L. Garrido, and P. I. Hurtado, 2013, Phys. Rev. E **87**, 032115.
Esposito, M., 2012, Phys. Rev. E **85**, 041125.
Esposito, M., U. Harbola, and S. Mukamel, 2007, Phys. Rev. E **76**, 031132.
Esposito, M., and J. M. R. Parrondo, 2015, Phys. Rev. E **91**, 052114.
Esposito, M., and C. Van den Broeck, 2010, Phys. Rev. E **82**, 011143.
Evans, D. J., E. G. D. Cohen, and G. P. Morriss, 1993, Phys. Rev. Lett. **71**, 2401.
Evans, D. J., and G. P. Morriss, 1990, in *Statistical Mechanics of Nonequilibrium Liquids*, Theoretical Chemistry Monograph Series, edited by D. P. Craig and R. McWeeny (Academic Press, London).
Evans, D. J., and D. J. Searles, 1994, Phys. Rev. E **50**, 1645.
Evans, D. J., and D. J. Searles, 2002, Adv. Phys. **51**, 1529.
Eyring, H., 1935, J. Chem. Phys. **3**, 107.
Falasco, G., and M. Baiesi, 2016a, New J. Phys. **18**, 043039.
Falasco, G., and M. Baiesi, 2016b, Europhys. Lett. **113**, 20005.
Falasco, G., F. Baldovin, K. Kroy, and M. Baiesi, 2016, New J. Phys. **18**, 093043.
Falasco, G., T. Cossetto, E. Penocchio, and M. Esposito, 2019, New J. Phys. **21**, 073005.
Falasco, G., and M. Esposito, 2020, Phys. Rev. Lett. **125**, 120604.
Falasco, G., and M. Esposito, 2021, Phys. Rev. E **103**, 042114.
Falasco, G., M. Esposito, and J.-C. Delvenne, 2020, New J. Phys. **22**, 053046.
Falasco, G., M. Esposito, and J.-C. Delvenne, 2022, J. Phys. A **55**, 124002.
Falasco, G., R. Rao, and M. Esposito, 2018, Phys. Rev. Lett. **121**, 108301.
Fernández Noa, C. E., P. E. Harunari, M. de Oliveira, and C. Fiore, 2019, Phys. Rev. E **100**, 012104.
Fiore, C. E., P. E. Harunari, C. E. Fernández Noa, and G. T. Landi, 2021, Phys. Rev. E **104**, 064123.
Fodor, E., C. Nardini, M. E. Cates, J. Tailleur, P. Visco, and F. van Wijland, 2016, Phys. Rev. Lett. **117**, 038103.
Forastiere, D., F. Avanzini, and M. Esposito, 2022, arXiv:2306.00911.
Forastiere, D., R. Rao, and M. Esposito, 2022, New J. Phys. **24**, 083021.
Freidlin, M. I., and A. D. Wentzell, 1998, *Random Perturbations of Dynamical Systems*, 2nd ed. (Springer, New York).
Freitas, J. N., and M. Esposito, 2022, Nat. Commun. **13**, 5084.
Freitas, N., J.-C. Delvenne, and M. Esposito, 2020, Phys. Rev. X **10**, 031005.
Freitas, N., J.-C. Delvenne, and M. Esposito, 2021, Phys. Rev. X **11**, 031064.
Freitas, N., and M. Esposito, 2021, Phys. Rev. E **103**, 032118.
Freitas, N., and M. Esposito, 2022, Phys. Rev. Lett. **129**, 120602.
Freitas, N., and M. Esposito, 2023, Phys. Rev. E **107**, 014136.
Freitas, N., G. Falasco, and M. Esposito, 2021, New J. Phys. **23**, 093003.
Freitas, N., K. Proesmans, and M. Esposito, 2022, Phys. Rev. E **105**, 034107.
Fruchart, M., R. Hanai, P. B. Littlewood, and V. Vitelli, 2021, Nature (London) **592**, 363.
Gallavotti, G., and E. G. D. Cohen, 1995a, Phys. Rev. Lett. **74**, 2694.
Gallavotti, G., and E. G. D. Cohen, 1995b, J. Stat. Phys. **80**, 931.
Gang, H., 1987, Phys. Rev. A **36**, 5782.
Gao, Y., and J.-G. Liu, 2022, J. Stat. Phys. **189**, 1.
Gardiner, C. W., 2004, *Handbook of Stochastic Methods for Physics, Chemistry and the Natural Sciences*, 3rd ed., Springer Series in Synergetics Vol. 13 (Springer-Verlag, Berlin).
Garrahan, J. P., R. L. Jack, V. Lecomte, E. Pitard, K. van Duijvendijk, and F. van Wijland, 2007, Phys. Rev. Lett. **98**, 195702.
Garrahan, J. P., R. L. Jack, V. Lecomte, E. Pitard, K. van Duijvendijk, and F. van Wijland, 2009, J. Phys. A **42**, 075007.
Garvey, J. E., and M. Whiles, 2016, *Trophic Ecology* (CRC Press, Boca Raton).
Gaspard, P., 2002a, J. Chem. Phys. **117**, 8905.
Gaspard, P., 2002b, J. Stat. Phys. **106**, 57.
Gaspard, P., 2005, *Chaos, Scattering and Statistical Mechanics*, Cambridge Nonlinear Science Series Vol. 9 (Cambridge University Press, Cambridge, England).
Gaspard, P., 2020, Chaos **30**, 113103.
Gaspard, P., 2022, *The Statistical Mechanics of Irreversible Phenomena* (Cambridge University Press, Cambridge, England).
Gaspard, P., and R. Kapral, 2020, Research 9739231.
Gaveau, B., M. Moreau, and J. Toth, 1997, Lett. Math. Phys. **40**, 101.
Gaveau, B., M. Moreau, and J. Toth, 1998, Phys. Rev. E **58**, 5351.
Gaveau, B., M. Moreau, and J. Toth, 1999, J. Chem. Phys. **111**, 7748.
Gaveau, B., and L. S. Schulman, 1998, J. Math. Phys. (N.Y.) **39**, 1517.
Ge, H., and H. Qian, 2010, Phys. Rev. E **81**, 051133.
Ge, H., and H. Qian, 2012, Chaos **22**, 023140.
Geitner, M., F. Aguilar Sandoval, E. Bertin, and L. Bellon, 2017, Phys. Rev. E **95**, 032138.

Gillespie, D. T., 1977, J. Phys. Chem. **81**, 2340.
Gillespie, D. T., 1992, Physica (Amsterdam) **188A**, 404.
Gillespie, D. T., 2000, J. Chem. Phys. **113**, 297.
Gingrich, T. R., G. M. Rotskoff, and J. M. Horowitz, 2017, J. Phys. A **50**, 184004.
Gingrich, T. R., S. Vaikuntanathan, and P. L. Geissler, 2014, Phys. Rev. E **90**, 042123.
Goldstein, S., D. A. Huse, J. L. Lebowitz, and P. Sartori, 2019, in *Stochastic Dynamics Out of Equilibrium*, edited by G. Giacomin, S. Olla, E. Saada, H. Spohn, and G. Stoltz (Springer International Publishing, Cham, Switzerland), pp. 581–596.
Gopal, A., M. Esposito, and N. Freitas, 2022, Phys. Rev. B **106**, 155303.
Grafke, T., T. Schäfer, and E. Vanden-Eijnden, 2017, in *Recent Progress and Modern Challenges in Applied Mathematics, Modeling and Computational Science*, Fields Institute Communications Vol. 79, edited by R. Melnik, R. Makarov, and J. Belair (Springer, New York), p. 17.
Graham, R., 1987, in *Fluctuations and Stochastic Phenomena in Condensed Matter* (Springer, New York), pp. 1–34.
Graham, R., and T. Tél, 1985, Phys. Rev. A **31**, 1109.
Graham, R., and T. Tél, 1986, Phys. Rev. A **33**, 1322.
Grassberger, P., and S. Manfred, 1980, Fortschr. Phys. **28**, 547.
Guioth, J., and E. Bertin, 2018, Europhys. Lett. **123**, 10002.
Guioth, J., and E. Bertin, 2019a, J. Chem. Phys. **150**, 094108.
Guioth, J., and E. Bertin, 2019b, Phys. Rev. E **100**, 052125.
Hajimiri, A., S. Limotyrakis, and T. H. Lee, 1999, IEEE J. Solid-State Circuits **34**, 790.
Hänggi, P., and P. Jung, 1988, IBM J. Res. Dev. **32**, 119.
Hänggi, P., P. Talkner, and M. Borkovec, 1990, Rev. Mod. Phys. **62**, 251.
Hao, G., and Q. Hong, 2011, J. R. Soc. Interface **8**, 107.
Harada, T., and S. Sasa, 2005, Phys. Rev. Lett. **95**, 130602.
Hartich, D., A. C. Barato, and U. Seifert, 2014, J. Stat. Mech. P02016.
Harunari, P. E., A. Dutta, M. Polettini, and É. Roldán, 2022, Phys. Rev. X **12**, 041026.
Hasegawa, Y., and T. Van Vu, 2019, Phys. Rev. Lett. **123**, 110602.
Hatano, T., and S. Sasa, 2001, Phys. Rev. Lett. **86**, 3463.
Henkel, C., 2017, Z. Naturforsch. A **72**, 99.
Herpich, T., T. Cossetto, G. Falasco, and M. Esposito, 2020, New J. Phys. **22**, 063005.
Herpich, T., and M. Esposito, 2019, Phys. Rev. E **99**, 022135.
Herpich, T., K. Shayanfard, and M. Esposito, 2020, Phys. Rev. E **101**, 022116.
Herpich, T., J. Thingna, and M. Esposito, 2018, Phys. Rev. X **8**, 031056.
Hohenberg, P. C., and B. I. Halperin, 1977, Rev. Mod. Phys. **49**, 435.
Horowitz, J. M., 2015, J. Chem. Phys. **143**, 044111.
Horowitz, J. M., and M. Esposito, 2014, Phys. Rev. X **4**, 031015.
Horowitz, J. M., and T. R. Gingrich, 2020, Nat. Phys. **16**, 15.
Huang, S., F. Li, J. X. Zhou, and H. Qian, 2017, J. R. Soc. Interface **14**, 20170097.
Hurtado, P. I., C. P. Espigares, J. J. del Pozo, and P. L. Garrido, 2014, J. Stat. Phys. **154**, 214.
Hurtado, P. I., and P. L. Garrido, 2011, Phys. Rev. Lett. **107**, 180601.
Ilker, E., and M. Hinczewski, 2019, Phys. Rev. Lett. **122**, 238101.
Ivlev, A. V., J. Bartnick, M. Heinen, C.-R. Du, V. Nosenko, and H. Löwen, 2015, Phys. Rev. X **5**, 011035.
Jarzynski, C., 2011, Annu. Rev. Condens. Matter Phys. **2**, 329.
Jiu-li, L., C. Van den Broeck, and G. Nicolis, 1984, Z. Phys. B **56**, 165.
Joyeux, M., and E. Bertin, 2016, Phys. Rev. E **93**, 032605.
Jun, Y., M. Gavrilov, and J. Bechhoefer, 2014, Phys. Rev. Lett. **113**, 190601.
Kac, M., G. Uhlenbeck, and P. Hemmer, 1963, J. Math. Phys. (N.Y.) **4**, 216.
Kawasaki, K., 1998, J. Stat. Phys. **93**, 527.
Keizer, J., 1978, J. Chem. Phys. **69**, 2609.
Keller, H. B., 2018, *Numerical Methods for Two-Point Boundary-Value Problems*, Dover Books on Mathematics (Dover Publications, New York).
Kikuchi, L., R. Singh, M. E. Cates, and R. Adhikari, 2020, Phys. Rev. Res. **2**, 033208.
Konarovskyi, V., T. Lehmann, and M. von Renesse, 2020, J. Stat. Phys. **178**, 666.
Koski, J. V., A. Kutvonen, I. M. Khaymovich, T. Ala-Nissila, and J. P. Pekola, 2015, Phys. Rev. Lett. **115**, 260602.
Koyuk, T., and U. Seifert, 2022, Phys. Rev. Lett. **129**, 210603.
Kraaij, R., A. Lazarescu, C. Maes, and M. Peletier, 2018, J. Stat. Phys. **170**, 492.
Kramers, H., 1940, Physica (Amsterdam) **7**, 284.
Kubo, R., K. Matsuo, and K. Kitahara, 1973, J. Stat. Phys. **9**, 51.
Kurchan, J., 1998, J. Phys. A **31**, 3719.
Kurchan, J., 2009, arXiv:0901.1271.
Kurtz, T. G., 1972, J. Chem. Phys. **57**, 2976.
Kuznets-Speck, B., and D. T. Limmer, 2021, Proc. Natl. Acad. Sci. U.S.A. **118**, e2020863118.
Landau, L. D., and E. M. Lifshitz, 1959, *Fluid Mechanics* (Pergamon Press, New York).
Landauer, R., and J. Swanson, 1961, Phys. Rev. **121**, 1668.
Lange, S., J. Pohl, and T. Santarius, 2020, Ecol. Econ. **176**, 106760.
Langer, J. S., 1969, Ann. Phys. (N.Y.) **54**, 258.
Lazarescu, A., T. Cossetto, G. Falasco, and M. Esposito, 2019, J. Chem. Phys. **151**, 064117.
Lebowitz, J. L., and H. Spohn, 1999, J. Stat. Phys. **95**, 333.
Lefever, R., G. Nicolis, and P. Borckmans, 1988, J. Chem. Soc., Faraday Trans. 1 **84**, 1013.
Lefevre, A., and G. Biroli, 2007, J. Stat. Mech. P07024.
Liero, M., and A. Mielke, 2013, Phil. Trans. R. Soc. A **371**, 20120346.
Loos, S. A., and S. H. Klapp, 2020, New J. Phys. **22**, 123051.
Luchinsky, D., P. V. McClintock, and M. Dykman, 1998, Rep. Prog. Phys. **61**, 889.
Luchinsky, D. G., R. S. Maier, R. Mannella, P. V. E. McClintock, and D. L. Stein, 1999, Phys. Rev. Lett. **82**, 1806.
Lynch, M., and G. K. Marinov, 2015, Proc. Natl. Acad. Sci. U.S.A. **112**, 15690.
Macieszczak, K., K. Brandner, and J. P. Garrahan, 2018, Phys. Rev. Lett. **121**, 130601.
Maes, C., 2018, *Non-Dissipative Effects in Nonequilibrium Systems* (Springer, New York).
Maes, C., 2020, Phys. Rev. Lett. **125**, 208001.
Maes, C., 2021, SciPost Phys. Lect. Notes **32**, 1.
Maes, C., and K. Netočný, 2007, C. R. Phys. **8**, 591.
Maes, C., and K. Netočný, 2008, Europhys. Lett. **82**, 30003.
Maes, C., and K. Netočný, 2010, J. Math. Phys. (N.Y.) **51**, 015219.
Maes, C., and K. Netočný, 2013, in Ann. Henri Poincaré **14**, 1193.
Maes, C., and K. Netočný, 2014, J. Stat. Phys. **154**, 188.
Maes, C., and K. Netočný, 2015, J. Stat. Phys. **159**, 1286.
Maier, R. S., and D. L. Stein, 1993, Phys. Rev. Lett. **71**, 1783.
Maier, R. S., and D. L. Stein, 1997, SIAM J. Appl. Math. **57**, 752.
Malinin, S. V., and V. Y. Chernyak, 2010, J. Chem. Phys. **132**, 01B602.
Manacorda, A., and A. Puglisi, 2017, Phys. Rev. Lett. **119**, 208003.

Mangeat, M., S. Chatterjee, R. Paul, and H. Rieger, 2020, Phys. Rev. E **102**, 042601.
Marchetti, M. C., J. F. Joanny, S. Ramaswamy, T. B. Liverpool, J. Prost, M. Rao, and R. A. Simha, 2013, Rev. Mod. Phys. **85**, 1143.
Marconi, U. M. B., and P. Tarazona, 1999, J. Chem. Phys. **110**, 8032.
Marini Bettolo Marconi, U., A. Puglisi, L. Rondoni, and A. Vulpiani, 2008, Phys. Rep. **461**, 111.
Markovich, T., E. Fodor, E. Tjhung, and M. E. Cates, 2021, Phys. Rev. X **11**, 021057.
Marsland III, R., W. Cui, and J. M. Horowitz, 2019, J. R. Soc. Interface **16**, 20190098.
Martynec, T., S. H. Klapp, and S. A. Loos, 2020, New J. Phys. **22**, 093069.
Martyushev, L. M., and V. D. Seleznev, 2006, Phys. Rep. **426**, 1.
McLennan, Jr., J. A., 1959, Phys. Rev. **115**, 1405.
Mehl, J., B. Lander, C. Bechinger, V. Blickle, and U. Seifert, 2012, Phys. Rev. Lett. **108**, 220601.
Meibohm, J., and M. Esposito, 2022, Phys. Rev. Lett. **128**, 110603.
Meibohm, J., and M. Esposito, 2023, New J. Phys. **25**, 023034.
Meibohm, J., and M. Esposito, 2024a, arXiv:2401.14982.
Meibohm, J., and M. Esposito, 2024b, arXiv:2401.14980.
Mielke, A., D. M. Renger, and M. A. Peletier, 2016, J. Non-Equilib. Thermodyn. **41**, 141.
Müller, B., J. Berner, C. Bechinger, and M. Krüger, 2020, New J. Phys. **22**, 023014.
Mura, F., G. Gradziuk, and C. P. Broedersz, 2018, Phys. Rev. Lett. **121**, 038002.
Murashita, Y., K. Funo, and M. Ueda, 2014, Phys. Rev. E **90**, 042110.
Nakamura, T., and A. Yoshimori, 2009, J. Phys. A **42**, 065001.
Nardini, C., É. Fodor, E. Tjhung, F. Van Wijland, J. Tailleur, and M. E. Cates, 2017, Phys. Rev. X **7**, 021007.
Negele, J. W., 2018, *Quantum Many-Particle Systems* (CRC Press, Boca Raton).
Neri, I., 2022, SciPost Phys. **12**, 139.
Nguyen, B., and U. Seifert, 2020, Phys. Rev. E **102**, 022101.
Nicolis, C., and G. Nicolis, 2010, Q. J. R. Meteorol. Soc. **136**, 1161.
Norris, J. R., 1997, *Markov Chains*, Cambridge Series in Statistical and Probabilistic Mathematics Vol. 2 (Cambridge University Press, Cambridge, England).
Nyawo, P. T., and H. Touchette, 2016, Europhys. Lett. **116**, 50009.
Onsager, L., 1931, Phys. Rev. **37**, 405.
Onsager, L., and S. Machlup, 1953, Phys. Rev. **91**, 1505.
Oono, Y., and M. Paniconi, 1998, Prog. Theor. Phys. Suppl. **130**, 29.
Öttinger, H. C., 2005, *Beyond Equilibrium Thermodynamics* (John Wiley & Sons, New York).
Owen, J. A., T. R. Gingrich, and J. M. Horowitz, 2020, Phys. Rev. X **10**, 011066.
Parrondo, J. M. R., J. M. Horowitz, and T. Sagawa, 2015, Nat. Phys. **11**, 131.
Pekola, J. P., 2015, Nat. Phys. **11**, 118.
Peliti, L., 1985, J. Phys. (Paris) **46**, 1469.
Peliti, L., and S. Pigolotti, 2021, *Stochastic Thermodynamics: An Introduction* (Princeton University Press, Princeton, NJ).
Pietzonka, P., and U. Seifert, 2018, J. Phys. A **51**, 01LT01.
Polettini, M., 2015, Lett. Math. Phys. **105**, 89.
Polettini, M., and M. Esposito, 2017, Phys. Rev. Lett. **119**, 240601.
Press, W. H., S. A. Teukolsky, W. T. Vetterling, and B. P. Flannery, 2007, *Numerical Recipes: The Art of Scientific Computing*, 3rd ed. (Cambridge University Press, Cambridge, England).
Prigogine, I., 1961, *Introduction to Thermodynamics of Irreversible Processes*, 2nd Ed. (Interscience Publishers, New York).
Prigogine, I., and R. Lefever, 1968, J. Chem. Phys. **48**, 1695.
Prinz, J.-H., H. Wu, M. Sarich, B. Keller, M. Senne, M. Held, J. D. Chodera, C. Schütte, and F. Noé, 2011, J. Chem. Phys. **134**, 174105.
Proesmans, K., and B. Derrida, 2019, J. Stat. Mech. 023201.
Proesmans, K., G. Falasco, A. Mohite, E. Fodor, and M. Esposito, 2024 (to be published).
Prost, J., J.-F. Joanny, and J. M. Parrondo, 2009, Phys. Rev. Lett. **103**, 090601.
Puglisi, A., S. Pigolotti, L. Rondoni, and A. Vulpiani, 2010, J. Stat. Mech. P05015.
Qian, H., P. Ao, Y. Tu, and J. Wang, 2016, Chem. Phys. Lett. **665**, 153.
Radunz, R., D. Rings, K. Kroy, and F. Cichos, 2009, J. Phys. Chem. A **113**, 1674.
Rahav, S., and C. Jarzynski, 2007, J. Stat. Mech. P09012.
Rana, S., and A. C. Barato, 2020, Phys. Rev. E **102**, 032135.
Rao, R., and M. Esposito, 2016, Phys. Rev. X **6**, 041064.
Rao, R., and M. Esposito, 2018a, J. Chem. Phys. **149**, 245101.
Rao, R., and M. Esposito, 2018b, New J. Phys. **20**, 023007.
Rao, R., and M. Esposito, 2018c, Entropy **20**, 635.
Redner, S., 2001, *A Guide to First-Passage Processes* (Cambridge University Press, Cambridge, England).
Remlein, B., and U. Seifert, 2024, J. Chem. Phys. **160**, 134103.
Remlein, B., V. Weissmann, and U. Seifert, 2022, Phys. Rev. E **105**, 064101.
Rezaei, E., M. Donato, W. R. Patterson, A. Zaslavsky, and R. I. Bahar, 2020, IEEE Trans. Device Mater. Reliab. **20**488.
Ruelle, D., 2009, Nonlinearity **22**, 855.
Rytov, S., 1958, Sov. Phys. JETP **6**, 130, http://jetp.ras.ru/cgi-bin/dn/e_006_01_0130.pdf.
Rytov, S. M., Y. A. Kravtsov, and V. I. Tatarskii, 1989, *Principles of Statistical Radiophysics, Vol. 3: Elements of Random Fields* (Springer, New York).
Sasa, S., and H. Tasaki, 2006, J. Stat. Phys. **125**, 125.
Schlögl, F., 1972, Z. Phys. **253**, 147.
Schmiedl, T., and U. Seifert, 2007, J. Chem. Phys. **126**, 044101.
Schnakenberg, J., 1976, Rev. Mod. Phys. **48**, 571.
Schuss, Z., 2009, *Theory and Applications of Stochastic Processes: An Analytical Approach*, Vol. 170 (Springer, New York).
Seifert, U., 2005, Phys. Rev. Lett. **95**, 040602.
Seifert, U., 2012, Rep. Prog. Phys. **75**, 126001.
Seifert, U., and T. Speck, 2010, Europhys. Lett. **89**, 10007.
Sekimoto, K., 2010, *Stochastic Energetics*, Lecture Notes in Physics Vol. 799 (Springer, New York).
Semenov, O., A. Vassighi, and M. Sachdev, 2006, IEEE Trans. Device Mater. Reliab. **6**, 17.
Sheth, J., S. W. F. Meenderink, P. M. Quiñones, D. Bozovic, and A. J. Levine, 2018, Phys. Rev. E **97**, 062411.
Shiraishi, N., 2023, *An Introduction to Stochastic Thermodynamics* (Springer, New York).
Shiraishi, N., K. Funo, and K. Saito, 2018, Phys. Rev. Lett. **121**, 070601.
Skellam, J. G., 1946, J. R. Stat. Soc. **109**, 296.
Skinner, D. J., and J. Dunkel, 2021a, Phys. Rev. Lett. **127**, 198101.
Skinner, D. J., and J. Dunkel, 2021b, Proc. Natl. Acad. Sci. U.S.A. **118**, e2024300118.
Smith, E., 2011, Rep. Prog. Phys. **74**, 046601.
Smith, E., 2020, Entropy **22**, 1137.
Smith, E., and H. J. Morowitz, 2016, *The Origin and Nature of Life on Earth: The Emergence of the Fourth Geosphere* (Cambridge University Press, Cambridge, England).
Snarski, M., 2021, arXiv:2108.00514.
Solon, A., H. Chaté, J. Toner, and J. Tailleur, 2022, Phys. Rev. Lett. **128**, 208004.

Solon, A. P., J. Stenhammar, R. Wittkowski, M. Kardar, Y. Kafri, M. E. Cates, and J. Tailleur, 2015, Phys. Rev. Lett. **114**, 198301.
Solon, A. P., and J. Tailleur, 2013, Phys. Rev. Lett. **111**, 078101.
Solon, A. P., and J. Tailleur, 2015, Phys. Rev. E **92**, 042119.
Speck, T., 2022, Phys. Rev. E **105**, L012601.
Speck, T., A. Engel, and U. Seifert, 2012, J. Stat. Mech. P12001.
Speck, T., and U. Seifert, 2005, J. Phys. A **38**, L581.
Speck, T., and U. Seifert, 2006, Europhys. Lett. **74**, 391.
Spohn, H., 2012, *Large Scale Dynamics of Interacting Particles* (Springer, New York).
Steffenoni, S., K. Kroy, and G. Falasco, 2016, Phys. Rev. E **94**, 062139.
Strasberg, P., and M. Esposito, 2019, Phys. Rev. E **99**, 012120.
Strogatz, S. H., 2015, *Nonlinear Dynamics and Chaos* (Taylor & Francis, London).
Sun, S. X., 2006, Phys. Rev. Lett. **96**, 210602.
Tailleur, J., J. Kurchan, and V. Lecomte, 2007, Phys. Rev. Lett. **99**, 150602.
Takatori, S. C., W. Yan, and J. F. Brady, 2014, Phys. Rev. Lett. **113**, 028103.
Thomas, P., and R. Grima, 2015, Phys. Rev. E **92**, 012120.
Timpanaro, A. M., G. Guarnieri, J. Goold, and G. T. Landi, 2019, Phys. Rev. Lett. **123**, 090604.
Tomita, K., and H. Tomita, 1974, Prog. Theor. Phys. **51**, 1731.
Touchette, H., 2009, Phys. Rep. **478**, 1.
Toyabe, S., T. Sagawa, M. Ueda, E. Muneyuki, and M. Sano, 2010, Nat. Phys. **6**, 988.
Vance, W., and J. Ross, 1996, J. Chem. Phys. **105**, 479.
Vance, W., and J. Ross, 1999, J. Phys. Chem. A **103**, 1347.
Van den Broeck, C., and M. Esposito, 2015, Physica (Amsterdam) **418A**, 6.
Van der Meer, J., B. Ertel, and U. Seifert, 2022, Phys. Rev. X **12**, 031025.
van Kampen, N., 1961, Can. J. Phys. **39**, 551.
van Kampen, N., 2007, *Stochastic Processes in Physics and Chemistry* (North-Holland, Amsterdam).
Van Vu, T., and K. Saito, 2023, Phys. Rev. X **13**, 011013.
Van Vu, T., V. Tuan Vo, and Y. Hasegawa, 2020, Phys. Rev. E **101**, 042138.
Vastola, J. J., and W. R. Holmes,2020, Phys. Rev. E **101**, 032417.
Vellela, M., and H. Qian, 2009, J. R. Soc. Interface **6**, 925.
Vo, V. T., T. Van Vu, and Y. Hasegawa, 2020, Phys. Rev. E **102**, 062132.
Weber, M. F., and E. Frey, 2017, Rep. Prog. Phys. **80**, 046601.
Weinan, E., and E. Vanden-Eijnden, 2004, Commun. Pure Appl. Math. **57**, 637.
Wiegel, F. W., 1986, *Introduction to Path-Integral Methods in Physics and Polymer Science* (World Scientific, Singapore).
Wolpert, D. H., 2019, J. Phys. A **52**, 193001.
Wolpert, D. H., A. Kolchinsky, and J. A. Owen, 2019, Nat. Commun. **10**, 1727.
Wu, F. Y., 1982, Rev. Mod. Phys. **54**, 235.
Wu, W., and J. Wang, 2013, J. Chem. Phys. **139**, 121920.
Xiao, T. J., Z. Hou, and H. Xin, 2008, J. Chem. Phys. **129**, 114506.
Yang, X., *et al.*, 2021, Proc. Natl. Acad. Sci. U.S.A. **118**, e2026786118.
Yoshimura, K., and S. Ito, 2021, Phys. Rev. Lett. **127**, 160601.
Yu, Q., and Y. Tu, 2022, Phys. Rev. Lett. **129**, 278001.
Zakine, R., and E. Vanden-Eijnden, 2023, Phys. Rev. X **13**, 041044.
Zakine, R., Y. Zhao, M. Knežević, A. Daerr, Y. Kafri, J. Tailleur, and F. van Wijland, 2020, Phys. Rev. Lett. **124**, 248003.
Zhou, P., and T. Li, 2016, J. Chem. Phys. **144**, 094109.
Zia, R., and B. Schmittmann, 2007, J. Stat. Mech. P07012.
Zinn-Justin, J., 2002, *Quantum Field Theory and Critical Phenomena*, 4th ed. (Clarendon Press, Oxford).
Zubarev, D., 1994, Condens. Matter Phys. **4**, 7.
Zubarev, D., and V. Morozov, 1983, Physica (Amsterdam) **120A**, 411.